

# **Redox enzymes in the fermentative degradation of glucose and gluconate**

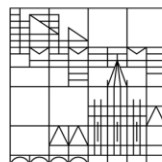
**Doctoral thesis for obtaining the  
academic degree Doctor of Natural Sciences  
(Dr. rer. nat.)**

Submitted by:

**Patil, Yogita**

**at the**

Universität  
Konstanz



Faculty of Sciences  
Department of Biology

**Konstanz, 2019**

Date of the oral examination: 19.06.2019

1. Reviewer: Prof. Dr. Bernhard Schink

2. Reviewer: Prof. Dr. Peter Kroth

3. Reviewer: Prof. Dr. Dieter Spiteller

---

## Table of Contents

---

Summary .....	5
Zusammenfassung.....	7
<b>Chapter 1. General introduction</b> .....	<b>9</b>
1. Anaerobic microbial degradation .....	10
1.1. Anaerobic degradation of sugars .....	11
1.2 Diversity of metabolic pathways .....	11
2. Energy conservation in anaerobic bacteria.....	14
2.1. Energy conservation via substrate level phosphorylation.....	14
2.2. Energy gain via electron transport phosphorylation (ETP).....	14
2.3. Flavin-based electron bifurcation (FBEB) for energy conservation .....	15
2.4 Anaerobic bacteria .....	18
2.4.1 <i>Bacillus stamsii</i> strain BoGlc83 .....	18
2.4.2 <i>Anaerobium acetethylicum</i> strain GluBS11 .....	18
3. Aim of the thesis .....	19
3.1. Research objective .....	19
3.2. Results outline.....	19
<b>Chapter 2. High-quality-draft genome sequence of the fermenting bacterium <i>A. acetethylicum</i> type strain GluBS11T (DSM 29698)</b> .....	<b>20</b>
1. Abstract.....	22
2. Introduction .....	23
3. Organism Information .....	24
4. Genome sequencing information .....	26
5. Insights from the genome sequence .....	31
6. Conclusions .....	41
<b>Chapter 3. Fermentation of glycerol by <i>Anaerobium acetethylicum</i> and its potential use in biofuel production Microbial and applied biotechnology</b> .....	<b>45</b>
1. Abstract.....	46
2. Introduction .....	47
3. Results .....	49
4. Discussion .....	61
5. Conclusion .....	66
6. Experimental procedures .....	67

---

<b>Chapter 4. Gluconate-fermentation by <i>Anaerobium acetethylicum</i>: an evidence for the involvement of modified ED pathway</b> .....	76
1. Abstract.....	77
2. Introduction .....	78
3. Results .....	80
4. Discussion.....	89
5. Conclusion.....	93
5. Materials and methods.....	93
<b>Chapter 5. Enzymes involved in re-oxidation of reducing equivalents in fermenting bacteria</b> .....	100
1. Abstract.....	101
2. Introduction .....	102
3. Results and Discussion .....	104
4. Conclusion.....	122
4. Materials and methods.....	122
<b>Chapter 6. General discussion/conclusions</b> .....	129
1. Fermentation of glycerol and gluconate by <i>A. acetethylicum</i> .....	130
2. Energy metabolism in BoGlc83 and GluBS11 .....	131
<b>List of publications</b> .....	135
<b>Achievements and individual contribution</b> .....	136
<b>References</b> .....	138
<b>Abbreviations</b> .....	165
<b>Acknowledgements</b> .....	166

---

## Summary

In my PhD project, the metabolically different model organisms, *Bacillus stamsii* strain BoGlc83, a syntrophic glucose fermenter and *Anaerobium acetethylicum* strain GluBS11, a classical gluconate/glucose fermenter were studied and compared for the identification of redox enzymes involved in the fermentation pathway to unravel enzyme systems involved in energy conservation during the anaerobic degradation of glucose and gluconate.

The genome of *A. acetethylicum* was sequenced to allow new insights in the genes encoding putative enzymes involved in glucose, gluconate and glycerol metabolism. The annotated genome sequence revealed the presence of a complete set of genes encoding for the enzymes of the Pentose-Phosphate (PP) pathway, the Embden-Meyerhof-Parnas (EMP) pathway, Tri-Carboxylic Acid (TCA) cycle as well as enzymes of the Entner-Doudoroff (ED) pathway. Enzymes involved in the glycerol as well as gluconate fermentation pathway by *A. acetethylicum* were investigated using the genomic information, performing biochemical assays in combination with proteome analysis. For gluconate fermentation the strain was found to utilize a modified ED pathway. The glycerol fermentation study revealed, that strain GluBS11 has a high tolerance towards elevated glycerol concentrations and ferments glycerol mainly to ethanol and bio-hydrogen.

Redox enzymes involved in the re-oxidation of reducing equivalents in *B. stamsii* and *A. acetethylicum* were investigated using biochemical assays and proteome analysis. *A. acetethylicum* was found to contain three different enzymes namely NADP-dependent hydrogenase, ferredoxin:NADP reductase and hydrogenase for NADPH and reduced ferredoxin oxidation and energy conservation in its anaerobic metabolism. In contrast, enzyme assays and proteomics results suggest, that *B. stamsii* rather uses a comproportionating pyruvate:ferredoxin oxidoreductase (PFOR) enzyme complex for the re-oxidation of reducing equivalents and energy conservation. In addition to this, pyruvate formate lyase seems also to be involved in the re-oxidation of NADH and reduced flavins or ferredoxin simultaneously. *In vitro* enzyme assays and proteomic results strongly indicate that the comproportionating PFOR is a flavin-containing/dependent enzyme system, where free flavins could be reduced by accepting electrons both from NADH and pyruvate oxidation. Additionally, ferredoxin and riboflavin could also be re-oxidized through the

---

formate dehydrogenase leading to the production of formate as fermentation product. In summary, both organisms were found to use different metabolic approaches and redox enzymes for balancing reducing equivalents and energy conservation during anaerobic metabolism.

---

## Zusammenfassung

In der vorliegenden Doktorarbeit wurden zwei metabolisch verschiedene Modellorganismen untersucht und verglichen, nämlich *Bacillus stamsii* Stamm BoGlc83, ein syntropher Glucose-Vergärer und *Anaerobium acetethylicum* Stamm GluBS11, ein ungewöhnlicher Gluconat/Glucose-Vergärer. Ziel der Arbeit war es, Redoxenzyme zu identifizieren, die am Fermentationsweg beteiligt sind, und die Enzymsysteme aufzuklären, die an der Energiekonservierung während des anaeroben Abbaus von Glucose und Gluconat beteiligt sind.

Das Genom von *A. acetethylicum* wurde sequenziert, um neue Erkenntnisse über die Gene zu gewinnen, die mutmaßliche Enzyme kodieren, die am Glucose-, Gluconat- und Glycerin-Metabolismus beteiligt sind. Die annotierte Genomsequenz zeigte das Vorhandensein eines vollständigen Satzes von Genen, die für die Enzyme des Pentose-Phosphat (PP) Weg, des Embden-Meyerhof-Parnas (EMP) Weg, des Tricarbonsäure-Zyklus sowie Enzyme des Entner-Doudoroff (ED) Weges kodieren. Enzyme, die am Glycerin- und Gluconat Fermentationsweg durch *A. acetethylicum* beteiligt sind, wurden anhand genomischer Informationen untersucht und biochemische Assays durchgeführt, die mit der Proteomanalyse kombiniert wurden. Für die Gluconat-Fermentation verwendete der Stamm einen modifizierten ED-Weg. Die Studie zur Glycerin-Fermentation ergab, dass der Stamm GluBS11 tolerant gegenüber hohen Glycerinkonzentrationen ist und Glycerin hauptsächlich zu Ethanol und Bio-Wasserstoff fermentiert.

Redoxenzyme, die an der Re-oxidation von Reduktionsäquivalenten in *B. stamsii* und *A. acetethylicum* beteiligt sind, wurden unter Verwendung biochemischer Assays und Proteomanalyse untersucht. Es wurde festgestellt, dass *A. acetethylicum* zur Re-oxidation von Reduktionsäquivalenten drei verschiedene Enzyme verwendet, nämlich NADP-abhängige Hydrogenase, Ferredoxin:NADP Reduktase und Hydrogenase zur Oxidation von NADPH und reduziertem Ferredoxin und zur Energieeinsparung im anaeroben Metabolismus. Im Gegensatz dazu legen Enzymassays, Aktivitätsfärbung und Proteomanalysen nahe, dass in *B. stamsii* Pyruvat:Ferredoxin Oxidoreduktase (PFOR)- Enzymkomplexe zur Re-oxidation von Reduktionsäquivalenten und zur Energiekonservierung verwendet werden. Darüber hinaus scheint Pyruvat:Formiat Lyase auch an der Re-oxidation von NADH beteiligt zu sein und reduziert gleichzeitig freie Flavine oder Ferredoxin. In vitro Enzymtests zeigen deutlich, dass

---

die Komproportionierungs-PFOR ein Flavin-enthaltendes Enzymsystem ist und bei dem freie Flavine Elektronen sowohl aus der Oxidation von NADH als auch von Pyruvat aufnehmen können, Ferredoxin und Riboflavin können durch eine Formiatdehydrogenase erneut reoxidiert und so Formiat als Gärprodukt freigesetzt werden. Zusammenfassend haben beide Organismen unterschiedliche metabolische Mechanismen und Redoxenzyme, um das Gleichgewicht zwischen Reduktionsäquivalenten und Energiekonservierung während des anaeroben Stoffwechsels zu halten.

# CHAPTER 1

---

## General Introduction

## 1. Anaerobic microbial degradation

In the presence of oxygen, aerobic bacteria are able to degrade organic matter like carbohydrates completely to  $\text{CO}_2$  and  $\text{H}_2\text{O}$  and also yield higher energy (Westermann 1993; Gibson 1984). By contrast, in the absence of oxygen, anaerobic bacteria need to perform this process in multiple steps that constitute a process called the anaerobic food chain constituting an important component of the global carbon cycle (Cole et al., 2007; Kortelainen et al., 2004). In this process at least five different groups of bacteria and archaea participate. Figure 1 shows the general steps of degradation of organic matter by anaerobic organisms including hydrolytic and primary fermenting bacteria, secondary fermenting bacteria and methanogenic archaea that finally transform organic matter to  $\text{CH}_4$  and  $\text{CO}_2$  (Schink 1997; Canfield et al., 2006).

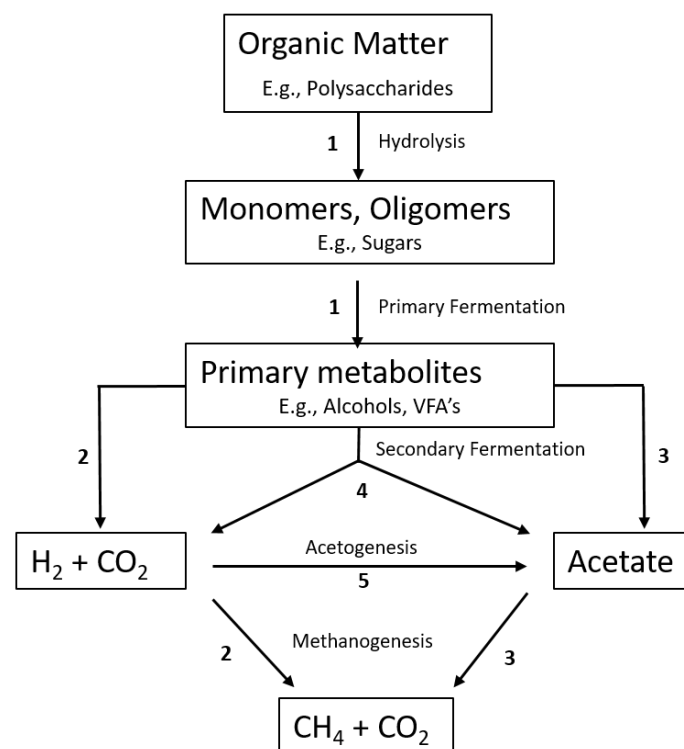


**Figure 1.** Anaerobic pathway of organic matter degradation: Group of bacteria involved: 1, primary fermenting bacteria; 2, hydrogen-oxidizing methanogens; 3, acetate-cleaving methanogens; 4, secondary-fermenting (“syntrophs”) bacteria; 5, acetogenic bacteria (Schink, 1997).

---

### 1.1. Anaerobic degradation of sugars

Primary fermenting bacteria perform extracellular enzymatic hydrolysis of polymers, such as polysaccharides, into their water-soluble building blocks, i.e., sugars. The same group of bacteria then ferments these monomers to smaller compounds such as volatile fatty acids (VFAs), alcohols, CO<sub>2</sub> and H<sub>2</sub> (Capone and Kiene, 1988). The anaerobic degradation of hexoses by primary fermenting bacteria or secondary fermenting bacteria to acetate, CO<sub>2</sub>, and H<sub>2</sub> is an exergonic process, however it is influenced by accumulating hydrogen. This reaction does not yield sufficient energy to support growth unless hydrogen pressure is minimized (Thauer et al., 1977; Schink, 1997). Therefore, fermentation of sugars by secondary fermenting bacteria (syntrophs) to acetate, CO<sub>2</sub>, H<sub>2</sub> and formate is performed in association with hydrogen consuming methanogens (Schink, 1997).

During syntrophic degradation, H<sub>2</sub> producing organisms couple those consuming it, a process called interspecies H<sub>2</sub> transfer. Besides H<sub>2</sub>, formate and acetate serve as metabolites for interspecies electron transfer during syntrophic degradation (Schink, 1997). In syntrophic microbial communities, methanogens, and homoacetogens are able to maintain low hydrogen partial pressure at the level of 10<sup>-4</sup> to 10<sup>-5</sup> atm, thereby yielding more energy per mole of substrate for the sugar-fermenting bacteria (Schink and Stams, 2006; Müller et al., 2008). On the other hand, when sugar-fermenting anaerobes are grown in pure culture, fermentation patterns generally shift to the production of more reducing end products such as butyrate, ethanol, or lactate due to the limited availability of ATP for use in substrate-level phosphorylation reactions (Iannotti et al., 1973; Thauer et al., 1977; Tewes and Thauer, 1980). This shift in fermentation patterns in the absence of a partner has been observed in a wide range of bacteria such as *Clostridia* spp. or *Ruminococcus albus* (Zeikus, 1983). In these organisms formation of butyrate, ethanol or lactate along with the excretion of H<sub>2</sub> serve as a way to dissipate reducing power (electrons).

### 1.2 Diversity of metabolic pathways

Anaerobic bacteria metabolize a wide variety of sugars, including glucose as well as sugar acids, e.g., gluconate, to pyruvate by employing one of the pathways that may include the Embden-Meyerhof-Parnas (EMP) or glycolysis, Entner-Doudoroff (ED), and the Pentose-Phosphate (PP) pathway (Peekhaus and Conway, 1998). In most cases, fermentation end-

---

products are predominantly produced from the common intermediate pyruvate. In respiring organisms, pyruvate is further oxidized through the citric acid cycle generating more energy (ATPs). One out of following three pathways can be used for the initial oxidation of carbohydrate-based substrates, e.g., glucose or gluconate that leads to the production of common intermediate pyruvate (Figure 2).

Glycolysis (EMP pathway) is the most common pathway which is not only found in bacteria, but occurs also in higher animals and plants, where glucose is oxidized to two molecules of pyruvate, and energy conserved in the form of ATP and NADH (Figure 2A). In the first step, glucose is phosphorylated with ATP to produce glucose-6-phosphate. The latter is then isomerized to fructose-6-phosphate and following another ATP-dependent phosphorylation fructose-1, 6-bisphosphate is produced. This reaction is catalyzed by phosphofructokinase, which is the key regulating enzyme of the glycolysis. Fructose-1, 6-bisphosphate is eventually metabolized to 3 carbons intermediate, glyceraldehyde-3-phosphate. Further oxidation of the one glyceraldehyde-3-phosphate to one pyruvate generates 2 ATP and the concomitant reduction of  $\text{NAD}^+$  to NADH. In glycolysis, bacteria gain first ATP through the substrate-level phosphorylation (SLP) of 1, 3-bisphosphoglycerate to 3-phosphoglycerate (Kim and Gadd, 2011; Voet et al., 2016). During EMP pathway one molecule of glucose is metabolized to two molecules of pyruvate and overall two ATP and two NADH (Figure 2A). Although less energy rewarding than EMP, the Entner-Doudoroff (ED) pathway involves production of common intermediate glyceraldehyde-3-phosphate which can be further oxidized to pyruvate. In 1952, the ED pathway was firstly reported in *Pseudomonas saccharophila* for the degradation of glucose and gluconate (Entner and Doudoroff, 1952). It has been reported that ED pathway is employed mainly for the degradation of gluconate (Peekhaus and Conway, 1998), where it is initially phosphorylated to 6-phosphogluconate. Following dehydration 2-keto-3-deoxy-6-phosphogluconate (KDPG) is formed. KDPG is finally cleaved yielding pyruvate and glyceraldehyde-3-phosphate (Entner and Doudoroff, 1952). The latter 3 carbon compound is then further metabolized to pyruvate by enzymes of the EMP pathway. Therefore, similar to EMP pathway, two molecules of pyruvate can be formed in ED pathway (Figure 2B). The key regulatory enzymes of the ED pathway are 6-phosphogluconate dehydratase and KDPG aldolase.

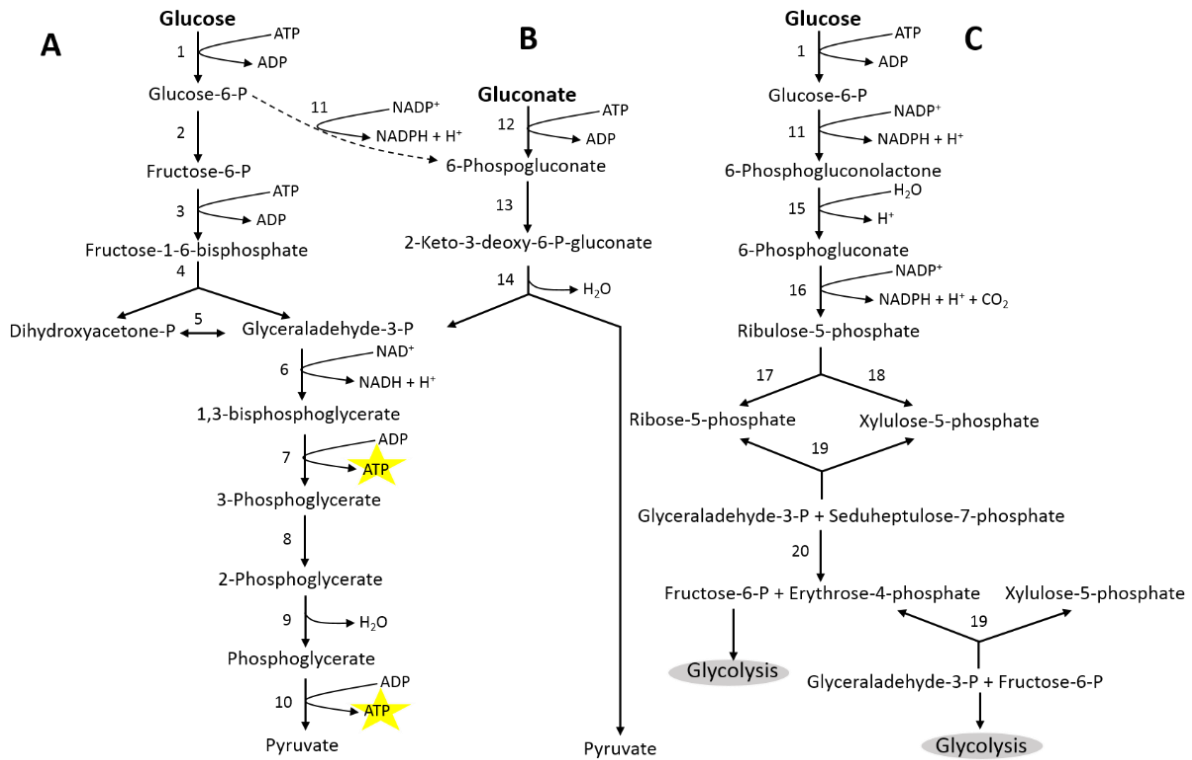


**Figure 2.** The schematic representation of common metabolic pathways employed by bacteria for sugar-based substrate degradation. A) Embden-Meyerhof-Parnas pathway (EMP, glycolysis); B) Entner-Doudoroff (ED) pathway; and C) pentose-phosphate pathway. The numbers represent the following enzymes: 1. Hexokinase; 2. Glucose-6-phosphate isomerase; 3. Phosphofruktokinase; 4. Fructose-1,6-bisphosphate aldolase; 5. Triosephosphate isomerase; 6. Glyceraldehyde-3-phosphate dehydrogenase; 7. 3-Phosphoglycerate kinase; 8. Phosphoglycerate mutase; 9. Enolase; 10. Pyruvate kinase. 11. Glucose-6-phosphate dehydrogenase; 12. Gluconate kinase; 13. 6-Phosphogluconate dehydratase; 14. KDPG aldolase; 15. 6-Phosphogluconolactonase; 16. 6-Phosphogluconate dehydrogenase; 17. Ribose-5-phosphate isomerase, 18. Ribulose 5-phosphate 3-epimerase; 19. Transketolases; 20. Transaldolase.

In some bacteria a third type of degradation pathway for glucose exists called the pentose-phosphate (PP) pathway (Figure 2C). Unlike to glycolysis, the PP pathway generates NADPH and pentoses (5-carbon sugars) as well as ribose-5-phosphate. The latter is used as a precursor for the biosynthesis of DNA nucleotides (Kruger et al., 2003). Thus, the PP pathway is considered primarily an anabolic metabolism generating precursors for the

---

synthesis of cellular biomass rather than a catabolic pathway for energy conservation (Kruger and von Schaewen, 2003). It generates no ATP, but only two NAD(P)H are formed in the oxidative branch (Figure 2C). Besides sugar metabolism, pyruvate can also be formed from other substrates like glycerol (discussed in Chapter 3).

## **2. Energy conservation in anaerobic bacteria**

In bacteria, the energy input is required for anabolic reactions, whereas catabolism involves the breakdown of substrates that allow an organism to gain energy. Energy conservation in organisms is generally dependent on the redox reactions and accomplished by electron transport phosphorylation or substrate level phosphorylation (Herrmann et al, 2008). Anaerobes operate with small amounts of energy, and syntrophically cooperating anaerobes have been found to be “experts” in the exploitation of minimal energy.

### **2.1. Energy conservation *via* substrate level phosphorylation**

During fermentation substrates are oxidized in the absence of external electron acceptors; i.e., the redox levels of the substrate and the metabolite(s) remain same. Therefore, the substrate serves not only as an electron donor, but also as a final electron acceptor (Thauer et al., 1971). In fermentation comparatively low amount of energy is conserved due to incomplete oxidation of substrate and relies on substrate level phosphorylation (SLP) for the generation of ATP (El-Mansi et al., 2006). The SLP is quicker, but less efficient source of ATP generation (Mitchell et al., 1975). In the SLP metabolism, anaerobic bacteria generate ATP by transferring a phosphoryl group to ADP (Voet et al., 2016). Fermentation of one mole of glucose yields 2-4 moles of ATP depending on the type of fermentation, while during aerobic respiration with O<sub>2</sub> as terminal electron acceptor yields can range between 32-36 ATP.

### **2.2. Energy gain *via* electron transport phosphorylation (ETP)**

Apart from SLP, energy conservation in chemotrophic bacteria also contains another mode of energy conservation *via* electron-transfer phosphorylation (ETP), also called as oxidative phosphorylation (Thauer et al., 1977). During electron transport phosphorylation (ETP),

---

electrons are transferred to a terminal electron acceptors, such as nitrate, sulfate etc., through which electrochemical ion-gradient  $H^+/Na^+$  is established across the membrane that finally is used for energy conservation in the form of ATP by ATP synthase (Buckel and Thauer, 2018). Thus, electrons are passed from one molecule to another, i.e., one substrate is oxidized (e.g., glucose to  $CO_2$ ) and the other is reduced (nitrate to dinitrogen). Apparently, bacterial fermentations are considered exceptions to this generalization because they are thought to lack ETP (Stadtman, 1966; Herrmann et al., 2008). In some cases the excretion of fermentation products results in a proton motive force, which can be exploited for membrane-facilitated ATP synthesis. Therefore, fermentation cannot be completely separated from a membrane electron transport in which energy can be conserved by ATP synthase (Braune et al., 1999; Wendt et al., 2003; Buckel et al., 2001). Oxidation phosphorylation is made of two main components: the electron transport phosphorylation (ETP), where electrons are passed from one substrate to another, and in chemiosmosis, energy released during electron transport is harvested to a built electrochemical gradient that is exploited to make ATP. In aerobic metabolism the final electron acceptor in ETP is molecular oxygen, while in anaerobic respiration a variety of other electron acceptors such as nitrate, sulfate are used as external electron acceptors.

### **2.3. Flavin-based electron bifurcation (FBEB) for energy conservation**

Electron bifurcation is a process in which electron pair is bifurcated to one electron with a more positive reduction potential and one with a more negative reduction potential than that of the electron pair (Buckel et al., 2013; when operating in reverse, the mechanism is referred to as electron confurcating). Electron bifurcation is a recently discovered energy conservation process that is driven by soluble multi-enzyme complexes found in cytoplasm (Fuchs et al., 2014). Electron bifurcation can be divided into two types: disproportionation (electrons from medium reduction potential electron donor are split and given to a high reduction potential acceptor and a low potential electron acceptor), and comproportionation (low reduction potential electron donor and high reduction potential electron donor deliver electrons to a medium reduction potential electron acceptor). In this process simultaneous coupling of exergonic and endergonic oxidation–reduction reactions are performed to circumvent thermodynamic barriers and minimize free energy loss (Peters et al., 2016).

---

When flavin-containing enzyme complexes (electron-transferring flavoprotein, Etf) are involved in electron bifurcation, the process is referred to as flavin-based electron bifurcation (FBEB; Müller et al., 2018). In addition to SLP and ETP, often FBEB is considered as a **‘third type of mechanism of energy conservation’** however, it is not directly coupled to ATP synthesis (Buckel and Thauer, 2018; Herrmann et al., 2008, Li et al., 2008). In this process, a biochemical reactions are catalyzed by flavin-based enzyme complex that involves the simultaneous reduction of two electron acceptors using a single electron donor, whereby a thermodynamically favorable exergonic reaction drives a unfavorable reaction (Buckel and Thauer, 2013; Peters et al., 2016). In 2008, a FBEB enzyme (Etf/Bcd) complex system was discovered in *C. kluyveri*. In recent years number of studies discovered the presence of flavin containing multi-enzyme complexes in many anaerobic bacteria as well as archaea. For instance, the multi-subunit [Fe-Fe] hydrogenase from hyperthermophilic fermenting bacterium *Thermotoga maritima* (Schut and Adams, 2009; Schuchmann and Müller, 2012), the hydrogenase (NfnAB) from *C. kluyveri* (Huang et al., 2012), the formate dehydrogenase from *C. acidiurici* (Wang et al., 2013), the lactate dehydrogenase from model acetogen *A. woodii* (Weghoff et al., 2014) as well as the [Ni-Fe] hydrogenase from methanogenic archaea (Kaster et al., 2011).

The electron-bifurcating flavoprotein complexes are categorized into four groups: (i) complexes containing EtfAB, each subunit harbor an FAD; (ii) NfnAB complex, each subunit harbor an FAD; (iii) protein complexes containing an FMN-binding, NAD(P)H dehydrogenase subunit; and (iv) complexes containing HdrABC with HdrA harboring FAD (Buckel and Thauer, 2018). In FBEB enzyme complexes, EtfAB subunits, and dehydrogenases are the key component involved in electron bifurcation reaction (Weghoff et al., 2015, Wang et al., 2010), except iron-only hydrogenase of *T. maritima* which does not contain Etf (Schut et al., 2009). A simple schematic illustration of flavin based electron bifurcation examples is shown below that explains the heart of the electron bifurcation mechanism (Figure 3).

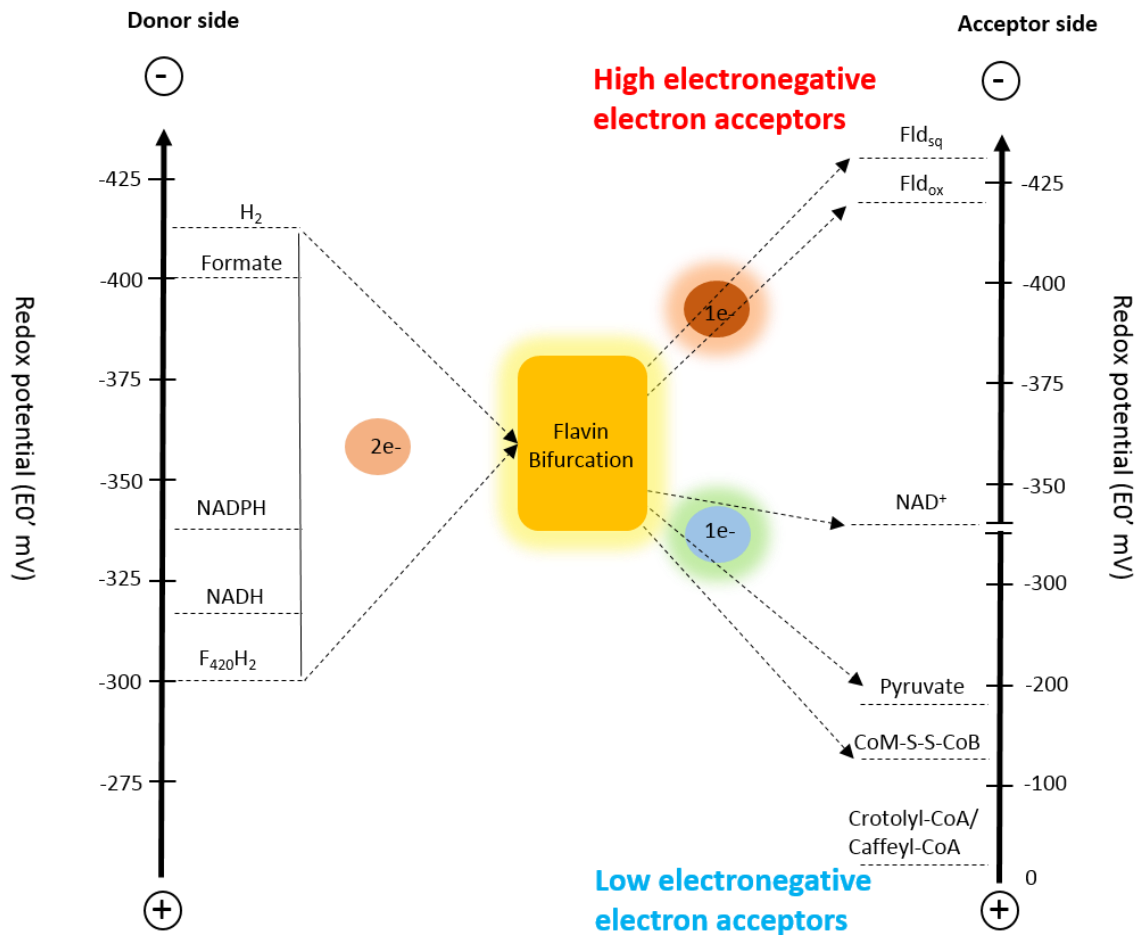


**Figure 3.** Schematic illustration of examples of flavin-based electron bifurcation (center) systems in anaerobic bacteria. Horizontal bars along the two scale indicate redox potentials ( $E_0'$  at pH 7.0) for different electron donors and acceptors. Two electrons originating from donors are bifurcated; in dark brown (one electron transferred to low potential acceptor) and sky blue (another electron is transferred to high-potential acceptor), respectively. Abbreviations: CoB, coenzyme B; CoM, coenzyme M;  $Fd^{ox}$ , oxidized ferredoxin;  $Fld^{sq}$ , semiquinone state flavodoxin (figure modified from Müller et al., 2018).

---

## 2.4 Anaerobic bacteria

### 2.4.1 *Bacillus stamsii* BoGlc83

*Bacillus* strain BoGlc83 is a metabolically highly versatile and flexible bacterium that was isolated from sediment of Lake Constance, Germany as a dominant sugar utilizer (Müller et al., 2008). It is a gram positive, facultative anaerobic but uniquely, it represents the first known strain that is capable of syntrophic degradation of sugars, e.g., glucose in association with hydrogen scavenging methanogenic partner organism *M. hungatei* (Müller et al., 2008).. Later it was found that strain BoGlc83 could also grow anaerobically in pure culture when provided with 10 mM pyruvate, 0.05% casamino acids and 0.05% yeast extract in addition to glucose (Mueller et al., 2015). This ability and metabolic versatility differ it from other *Bacillus* spp., which have been described so far (Müller et al., 2008, Sneath, 1986) The genome of strain BoGlc83 has recently been sequenced (Müller et al., 2016 unpublished data). Glucose fermentation by the *Bacillus stamsii* occurs through the classical Embden-Meyerhof-Parnas pathway (Müller et al., 2008) and generate two molecules of pyruvate plus 4 reducing equivalents (2 NADH and 2 Fd<sup>red</sup>).

### 2.4.2 *Anaerobium acetethylicum* strain GluBS11

Strain GluBS11 is a classical sugar fermenting bacterium isolated from biogas slurry samples using gluconate as a substrate. It is very closely related to genus *Clostridium* (family *Lachnospiraceae*). Strain GluBS11 ferment a wide range of sugars, including glucose and sugar acids such as gluconate uniquely to ethanol, acetate, formate and hydrogen as main end products, but no butyrate (Patil et al., 2015). GluBS11 ferment glucose and/or gluconate through modified ED pathway producing pyruvate, and generate 2 NADPH and 2 reduced ferredoxins. Similar to EMP pathway, these 2 NA(D)H and reduced ferredoxin have to be re-oxidized to NAD(P)<sup>+</sup> with the release of two electrons to form hydrogen or formate. Under physiological conditions, this redox reaction is endergonic and non-spontaneous, enzymes involved are unknown for the both strains. However, a hypothetical bifurcating enzyme system was proposed to catalyze such reactions based on the discovery enzymes found in other anaerobic bacteria like *T. maritima* (Schut et al., 2009).

---

### 3. Aims of the thesis

The aim of this work was to investigate the involvement of redox enzymes in syntrophically glucose-fermenting and classical glucose/gluconate-fermenting anaerobic bacteria: *Bacillus stamsii* BoGlc83 and *Anaerobium acetilylicum* GluBS11, and compare the energy metabolism difference in these organisms. Specifically the following research questions were raised:

#### 3.1 Description of specific objectives

- Genome sequencing of GluBS11 and comparative genome analysis of GluBS11 and BoGlc83 for the presence of genes encoding enzymes involved in anaerobic fermentative metabolism
- Investigation of enzymes involved in glycerol and gluconate-fermentation by strain GluBS11 using biochemical assay and proteomic analysis
- Investigation of redox enzymes involved in re-oxidation reducing equivalents in strain BoGlc83 and GluBS11, and comparative analysis of energy metabolism

#### 3.2 Results outline.

During the course of my PhD work following results were obtained that are divided into four main chapters.

**Chapter 2.** Describes the genome sequencing of *A. acetethylicum* and provide novel insights into identification of gene encoding enzymes in metabolic pathways (published).

**Chapter 3.** Describes the biochemical investigation of glycerol fermentation pathway by *A. acetethylicum* for conservation of glycerol to biofuel (published).

**Chapter 4.** Describes the biochemical evidence for the involvement of modified ED-pathway in gluconate fermentation by GluBS11 (submitted).

**Chapter 5.** Describes the involvement of redox enzymes in energy metabolism of syntrophic- and classical-fermenting anaerobic bacteria (draft manuscript).

---

# CHAPTER 2

---

**High-quality-draft genome sequence of the  
fermenting bacterium *Anaerobium acetethylicum*  
type strain GluBS11<sup>T</sup> (DSM 29698)**

**Yogita Patil**, Nicolai Müller, Bernhard Schink, et al.,

Published in Standards in Genomic Sci. 2016; doi: 10. 1186/s40793-017-0236-

4.

---

## 1. Abstract

*Anaerobium acetethylicum* strain GluBS11<sup>T</sup> belongs to the family *Lachnospiraceae* within the order *Clostridiales*. It is a Gram-positive, non-motile and strictly anaerobic bacterium isolated from biogas slurry that was originally enriched with gluconate as carbon source (Patil, et al., *Int J Syst Evol Microbiol* 65:3289-3296, 2015). Here we describe the draft genome sequence of strain GluBS11<sup>T</sup> and provide a detailed insight into its physiological and metabolic features. The draft genome sequence generated 4,609,043 bp, distributed among 105 scaffolds assembled using the SPAdes genome assembler method. It comprises in total 4,132 genes, of which 4,008 were predicted to be protein coding genes, 124 RNA genes and 867 pseudogenes. The G+C content was 43.51 mol %. The annotated genome of strain GluBS11<sup>T</sup> contains putative genes coding for the pentose phosphate pathway, the Embden-Meyerhoff-Parnas pathway, the Entner-Doudoroff pathway and the tricarboxylic acid cycle. The genome revealed the presence of most of the necessary genes required for the fermentation of glucose and gluconate to acetate, ethanol, and hydrogen gas. However, a candidate gene for production of formate was not identified.

## Keywords

Anaerobic, Gluconate, Glycerol, Microcompartments, Lachnospiraceae, Firmicutes, Gram-staining positive, Embden-Meyerhoff-Parnas pathway, Entner-Doudoroff pathway, Ferredoxin, Transporters.

## Abbreviations

NADH: nicotinamide adenine dinucleotide reduced; CDS: coding DNA sequence; COG: clusters of orthologous groups; MEGA: molecular evolutionary genetics analysis; CTAB: cetyl trimethyl ammonium bromide; KEGG: kyoto encyclopedia of genes and genomes

---

## 2. Introduction

Strain GluBS11<sup>T</sup> (= DSM 29698) is the type strain of the newly described species *Anaerobium acetethylicum* (Patil et al., 2015). The genus *Anaerobium* belongs to the family *Lachnospiraceae* (Rainey et al., 2009) within the class *Clostridia* (Rainey et al., 2009a) of the order *Clostridiales* (Prévot 1953) that is largely synonymous with *Clostridium* rRNA cluster XIVa (Collins et al., 1994, Stackebrandt et al., 1999). Members of the family *Lachnospiraceae* have been isolated from diverse habitats, but are mainly constituents of mammalian intestinal microbiota, especially from ruminants (Kittelman et al., 2013) and humans (Gosalbes et al., 2011). They are strictly anaerobic and primarily non-spore forming (Cotta et al., 2006), and ferment polysaccharides to short-chain fatty acids such as acetate and propionate as fermentation products (Biddle et al., 2013), e.g., *Eubacterium rectale* ATCC 33656<sup>T</sup>, *Eubacterium ventriosum* ATCC 27560<sup>T</sup>, *Coprococcus* sp. and *Roseburia* sp. (Barcenilla et al., 2000, Duncan et al., 2002). The family *Lachnospiraceae* as currently described in the National Center for Biotechnology Information homepage comprises 41 named genera and several unclassified isolates, of which a total of 143 draft or complete genome sequences are available. Strain GluBS11<sup>T</sup> was isolated due to its ability to ferment gluconate, and the species epithet '*acetethylicum*' refers to its main fermentation products acetate and ethanol during gluconate fermentation (Patil et al., 2015). Within the diverse family of *Lachnospiraceae*, strain GluBS11<sup>T</sup> is phylogenetically closely related to the type strains of *C. herbivorans* strain 54408 ((94% 16S rRNA sequence similarity); Varel et al., 1995), *C. populeti* ATCC 35295<sup>T</sup> ((93.3% similarity); Sleat and Mah, 1985), *Eubacterium uniforme* ATCC 35992<sup>T</sup> (92.4% similarity), and *C. polysaccharolyticum* ATCC 33142<sup>T</sup> ((91.5% similarity); van Gylswyk et al., 1980). Of these, all strains were reported to ferment sugars mainly to butyrate plus formate, acetate, ethanol or lactate, except for *E. uniforme*, which does not produce butyrate. Similar to *E. uniforme* ATCC 35992<sup>T</sup>, strain GluBS11<sup>T</sup> does not produce butyrate during the fermentation of sugars or glycerol (Patil et al., 2015, Patil et al., 2017). Moreover, none of the above strains except for strain GluBS11<sup>T</sup> was tested for fermentation of gluconate.

The most prominent feature of *A. acetethylicum* strain GluBS11<sup>T</sup> is its ability to ferment sugars (including oxidized sugar such as gluconate) and glycerol mainly to acetate, ethanol, hydrogen, and formate (Patil et al., 2015, Patil et al., 2017). Therefore, we selected strain

---

GluBS11<sup>T</sup> as a candidate for studying its potential to ferment gluconate or glycerol. Moreover, most of the described bacterial glycerol fermentations lead to 1,3-propanediol (Homann et al., 1980) and other undesired products such as butyrate or 2,3-butanediol. In contrast to this, strain GluBS11<sup>T</sup> ferments glycerol mainly to ethanol and hydrogen gas as well as negligible amounts of acetate and formate (Patil et al., 2017). Here we present the summary of the taxonomic classification and the features of *A. acetethylicum* strain GluBS11<sup>T</sup> together with the description of the genome sequencing and annotation. Emphasis is given on understanding the central metabolism and fermentation pathways. The putative enzymes involved in the fermentation of gluconate, glucose, and glycerol were also reconstructed from the genomic data.

### 3. Organism Information

#### 3.1 Classification and features

*A. acetethylicum* strain GluBS11<sup>T</sup> is a member of the family Lachnospiraceae in the phylum Firmicutes (Gibbons and Murray, 1978). Cells were strictly anaerobic, non-motile and stained Gram-positive (Patil et al., 2015). Figure 1A shows the ultrathin trans-section of a rod-shaped cell and figure 1B shows details of the Gram-positive membrane structure. For transmission electron microscopy, fixation of bacterial cells was done with glutaraldehyde and osmium tetroxide followed by staining with uranylacetate. Samples were dehydrated in a graded ethanol series, embedded in Spurr resin and viewed in a Zeiss 912 Omega transmission electron microscope (Oberkochen, Germany) at 80kV. Classification and general features are summarized in Table 1. Strain GluBS11<sup>T</sup> ferments various substrates including glucose, lactose, sucrose, fructose, maltose, xylose, galactose, melibiose, melezitose, gluconate, mannitol, erythritol, glycerol and esculin, and mainly produces acetate, ethanol, hydrogen and formate as fermentation end products (Patil et al., 2015). Although strain GluBS11<sup>T</sup> was tested negative for catalase and peroxidase (Patil et al., 2015). A gene coding for a putative catalase-peroxidase (IMG gene locus tag Ga0116910\_10254) was identified in the draft genome. Besides this, strain GluBS11<sup>T</sup> contains putative genes coding for thioredoxin reductase (Ga0116910\_100846) and thioredoxin (Ga0116910\_100229) and no gene coding for superoxide dismutase was identified in the genome. Strain GluBS11<sup>T</sup> was tested positive for fermentation (API Rapid 32A reactions) of  $\alpha$ -galactosidase,  $\alpha$ -glucosidase and  $\beta$ -

---

glucosidase (Patil et al., 2015). The genome-based analysis identified genes coding for a putative  $\beta$ -galactosidase (Ga0116910\_1001515 and Ga0116910\_100295), a  $\beta$ -glucosidase (Ga0116910\_100187 and Ga0116910\_100196) and  $\alpha$ -galactosidase (Ga0116910\_10579, Ga0116910\_100577 and Ga0116910\_102538), respectively.

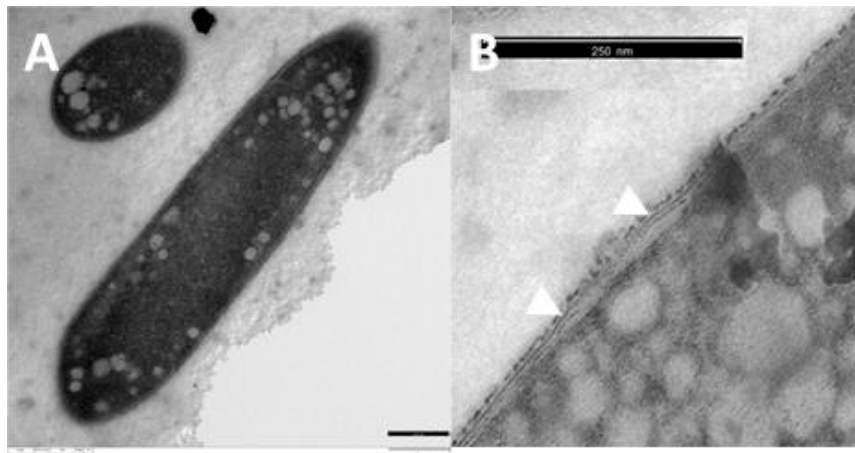


**Figure 1.** Transmission electron micrograph of *A. acetethylicum* strain GluBS11<sup>T</sup> cells grown with gluconate. A) Ultrathin trans-section of cell; B) details of the Gram-positive membrane structure (white arrows).

BLAST search results of the partial 16S rRNA gene sequence of *A. acetethylicum* strain GluBS11<sup>T</sup> (KP233894) revealed closest sequence similarities with the uncultured Lachnospiraceae bacterium strain UY038 (94% similarity; HM099641) that was isolated from an oral sample, *C. populeti* ATCC 35295<sup>T</sup> (94%; X71853) and *Robinsoniella* sp. MCWD5 (94%; KU886099). The draft genome sequence of *A. acetethylicum* GluBS11<sup>T</sup> has one full-length 16S rRNA gene (1,536 bp; locus tag Ga0116910\_1073) that was compared with the partial 16S rRNA gene sequence (1,402 bp; KP233894) from the original species description (Patil et al., 2015). Sequence alignment indicated, that both 16S rRNA sequences were about 99% identical and the complete 16S rRNA gene sequence differs from the partial 16S rRNA gene sequence by the presence of an additional stretch of 45 bp nucleotides sequence at the beginning, 5 gaps (53-55, 65 and 68 positions), and 9 base change at position 51 (T-A), 96 (G-A), 104 (A-T), 1,008 (T-A), 1423 (A-T), 1,434 (A-G), 1,435 (T-G), 1,442 (A-C) and 1,443 (T-C), followed by an additional long stretch of a 83 bp nucleotide sequence

---

at the end. Figure 2 shows the current phylogenetic position of *A. acetethylicum* strain GluBS11<sup>T</sup> in a phylogenetic tree constructed in MEGA 7 (Kumar et al., 2016) using the Minimum Evolution method (Rzhetsky and Nei, 1992), and the evolutionary distances were computed using the Jukes-Cantor method (Jukes and Cantor, 1969) and the Neighbor-Joining algorithm (Saitou and Nei, 1978).

## **4. Genome sequencing information**

### **4.1 Genome project history**

Strain GluBS11<sup>T</sup> was selected for genome sequencing because of its ability to ferment gluconate or glycerol mainly to acetate, ethanol, hydrogen and small amounts of formate. Genome sequencing was performed through the community science program as part of the “Genomic Encyclopedia of Bacterial and Archaeal Type Strains, Phase III: the genomes of soil and plant-associated and newly described type strains” (Kyrpides et al., 2014, Whitman et al., 2015). The draft genome of *A. acetethylicum* strain GluBS11<sup>T</sup> is listed in the Genomes OnLine Database (GOLD) under the GOLD project ID Gp0139288 (Reddy et al., 2015), and the assembled and annotated high-quality permanent draft genome sequence is deposited in IMG under submission ID 88715 (Markowitz et al., 2014). Whole genome shotgun (WGS) sequencing project was also submitted to the Genbank/NCBI under the accession no., FMKA00000000 and consists of 105 contigs (FMKA01000001-FMKA01000105). Sequencing, finishing and annotation were performed by the Department of Energy (DOE), Joint Genome Institute (JGI) using state-of-the-art sequencing technology (Mavromatis et al., 2012). A summary of the project information is shown in Table 2.

**Table 1.** Classification and general features of *Anaerobium acetethylicum* strain GluBS11<sup>T</sup> according to the MIGS recommendations (Field et al., 2008).

MIGS ID	Property	Term	Evidence code <sup>a</sup>
	Classification	Domain <i>Bacteria</i>	TAS (Woese et al., 1990)
		Phylum <i>Firmicutes</i>	TAS (Gibbons and Murray, 1978, Murray, 1984)
		Class <i>Clostridia</i>	TAS (Rainey, 2009, Nei and Kumar, 2000)
		Order <i>Clostridiales</i>	TAS (Prévot, 1953, Felsenstein, 1985)
		Family <i>Lachnospiraceae</i>	TAS (Rainey, 2009b, Nei and Kumar, 2000)
		Genus <i>Anaerobium</i>	TAS (Patil et al., 2015)
		Species <i>Anaerobium acetethylicum</i>	TAS (Patil et al., 2015)
		Type strain: <i>GluBS11<sup>T</sup> (DSM 29698)</i>	
	Gram stain	<i>positive</i>	IDA, (Patil et al., 2015)
	Cell shape	<i>rod-shaped</i>	IDA, (Patil et al., 2015)
	Motility	<i>non-motile</i>	TAS (Patil et al., 2015)
	Sporulation	<i>spore formation not reported</i>	TAS (Patil et al., 2015)
	Temperature range	<i>15-37°C</i>	IDA (Patil et al., 2015)
	Optimum temperature	<i>30°C</i>	IDA, (Patil et al., 2015, Patil et al., 2017)
	pH range; Optimum	<i>3.5–6.5; 7.3</i>	TAS (Patil et al., 2015)
	Carbon source	<i>gluconate, glucose, glycerol.</i>	TAS (Patil et al., 2015, Patil et al., 2017)
MIGS-6	Habitat	<i>biogas slurry</i>	TAS (Patil et al., 2015)
MIGS-6.3	Salinity	<i>not determined</i>	
MIGS-22	Oxygen requirement	<i>anaerobe</i>	TAS (Patil et al., 2015, Patil et al., 2017)
MIGS-15	Biotic relationship	<i>free-living</i>	IDA
MIGS-14	Pathogenicity	<i>non-pathogenic</i>	NAS
MIGS-4	Geographic location	<i>Germany</i>	IDA
MIGS-5	Sample collection	<i>2014</i>	IDA
MIGS-4.1	Latitude	<i>50.64 N</i>	NAS
MIGS-4.2	Longitude	<i>6.88 E</i>	NAS
MIGS-4.4	Altitude	<i>170 meter</i>	NAS

<sup>a</sup>Evidence codes - IDA: Inferred from Direct Assay; TAS: Traceable Author Statement (i.e., a direct report exists in the literature); NAS: Non-traceable Author Statement (i.e., not directly observed for the living, isolated sample, but based on a generally accepted property for the species, or anecdotal evidence). These evidence codes are from the Gene Ontology project (Euzéby 2010).

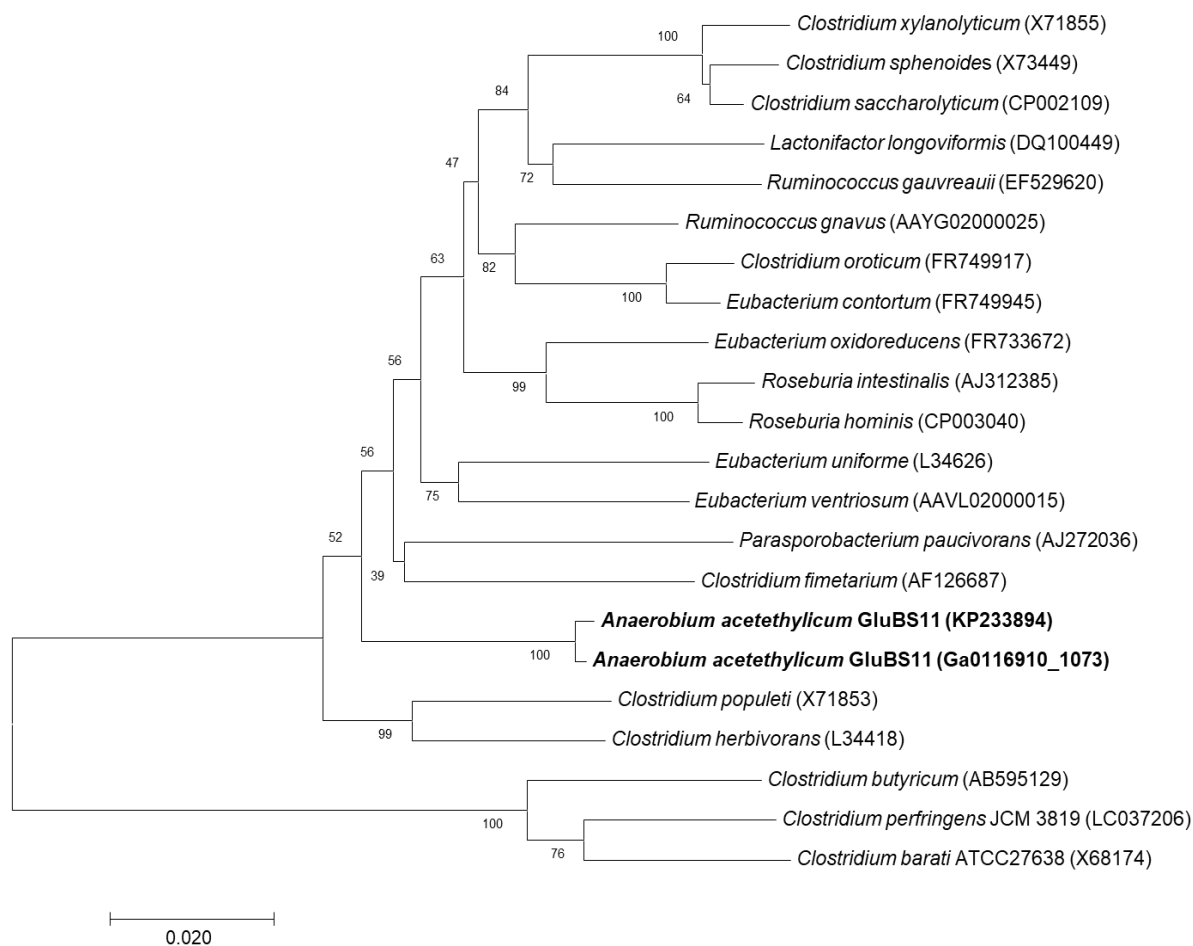


**Figure 2.** Phylogenetic tree constructed using MEGA 7 (Kumar et al., 2016) showing the current position of the *A. acetethylicum* strain GluBS11<sup>T</sup> with respect to the selected members from the order *Clostridiales*. The evolutionary distances were computed using the Jukes-Cantor method (Jukes and Cantor, 1969) and are in the units of the number of base substitutions per site. The phylogenetic tree was searched using the Close-Neighbor-Interchange algorithm (Skerman et al., 1980) at a search level of 1. All positions containing gaps and missing data were eliminated. There were a total of 1,300 positions in the final dataset. Numbers at the nodes indicates the bootstrap values from 1,000 replicates (Ashburner et al., 2000) and accession numbers are given in parentheses. Bar indicates 2% estimated sequence divergence.

---

**Table 2.** Project information.

MIGS ID	Property	Term
MIGS 31	Finishing quality	High-quality-draft
MIGS-28	Libraries used	An Illumina 300 bp insert standard shotgun (AZHBB)
MIGS 29	Sequencing platforms	Illumina HiSeq 2500-1TB
MIGS 31.2	Fold coverage	336.0X
MIGS 30	Assemblers	SPAdes
MIGS 32	Gene calling method	Prodigal
	Locus Tag	BJR36
	Genbank ID	FMKA00000000
	GenBank Date of Release	September 23, 2016
	GOLD ID	Gp0139288
	BioProject	PRJEB15475
	MIGS 13	Source Material Identifier
	Project relevance	Sugar and glycerol fermenting bacterium

---

## 4.2 Growth conditions and genomic DNA preparation

*A. acetethylicum* strain GluBS11<sup>T</sup> was cultivated in anoxic mineral medium supplemented with 10 mM gluconate as growth substrate at 30°C for three days until OD<sub>600nm</sub> 1.0 was reached. Genomic DNA was isolated from the cell pellet obtained from about 500 ml of grown culture using a CTAB-based method (Porebski et al., 1997) with slight modifications (Junghare et al., 2015). After RNase treatment, the purity and quality of the genomic DNA preparation were assessed by DNA absorption at 260nm and size by agarose gel electrophoresis (1% w/v; Fig. S1). The concentration of the isolated genomic DNA was 2.4 µg µl<sup>-1</sup> (A<sub>260/280</sub>= 2.03 and A<sub>260/230</sub>=2.47). Finally, the DNA was used to amplify the 16S rRNA gene to confirm the identity of genomic DNA by comparing with the described partial 16S rRNA gene sequence (KP233894) of *A. acetethylicum* strain GluBS11<sup>T</sup>. The pure and high-quality genomic DNA was shipped to the DOE, JGI for genome sequencing.

---

### **4.3 Genome sequencing and assembly**

The draft genome sequencing was performed at the DOE, JGI using the Illumina technology (Bennett and Solexa, 2004). An Illumina 300 bp insert standard shotgun library was constructed and sequenced using the Illumina HiSeq-2500 1TB platform, which generated 11,508,336 reads totaling 1,726.3 Mbp. All details on library construction and sequencing performed at the JGI can be found on the website. All raw Illumina sequence data were filtered using BBDuk (Bushnell), which removes known Illumina artifacts and PhiX. Reads with more than one “N” or with quality scores (before trimming) averaging less than 8 or reads shorter than 51 bp (after trimming) were discarded. Remaining reads were mapped to masked versions of human, cat and dog references using BMap (Bushnell) and discarded if the identity exceeded 95%. Sequence masking was performed with BMask (Bushnell). The following steps were performed for assembly: (1) artifact filtered Illumina reads were assembled using the SPAdes genome assembler ((version 3.6.2); 33), (2) assembly contigs were discarded if their length was <1 kbp. Parameters for the SPAdes assembly were -cov-cutoff auto -phred-offset 33 -t 8 -m 40 -careful -k 255,595 -12. The final draft assembly contained 108 contigs in 105 scaffolds, totaling 4.609 Mbp in size, and was based on 1,500.0 Mbp of Illumina data with a mapped coverage of 336.0X.

### **4.4 Genome annotation**

Genes were identified with Prodigal (Hyatt et al., 2010) using standard microbial genome annotation pipeline (Huntemann et al., 2015). The predicted CDSs were translated and used to search the NCBI non-redundant database, UniProt, TIGRFam, Pfam, KEGG, COG, and InterPro databases. The tRNAScanSE tool (Lowe et al., 1996) was used to find tRNA genes, whereas rRNA genes were found by searches against models of the rRNA genes built from SILVA (Pruesse et al., 2007). Other non-coding RNAs such as the RNA components of the protein secretion complex and the RNase P were identified by searching the genome for the corresponding Rfam profiles using INFERNAL (Nawrocki et al., 2013). Additional gene prediction analysis and manual functional annotation (IMG taxon ID 2675903067) were performed within the Integrated Microbial Genomes-Expert Review (IMG-ER) platform (Markowitz et al., 2009) developed by the JGI, Walnut Creek, CA, USA.

---

## 4.5 Genome Properties

The draft genome sequence of *A. acetethylicum* strain GluBS11<sup>T</sup> was based on an assembly of 105 DNA scaffolds (108 contigs) amounting to 4,609,043 (4.6 Mb) nucleotide base pairs with a calculated G+C content of 43.51 %mole (Table 3). Of the total of predicted CDSs of 4,132 genes (100%), 4,008 were assigned to protein-coding genes, of which 2,640 were assigned to COGs (63.89%), and the rest of 124 were assigned to RNA genes (3.0%). The majority of protein-coding genes (3,141 genes or 76.02%) were assigned to putative functions whilst the remaining genes were annotated as hypothetical proteins of unknown function. The draft genome properties, the statistics and the distribution of genes into COGs functional categories are summarized in Table 3 and Table 4. The draft genome comparison of *A. acetethylicum* strain GluBS11<sup>T</sup> using the BLASTn revealed top hits with the genomes of *C. nexile* DSM 1787<sup>T</sup> (85% identity; NZ\_DS995342.4), *Anaerostipes hadrus* DSM 3319<sup>T</sup> (85%; NZ\_KB290653.1), *Acetonema longum* DSM 6540<sup>T</sup> (84%; NZ\_AFGF01000168.1), *Anaerostipes caccae* DSM 14662<sup>T</sup> (83%; NZ\_DS499733.1), *Blautia hansenii* DSM 20583<sup>T</sup> (83%; NZ\_GG698589.1), and a ruman-associated strain, *Ruminococcus torques* ATCC 27756<sup>T</sup> (82%; NZ\_DS264349.1), and *C. phytofermentans* ATCC 700394<sup>T</sup> (74%), respectively.

## 5. Insights from the genome sequence

### 5.1 General metabolic features

The draft genome of strain GluBS11<sup>T</sup> was further examined to understand the organism's physiology and fermentation metabolism. The draft genome encodes most of the key enzymes of the pentose phosphate pathway, Embden-Meyerhoff-Parnas pathway, Entner-Doudoroff pathway and tricarboxylic acid cycle (Table S1). Thus, strain GluBS11<sup>T</sup> is very likely to use these pathways for its central metabolism and biosynthesis. Besides this, the genome also contains the genes coding for putative enzymes of anaplerotic pathways, such as oxaloacetate decarboxylase ( $\alpha$ -subunit, Ga0116910\_1001318 and  $\beta$ -subunit, Ga0116910\_1001319), pyruvate kinase (Ga0116910\_1001611), fructose-1,6-bisphosphatase (Ga0116910\_1001181 and 10346), phosphoenolpyruvate carboxykinase (Ga0116910\_1001300) and pyruvate carboxylase  $\beta$ -subunit (Ga0116910\_101716). Genes for biosynthesis of amino acids and most co-factors were also present (Table S1).

---

Although cells of strain GluBS11<sup>T</sup> are non-motile (Patil et al., 2015), the genome possesses genes that are predicted to encode flagellum components (Ga0116910\_1001565, Ga0116910\_1002133- Ga0116910\_1002135, Ga0116910\_100329, Ga0116910\_1002133- Ga0116910\_1002135) such as flagellar protein FliO/FliZ, flagellar motor switch protein FliN/FliY/FliM, flagellar FliL protein, and pilus assembly-protein (Flp/PilA), which are located in a single gene cluster (locus tag Ga0116910\_100336 to Ga0116910\_100363), including the chemotaxis protein (MotB/A). The draft genome also contains genes predicted to encode seven universal stress proteins of the UspA family (gene loci Ga0116910\_103114, 1003225, 10025, 10028, 10027, 104111 and 100540), 2 heat-shock proteins such as GrpE (Ga0116910\_10476 and 100386), one heat-inducible transcriptional repressor (Ga0116910\_100387), and six cold-shock proteins of the CspA family (Ga0116910\_10067, 1002200, 1001175, 1004187, 1005160 and 1002190). Also a DNA-directed RNA polymerase with sigma-70/32 factor (ECF family) and a heat-inducible transcriptional repressor (HrcA) along with the RNA polymerase sigma factor for flagellar operon FliA were detected in the draft genome.

Clustered regularly interspaced short palindromic repeats (CRISPRs) are segments of prokaryotic DNA containing short repetitions of base sequences followed by a short segment of ‘spacer DNA’ that function as a defense system against the introduction of foreign genetic materials (e.g., phage infection, plasmid or horizontal gene transfer). CRISPRs were found in approximately 40% of all sequenced bacterial genomes (Grissa et al., 2007). Genome analysis of strain GluBS11<sup>T</sup> suggests that the genome does not contain CRISPR regions, although the genome of the phylogenetically closely related strain *C. populeti* ATCC 35295<sup>T</sup> contains two gene coding for CRISPR-associated proteins (cas9 family protein; Ga0056054\_02523 and Ga0056054\_00025).

---

**Table 3.** Genome statistics.

Attribute	Value	% of Total
Genome size (bp)	4,609,043	100
DNA coding (bp)	4,001,559	86.82
DNA G+C (bp)	2,005,619	43.51
DNA scaffolds	105	100
Total genes	4,132	100
Protein coding genes	4,008	97.00
RNA genes	124	3.00
Pseudo genes	867	20.98
Genes in internal clusters	1,252	30.30
Genes with function prediction	3,141	76.02
Genes assigned to COGs	2,633	63.72
Genes with Pfam domains	3,303	79.94
Genes with signal peptides	186	4.50
Genes with transmembrane helices	984	23.81
CRISPR repeats	0	0

---

The total is based on either the size of the genome in the base pairs or the total numbers of proteins coding genes in the annotated genome of *A. acetethylicum* GluBS11<sup>T</sup>.

---

**Table 4.** Number of genes associated with general COG functional categories.

Code	Value	%age	Description
J	199	6.69	Translation, ribosomal structure and biogenesis
A	-	-	RNA processing and modification
K	284	9.55	Transcription
L	121	4.07	Replication, recombination and repair
B	-	-	Chromatin structure and dynamics
D	32	1.08	Cell cycle control, Cell division, chromosome partitioning
V	57	1.92	Defense mechanisms
T	165	5.55	Signal transduction mechanisms
M	120	4.03	Cell wall/membrane biogenesis
N	63	2.12	Cell motility
U	43	1.45	Intracellular trafficking and secretion
O	89	2.99	Posttranslational modification, protein turnover, chaperones
C	174	5.85	Energy production and conversion
G	539	18.12	Carbohydrate transport and metabolism
E	224	7.53	Amino acid transport and metabolism
F	88	2.96	Nucleotide transport and metabolism
H	135	4.54	Coenzyme transport and metabolism
I	86	2.89	Lipid transport and metabolism
P	111	3.73	Inorganic ion transport and metabolism
Q	47	1.58	Secondary metabolites biosynthesis, transport and catabolism
R	233	7.83	General function prediction only
S	124	4.17	Function unknown
-	1,499	36.28	Not in COGs

The total is based on the total number of protein coding genes predicted in the genome of *A. acetethylicum* strain GluBS11<sup>T</sup>. – no data available.

---

## 5.2 Transporters

Transporters enable bacteria to accumulate required nutrients and also contribute for excretion of unwanted metabolic products. They also help to maintain the osmotic balance and the cytoplasmic pH by transporting H<sup>+</sup> and various salts. Genome analysis of strain GluBS11<sup>T</sup> identified various membrane transporters including the ABC solute transporters (ATP-dependent) that could take part in the transport of various substrates such as ions, vitamins, sugars, amino acids, and metabolites (Table S2). Most of these identified transporters belong to diverse transporter families such as the amino acid/polyamine antiporter (APA) family, the drug/metabolite transporter (DMT) superfamily, and the major facilitator superfamily (MFS) that is used for transport of a diverse set of small solutes in response to chemiosmotic ion gradients (González et al., 2008). The draft genome sequence also contains several genes coding for proton symporters (Table S2). Thus, strain GluBS11<sup>T</sup> could generate a proton gradient using FoF<sub>1</sub>-type ATP synthase in reverse direction (Grupe et al., 1992, Al-Awqati 1986).

## 5.3 Metabolic pathways for glucose, gluconate and glycerol utilization

Strain GluBS11<sup>T</sup> ferments sugars, e.g., glucose and gluconate or glycerol mainly to ethanol and hydrogen, including the production of acetate and small amounts of formate as fermentation end products (Patil et al., 2015, Patil et al., 2017). In the present study, a metabolic network for the utilization of glucose and gluconate including glycerol was constructed based on the genome as shown in Figure 3, from the genome annotation provided by the IMG-ER. To determine which pathway was utilized for glycerol fermentation, a recent study by Patil et al., (Patil et al., 2017) provided insight into glycerol fermentation of strain GluBS11<sup>T</sup> using biochemical and proteomic approaches. There are three possible alternatives for gluconate metabolism: first, the phosphorylation to gluconate 6-phosphate (the Entner-Doudoroff pathway), second, the reduction to glucose or lastly, the dehydration to 2-keto-3-deoxy-gluconate ((KDG, modified Entner-Doudoroff pathway); Ramachandran et al., 2006). In the last four decades, several studies reported that gluconate fermentation by numerous anaerobic bacteria, e.g., *Clostridium acetivum* DSM 1496<sup>T</sup> (Andreesen, et al., 1969) or *E. coli* ML30 (DSM 1328<sup>T</sup>) (Eisenberg and Dobrogosz, 1967) proceeds through a modified Entner-Doudoroff pathway.

---

The genome annotation predicted the presence of four gluconate:proton symporters (Gnt family) encoded by Ga0116910\_10413, Ga0116910\_10069, Ga0116910\_100214 and Ga0116910\_10418. In a previous study, it was shown that *C. acetobutylicum* ATCC 824<sup>T</sup> takes up gluconate by gluconate:proton symporters ((CA\_C2835); Servinsky et al., 2014) which showed amino acid sequence identity (24 to 41%) with the four predicted genes with highest identity (Ga0116910\_10418; 42%). Thus, the product of the Ga0116910\_10418 gene is the most likely candidate for uptake of gluconate. Based on the genome annotation, *A. acetethylicum* strain GluBS11<sup>T</sup> most likely uses the Entner-Doudoroff pathway for gluconate metabolism, through which gluconate is first phosphorylated to 6-phosphogluconate by gluconokinase (EC 2.7.1.12) followed by dehydration to 2-keto-3-deoxy-phosphogluconate (KDPG) by 6-phosphogluconate dehydratase (EC 4.2.1.12). Alternatively, gluconate could be first dehydrated (modified Entner-Doudoroff pathway) to 2-keto-3-deoxy gluconate (KDG) by gluconate dehydratase (EC 4.2.1.39) followed by phosphorylation to KDPG by 2-keto-3-deoxygluconokinase (EC 2.7.1.45). KDPG would be further converted to pyruvate and glyceraldehyde 3-phosphate by KDPG aldolase (EC 4.1.2.14). The presence of a putative gene coding for KDPG aldolase (Ga0116910\_101517) indicates that gluconate is most likely metabolized *via* KDPG. However, no putative genes coding for the initial enzymes that could convert gluconate to KDPG (according to two ways as mentioned above) was identified in the draft genome of strain GluBS11<sup>T</sup>. However, two putative genes were annotated as dihydroxy acid dehydratase/phosphogluconate dehydratase (Ga0116910\_10068 and Ga0116910\_101679) that could have this activity. The predicted dihydroxy acid dehydratase (EC 4.2.1.9) is possibly involved in the biosynthesis of amino acids (valine, isoleucine, and isoleucine). A similar observation was also reported for the gluconate-fermenting *C. acetobutylicum* ATCC 824<sup>T</sup>, where the gene CA\_C3170 was predicted to encode a 6-phosphogluconate dehydratase and BlastP analysis indicated that it is a dihydroxy acid dehydratase primarily involved in the synthesis of amino acids (Servinsky et al., 2014, Altschul et al., 1990). BlastP search of amino acid sequence analysis of genes Ga0116910\_10068 and Ga0116910\_101679 showed more than 80% identity with the dihydroxy acid dehydratase of *C. phytofermentans* ATCC 700394<sup>T</sup> (A9KL28) and *Anaerostipes caccae* DSM 14662<sup>T</sup>, respectively, and showed only 40-60% identity with gene CA\_C3170 of *C. acetobutylicum* ATCC 824<sup>T</sup>. Therefore, genes Ga0116910\_10068 and Ga0116910\_101679 most likely encode a dihydroxy acid dehydratase that is involved in

---

amino acid synthesis rather than in KDPG formation. Based on this information, gluconate degradation *via* the Entner-Doudoroff pathway involving gluconate phosphorylation to 6-phosphogluconate by gluconokinase (EC 2.7.1.12) followed by dehydration to KDPG by 6-phosphogluconate dehydratase (EC 4.2.1.12) can be ruled out. Furthermore, the presence of a putative gene coding for KDPG aldolase (Ga0116910\_101517) indicates that gluconate is most likely metabolized via the modified Entner-Doudoroff pathway, which would be consistent with previous studies of the anaerobic gluconate metabolism (Andreesen and Gottschalk, 1969, Servinsky et al., 2014, Bender et al., 1971). Even though no genes coding for the gluconate dehydratase (EC 4.2.1.39) and KDG kinase (EC 2.7.1.178) required for initial activation of gluconate to KDPG were identified in the genome of strain GluBS11<sup>T</sup>.

While gluconate is predicted to be metabolized via the modified Entner-Doudoroff pathway, glucose could be metabolized through glycolysis. For uptake of glucose, strain GluBS11<sup>T</sup> most likely uses a phosphotransferase system (PTS) which couples glucose import to its phosphorylation with phosphoenolpyruvate, yielding glucose-6-phosphate and pyruvate (Servinsky et al., 2014). Genes Ga0116910\_100991 and Ga0116910\_100370 are predicted to encode PTS proteins which are most likely involved in glucose transport in strain GluBS11<sup>T</sup>. Thus, genome analysis suggests that glucose is most probably metabolized through glycolysis *via* glucose 6-phosphate by glucose-6-phosphate isomerase (Ga0116910\_1004120 and Ga0116910\_10539), 6-phosphofructokinase (Ga0116910\_103531, Ga0116910\_100239, Ga0116910\_102039 and Ga0116910\_101135), and fructose-bisphosphate aldolase (Ga0116910\_101128 and Ga0116910\_102024) to glyceraldehyde 3-phosphate. In the glycolysis pathway, glyceraldehyde 3-phosphate is further metabolized through the lower part of glycolysis to ethanol, acetate, hydrogen, and formate. During gluconate fermentation, KDPG aldolase would then convert KDPG to glyceraldehyde-3-phosphate and pyruvate, and only glyceraldehyde-3-phosphate passes through the lower glycolysis pathway.

Previous studies with other bacteria reported that gluconate fermentation mainly yielded acetate and butyrate as fermentation products (Andreesen and Gottschalk, 1969, Servinsky et al., 2014, Bender et al., 1971). Although, the draft genome of strain GluBS11<sup>T</sup> contains genes predicted to code for a putative butyrate kinase (Ga0116910\_101723 and Ga0116910\_102110), gluconate, glucose or glycerol fermentation by strain GluBS11<sup>T</sup> does not produce butyrate (Patil et al., 2015, Patil et al., 2017). The pathways were easily

---

constructed based on the genome analysis and genes for acetate metabolism, e.g., acetate kinase (Ga0116910\_103636, Ga0116910\_1001586 and Ga0116910\_104214), ethanol metabolism, e.g., alcohol hydrogenase (Ga0116910\_101528, Ga0116910\_102038, Ga0116910\_102215, Ga0116910\_1004154 and Ga0116910\_102016), and hydrogen metabolism, e.g., putative iron-only hydrogenases and subunits coding for an NADP<sup>+</sup>-reducing hydrogenase (Ga0116910\_1001473, Ga0116910\_1001466, Ga0116910\_1001467, Ga0116910\_1001468, Ga0116910\_1001470, Ga0116910\_100545 and Ga0116910\_1001473). No candidate gene was found to code for a putative formate-producing formate dehydrogenase in the draft genome of strain GluBS11<sup>T</sup> even though formate dehydrogenase activities were detected in cell-free extracts using benzyl viologen as an artificial electron acceptor (Patil et al., 2017). On the other hand, genes annotated as pyruvate:formate lyase or formate C-acetyltransferase were identified in the genome (Ga0116910\_1004109, Ga0116910\_100860, Ga0116910\_102934 and Ga0116910\_102935), but no activity for a possible pyruvate:formate lyase could be detected (Patil et al., unpublished results). This indicates that the genomic information is sometimes insufficient to predict metabolic pathways. Thus, further biochemical and proteomics studies would be needed to investigate and confirm the gluconate and glucose fermentation pathway utilized by this bacterium.

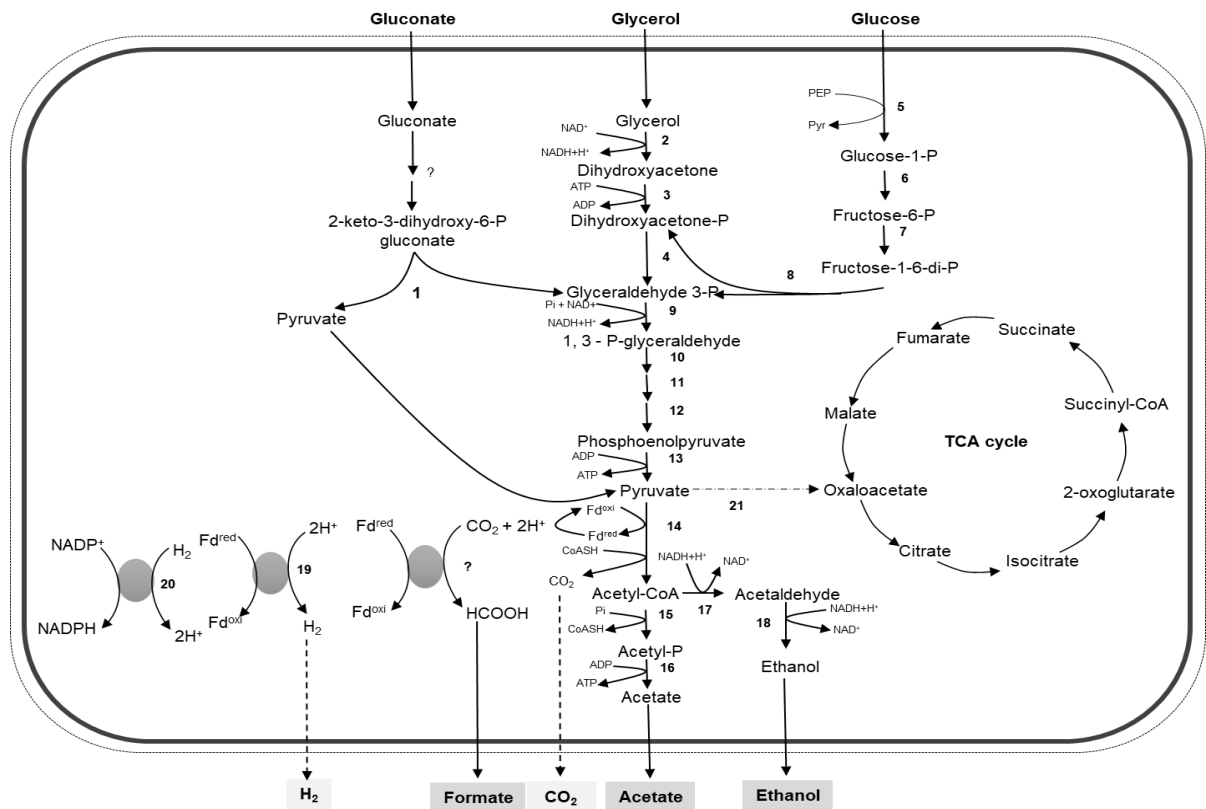


**Figure 3.** Metabolic network of glucose and gluconate, including glycerol (Patil et al., 2017) metabolism by *A. acetethylicum* strain GluBS11<sup>T</sup> reconstructed from the IMG annotated draft genome sequence. Numbers adjacent to arrows represent putative enzymes. 1) 2-keto-3-deoxphosphogluconate (KDPG) aldolase (locus tag, Ga0116910\_101517); 2) glycerol dehydrogenase (Ga0116910\_101526 and 101551); 3) dihydroxyacetone kinase (Ga0116910\_1001186, 1001188, 101527, 101552 and 101085); 4) triosephosphate isomerase (Ga0116910\_1001390, 102914, 101435 and 101134); 5) phosphotransferase system (PTS; Ga0116910\_100991 and Ga0116910\_100370); 6) phosphogluconomutase (Ga0116910\_1007105, 10644, 1002181 and 10031112); 7) phosphofructokinase (Ga0116910\_100239); 8) fructose 1, 6-bisphosphate aldolase (Ga0116910\_100167); 9) glyceraldehyde 3-phosphate dehydrogenase (Ga0116910\_1001391); 10) phosphoglycerate kinase (Ga0116910\_1001391); 11) phosphoglycerate mutase (Ga0116910\_1001389 and Ga0116910\_103027); 12) enolase (Ga0116910\_1001503); 13) pyruvate kinase (Ga0116910\_1004153); 14) pyruvate ferredoxin oxidoreductase (Ga0116910\_103224 and Ga0116910\_101718); 15) phosphoacetyl transferase (Ga0116910\_1001587); 16) acetate kinase (Ga0116910\_1001586); 17) CoA-dependent acetaldehyde dehydrogenase (Ga0116910\_1004188); 18) alcohol dehydrogenase (Ga0116910\_101528 and 101313); 19) iron-only hydrogenases (Ga0116910\_100545, Ga0116910\_1001473 and Ga0116910\_100543); 20) NADP-reducing hydrogenases (Ga0116910\_1001466, Ga0116910\_1001467, Ga0116910\_1001468, Ga0116910\_1001470) and 21) putative pyruvate carboxylase (Ga0116910\_101716).

---

## 5.5 Microcompartments and fucose utilization

The genome of *A. acetethylicum* strain GluBS11<sup>T</sup> harbors five genes that putatively code for bacterial microcompartment shell proteins (BMCs). Four of these genes are annotated as “BMC-domain-containing protein” (Ga0116910\_1005148, Ga0116910\_1005149, Ga0116910\_1005150 and Ga0116910\_1005151), and one gene is annotated as “Carboxysome shell and ethanolamine utilization microcompartment protein CcmL/EutN” (Ga0116910\_1005155). Microcompartments are protein complexes that form discrete spaces within the cell, thus enabling enzyme reactions that either produce toxic intermediates or require accumulation of a certain metabolite, e.g., the ethanolamine utilization microcompartment in *Salmonella typhimurium* ATCC 13311<sup>T</sup> or the carboxysomes in cyanobacteria (Garsin, 2010, Rae et al., 2013). An IMG gene search for microcompartments and subsequent comparison to other genomes using the IMG Gene Ortholog Neighborhoods viewer, revealed that the microcompartment genes in *A. acetethylicum* strain GluBS11<sup>T</sup> are located in a putative operon that also contains genes associated with fucose utilization in *Clostridium phytofermentans* ATCC 700394<sup>T</sup> (52). Fucose, a deoxyhexose derived from plant biomass degradation, can be fermented to propionate, propanol, mixed acids, and ethanol by *C. phytofermentans* ATCC 700394<sup>T</sup>, and the responsible genes are located in two different operons in this organism (Petit et al., 2013). Initially, fucose is converted to fuculose-phosphate by fucose mutarotase, fucose isomerase and fucose kinase ((Cphy\_3153 – Cphy\_3155); Petit et al., 2013). Likewise, the orthologs in *A. acetethylicum* strain GluBS11<sup>T</sup> are located in a similar operon (L-fucose isomerase Ga0116910\_100812, rhamnulokinase/L-fuculokinase Ga0116910\_100813 and L-fucose mutarotase Ga0116910\_100815). Fuculose-phosphate is then further degraded to lactaldehyde and dihydroxyacetone-phosphate by fuculose-phosphate aldolase (Ga0116910\_102223 in *A. acetethylicum* strain GluBS11<sup>T</sup>, Cphy\_1177 in *C. phytofermentans*). Dihydroxyacetone phosphate can then be processed through glycolysis, while lactaldehyde is reduced to 1,2-propanediol with NADH. 1,2-propanediol is then disproportionated in microcompartments to propionate and propanol by 1,2-propanediol oxidoreductase (Cphy\_1185, Ga0116910\_1005154), 1,2-propanediol dehydratase (Cphy\_1174, Ga0116910\_100557 - Ga0116910\_100559 in a different area of the genome), propionaldehyde dehydrogenase (Cphy\_1178, Ga0116910\_1005146), phosphate propanoyl transferase (Cphy\_1183, Ga0116910\_1005152), acetate/propionate kinase (Cphy\_1327, Ga0116910\_104214, Ga0116910\_1001586, or Ga0116910\_103636) and

---

propanol dehydrogenase (Cphy\_1179, Ga0116910\_1005147). Rhamnose can be degraded in a similar way by *C. phytofermentans* ATCC 700394<sup>T</sup>, and the respective genes leading to lactaldehyde and dihydroxyacetone-phosphate were also identified in the genome of *A. acetethylicum* strain GluBS11<sup>T</sup> (L-rhamnose mutarotase Ga0116910\_10513, L-rhamnose isomerase Ga0116910\_1001301, rhamnulokinase/L-fuculokinase Ga0116910\_100813); Petit et al., 2013). However, earlier results demonstrated that rhamnose cannot be utilized by *A. acetethylicum* strain GluBS11<sup>T</sup> (Petit et al., 2013). Even though the genes for fucose degradation are present in the genome, it is still doubtful whether this sugar can serve as a growth-supporting substrate for strain GluBS11<sup>T</sup>.

## 6. Conclusions

Taken together, the draft genome sequence of *A. acetethylicum* strain GluBS11<sup>T</sup> expands our view on the metabolic capacities of this sugars and glycerol-fermenting bacterium. The genome sequence gives us insights into the putative enzymes involved in the pathway of glucose and gluconate (including glycerol) fermentation, and provides a brief summary of the key reactions involved. Lastly, the hypotheses concerning the glucose and gluconate fermentation pathways based on genomic data are still preliminary, and additional biochemical and functional proteomic studies will be necessary for confirmation and further insights.

## Competing interests

All authors declare no competing interest.

## Funding

During this research YP was funded by a LGFG scholarship. The genome sequencing was performed under the auspices of the US Department of Energy's Office of Science, Biological and Environmental Research Program, and by the University of California, Lawrence Berkeley National Laboratory under contract No. DE-AC02-05CH11231.

---

### **Authors' contributions**

YP, MJ, NM and BS initiated the project and YP performed DNA preparation. MJ and YP performed the comparative genomics, investigated the genome for general metabolic features and fermentation pathways. MJ, YP and NM drafted the manuscript that was critically reviewed and corrected by BS, NM, WW, NS and NK, respectively. Marcel Huntemann, Alicia Clum, Manoj Pillay, Krishnaveni Palaniappan, Neha Varghese, Natalia Mikhailova, Dimitrios Stamatis, T.B.K. Reddy, Chris Daum, Natalia Ivanova, and Tanja Woyke performed the technical work for sequencing, assembly and annotation of the genome. All authors read and approved the final manuscript.

### **Acknowledgements**

YP thanks the LGFG scholarship funding program of the University of Konstanz for providing scholarship during this research work. The authors appreciate the service of the Electron Microscopy Center of the University of Konstanz.

---

## Supplementary information

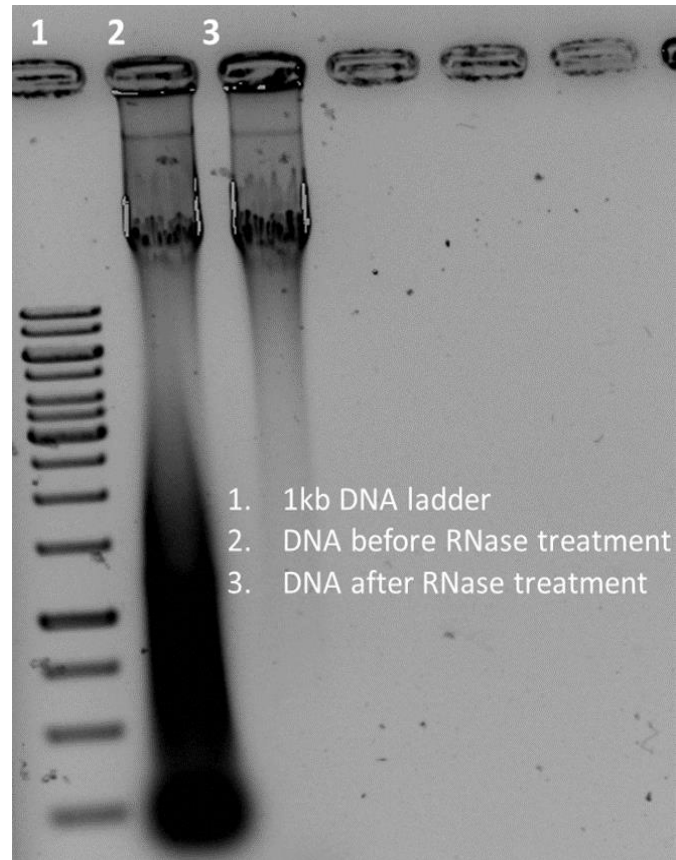


**Figure S1.** Gel electrophoresis of genomic DNA isolated from GluBS11<sup>T</sup> cells grown with gluconate.

**Table S1.** IMG annotated functions of selected putative key enzymes involved in the metabolic pathways identified in the draft genome sequence of *A. acetethylicum* strain GluBS11<sup>T</sup>.

Main pathways	Key enzymes identified	Gene loci (Ga0116910_ )
Glycolysis	Phosphofructokinase	100239
	Fructose 1, 6-biphosphate aldolase	101258
	Pyruvate kinase	100167
Pentose phosphate pathway	Gluconolactonase	1001376
	Ribulose-5-phosphate 3-epimerase	100910, 10099, 103543
	Transketolase	10533, 103542
	Transaldolase	101534
ED pathway	2-keto-3-deoxphosphogluconate aldolase	101517
TCA cycle	Malate dehydrogenase	103828
	Citrate synthase	1001297
	Aconitase	1004146
	Fumarate hydratase $\alpha\beta$ subunit	1004208, 100771, 100772, 1004209
		1001415
	Isocitrate dehydrogenase (NAD <sup>+</sup> )	1005157, 103224, 101718
	Pyruvate-ferredoxin/flavodoxin oxidoreductase	1001318
	Oxaloacetate decarboxylase, alpha subunit	101716
Anaplerotic pathway	Pyruvate carboxylase subunit B	101716
	Oxaloacetate decarboxylase, alpha subunit	1001318
	Malate dehydrogenase (malic enzyme)	1002215
Amino acid metabolism	Tryptophan synthase, alpha chain	1005144
	Tryptophan synthase beta chain/phosphoribosyl anthranilate isomerase	1005143
	Anthranilate phosphoribosyl transferase	10594
	Phosphoribosyl anthranilate isomerase	1005142
	Histidinol dehydrogenase	1001211
	Histidyl-tRNA synthetase	1008100
	Glutamine amido transferase	1001617
	Dihydroxy-acid dehydratase	10068
	Threonine synthase	1001330
	Threonine dehydratase	1001578
Lipid metabolism	L-threonine aldolase	10256
	Glycerol kinase	1005138, 104021
	glycerol-3-phosphate acyltransferase PlsX, PlsY	1001583, 1001559
Glycerol metabolism	Diacylglycerol kinase (ATP)	1001177, 101168
	Glycerol dehydrogenase	101526, 101551
Acetate metabolism	Dihydroxyacetone kinase	101527
	Phosphoacetyl transferase	1001587
Ethanol metabolism	Acetate kinase	1001586
	Alcohol dehydrogenase	101528, 101313
	Phosphoacetyl transferase	1001587

**Table S2.** Putative transporters identified in the draft genome of *A. acetethylicum* GluBS11<sup>T</sup>.

<b>Locus tag</b>	<b>IMG annotated putative function</b>
Ga0116910_	
100948 and 1003216	F-type H <sup>+</sup> -transporting ATPase β subunit
100946 and 1003223	F-type H <sup>+</sup> -transporting ATPase α subunit
100947 and 1003224	F-type H <sup>+</sup> -transporting ATPase γ subunit
100949	F-type H <sup>+</sup> -transporting ATPase ε subunit
100941 and 1003220	F-type H <sup>+</sup> -transporting ATPase α subunit
100944	F-type H <sup>+</sup> -transporting ATPase β subunit
1003222	ATP synthase, F <sub>0</sub> β subunit
100945	F-type H <sup>+</sup> -transporting ATPase β subunit
1003221	F-type H <sup>+</sup> -transporting ATPase c subunit
1001457	basic amino acid/polyamine antiporter, APA family
101710	Threonine/homoserine efflux transporter RhtA
1001459, 1001490, 101535, 101643	Permease of the drug/metabolite transporter (DMT) superfamily
1001465, 101045 1001610	Formate/nitrite transporter FocA, FNT family Succinate-acetate transporter protein
101480	Energy-coupling factor transport system permease protein
101478, 101479	Energy-coupling factor transporter ATP-binding protein EcfA2
1004161	Energy-coupling factor transporter transmembrane protein EcfT
101945, 10248, 101156	zinc transporter, ZIP family/zinc and cadmium transporter cation diffusion facilitator family transporter
1001613, 101280 1004168	magnesium transporter
1001353	metal ion transporters
101328	MFS transporter, UMF1 family
100689	MFS-type transporter involved in bile tolerance, Atg22 family
1001269	MFS transporter, DHA3 family, macrolide efflux protein
101142, 101141, 1001269	sulfate permease, SulP family
10648, 100776, 103213	Na <sup>+</sup> /melibiose symporter or related transporter
102731, 102841	Glycoside/pentoside/hexuronide:cation symporter, GPH family/probable glucitol
10279, 101232, 1003206, 100796	transport protein GutA
100186, 10275	Probable glucitol transport protein GutA
1001150, 1005134	ATPase components of ABC transporters with duplicated ATPase domains
10308	ATP-binding cassette, subfamily F, member 3
100156, 101276	Di- and tricarboxylate transporter
100698	lincosamide and streptogramin A transport system ATP-binding/permease protein
1001413	ATP-binding cassette, subfamily F, member 3
102822	
102820	Putative tricarboxylic transport membrane protein  Tripartite-type tricarboxylate transporter, receptor component TctC
1005156, 100912	Biotin transport system substrate-specific component

# CHAPTER 3

---

## **Fermentation of glycerol by *Anaerobium acetethylicum* and its potential use in biofuel production**

**Yogita Patil**, Madan Junghare, Nicolai Müller

Published in *Microbial Biotechnology* (2017), 10 (1), 203 – 217.

---

## 1. Abstract

Growth of biodiesel industries resulted in increased coproduction of crude glycerol which is therefore becoming a waste product instead of a valuable ‘coproduct’. Glycerol can be used for the production of valuable chemicals, e.g. biofuels, to reduce glycerol waste disposal. In this study, a novel bacterial strain is described which converts glycerol mainly to ethanol and hydrogen with very little amounts of acetate, formate and 1,2-propanediol as coproducts. The bacterium offers certain advantages over previously studied glycerol-fermenting microorganisms. *Anaerobium acetethylicum* during growth with glycerol produces very little side products and grows in the presence of maximum glycerol concentrations up to 1500 mM and in the complete absence of complex organic supplements such as yeast extract or tryptone. The highest observed growth rate of  $0.116 \text{ h}^{-1}$  is similar to that of other glycerol degraders, and the maximum concentration of ethanol that can be tolerated was found to be about 60 mM ( $2.8 \text{ g l}^{-1}$ ) and further growth was likely inhibited due to ethanol toxicity. Proteome analysis as well as enzyme assays performed in cell-free extracts demonstrated that glycerol is degraded via glyceraldehyde-3-phosphate, which is further metabolized through the lower part of glycolysis leading to formation of mainly ethanol and hydrogen. In conclusion, fermentation of glycerol to ethanol and hydrogen by this bacterium represents a remarkable option to add value to the biodiesel industries by utilization of surplus glycerol.

**Keywords:** Glycerol, bioethanol, biohydrogen, renewable energy, biodiesel, fossil fuels, proteomics, enzyme assays.

---

## 2. Introduction

Fossil fuels are the main source of energy being used worldwide and cover about 80% of the global energy demand (Sarma et al., 2012). Fossil fuels are limited, non-renewable and associated with many problems such as global warming, ecosystem imbalance and health hazards (da Silva et al., 2009). Therefore, there is a huge demand for alternative energy sources that are renewable, eco-friendly and sustainable to replace the conventional fossil fuels. Moreover, Campbell and Laherrere (1998) predicted that petroleum reserves will be completely depleted by 2050 (Nwachukwu et al., 2012). This concern has highlighted the future need for the use of biofuels such as ethanol, biodiesel, butanol, hydrogen or electricity produced from renewable plant biomass as one of the promising alternatives over fossil fuels (Elmekawy et al., 2013; Speers et al., 2014). Therefore, in recent years there has been a significant increase in the production and use of biofuels worldwide, such as biodiesel and bioethanol.

In the last decade, the European Union (EU) was the principal biodiesel producer which contributed about 82% of global biodiesel production (Demirbas and Balat, 2006). According to the European Biodiesel Board (EBB, 2006), the estimated production of biodiesel in 2005 was about 3.2 million tons with a production capacity of 6 million tons (da Silva et al., 2009), which has now increased to about 10.4 million tons in 2013 with a production capacity of 23 million tons. Germany is currently the largest producer and consumer of biodiesel in the EU, producing more than 2.5 million tons in 2013 (EBB, 2013; <http://www.ebb-eu.org/stats.php>). The top five global producers of biodiesel are Argentina, Brazil, France, Germany and the United States of America (Sarma et al., 2012).

Glycerol (1,2,3-propanetriol) is a simple trivalent alcohol that results from the natural degradation of the glyceride component of plant cell wall phospholipids or reserve lipids of plant seeds (Roger et al., 1992; Nwachukwu et al., 2013). It is produced in major amounts during trans esterification of vegetable oils and animal fats (Solomon et al., 1995; Barbirato et al., 1997a,b, 1998; Colin et al., 2001) and has wide applications in different industries such as food and drinks, toothpaste, cosmetics, toiletries, plastics, tobacco, pulp and paper, paint, leather and textile, pharmaceuticals and automotive (Choi, 2008; Nicol et al., 2012; Rossi et al., 2012). The economic value of industrial glycerol has decreased due to the surplus crude glycerol generated during biodiesel production, and it cannot be utilized directly in any

---

industrial applications due to the presence of impurities. Furthermore, it cannot be directly released into the environment without treatment as the cost of such treatment is not economical (Nwachukwu et al., 2013). Recently, fermentative conversion of crude glycerol into valuable products such as, e.g., bioethanol has gained interest for the development of biodiesel- producing industries, and also for replacing conventional carbohydrate sugars used in industrial microbial fermentation processes to convert it into a broad range of value- added organic products such as bioethanol (Dharmadi et al., 2006; Rossi et al., 2012).

Bioethanol is considered as an alternative to fossil fuels, as it is a renewable, bio-based resource, and provides the potential to reduce particulate emissions (Hansen et al., 2005). Several microorganisms produce ethanol as a natural fermentation end-product, sometimes even in a homo- ethanogenic type of fermentation (Otero et al., 2007). Bioethanol is one of the fermentation products that can be generated from glycerol via anaerobic fermentation, which is more economical than the use of corn or lignocellulosic biomass for bioethanol production (Choi, 2008). Moreover, the cost of ethanol produced from glycerol is about 40% lower than when it is produced from corn (Yazdani and Gonzalez, 2007).

Fermentation of glycerol most often leads to 1,3-propanediol as reduced end- product (Homann et al., 1990). *Escherichia coli* was shown to ferment glycerol anaerobically to ethanol, hydrogen and formate, thus providing a bioagent to produce value-added biofuel from glycerol (Dharmadi et al., 2006; Trchounian and Trchounian, 2015). Other microorganisms are able to perform similar fermentations of glycerol, especially several members of the genus *Clostridium* (Biebl, 2001). Also mixtures of microorganisms, e.g. buffalo slurry, were used to optimize hydrogen production from glycerol (Marone et al., 2015). The main problems with glycerol- fermenting bacteria are the accumulation of undesired by- products such as 2,3-butanediol or butyric acid, and the low tolerance of these strains towards solvents, i.e. glycerol and ethanol. The latter two dissolve cellular membranes at higher concentrations and are therefore lethal for any kind of microorganism. However, yeasts can tolerate ethanol concentrations up to about 120 g l<sup>-1</sup> (15% v/v; Lam et al., 2014), which is similar to some bacteria, e.g. *Zymomonas* sp. (Swings and De Ley, 1977).

Recently, an anaerobic bacterium representing the new genus *Anaerobium* within the order *Clostridiales* was enriched and isolated from sludge samples obtained from a biogas reactor at Odendorf, Germany. *Anaerobium acetethylicum* strain GluBS11<sup>T</sup> was originally described

---

for gluconate fermentation, but it grows also with glycerol under strictly anoxic conditions (Patil et al., 2015). Unlike many other members of the order *Clostridiales*, fermentation of glycerol by *A. acetethylicum* mainly produces ethanol and hydrogen and does not coproduce undesired by-products such as butyrate, 1,3-propanediol or 2,3-butanediol under any growth condition (Patil et al., 2015). In this study, we describe the optimum conditions for glycerol fermentation to ethanol and hydrogen by *A. acetethylicum* using pure glycerol at different concentrations and elucidate the biochemical reactions involved in anaerobic glycerol fermentation based on proteomics and *in vitro* enzyme assays. Based on our findings, we propose a glycerol fermentation pathway that mainly leads to ethanol and hydrogen and does not involve the formation of 1, 3-propanediol or 2,3-butanediol. Application of *A. acetethylicum* as a potential future candidate for bioethanol and biohydrogen production from glycerol is discussed in the context of the proposed pathway.

### 3. Results

#### 3.1 Anaerobic glycerol fermentation by *A. acetethylicum*

In strictly anaerobic growth experiments with *A. acetethylicum*, glycerol is fermented mainly to ethanol, hydrogen and small amounts of acetate, formate and propylene glycol (1,2-propanediol). In cultures with different initial concentrations of glycerol (10, 50, 100 and 200 mM added to cultures, actual concentrations 10.8, 48.7, 97.4 and 189.6 mM, respectively), the strain exhibited different lag phase periods which increased with increasing glycerol concentrations (Fig. 1A and B). Maximal growth rates ( $\mu_{max}$ ) observed in the exponential phase were 0.101, 0.116, 0.107 and 0.070 h<sup>-1</sup> at 10, 50, 100 and 200 mM of glycerol respectively (Fig. 1A). Growth was exponential within 28 and 44 h as shown in the half-logarithmic plot (Fig. 1A inset). After 44 h, growth was not exponential any more (Fig. 1A). At all tested glycerol concentrations, the strain consumed glycerol within 91–98 h of incubation and produced ethanol and hydrogen as major fermentation products, whereas the concentrations of formate, acetate and propylene glycol were comparatively low (Table 1). The maximum ethanol concentration produced after 91–98 h of incubation was about 38 mM when the cells were cultivated with 100 mM of initial glycerol (Fig. 2). In another growth experiment, final concentrations were measured after 166 h, i.e. when the cells were in late

stationary to decline phase, and the maximum average ethanol concentration observed was 62 mM at 100 mM of initial glycerol concentration (Fig. 2, growth curve not shown).

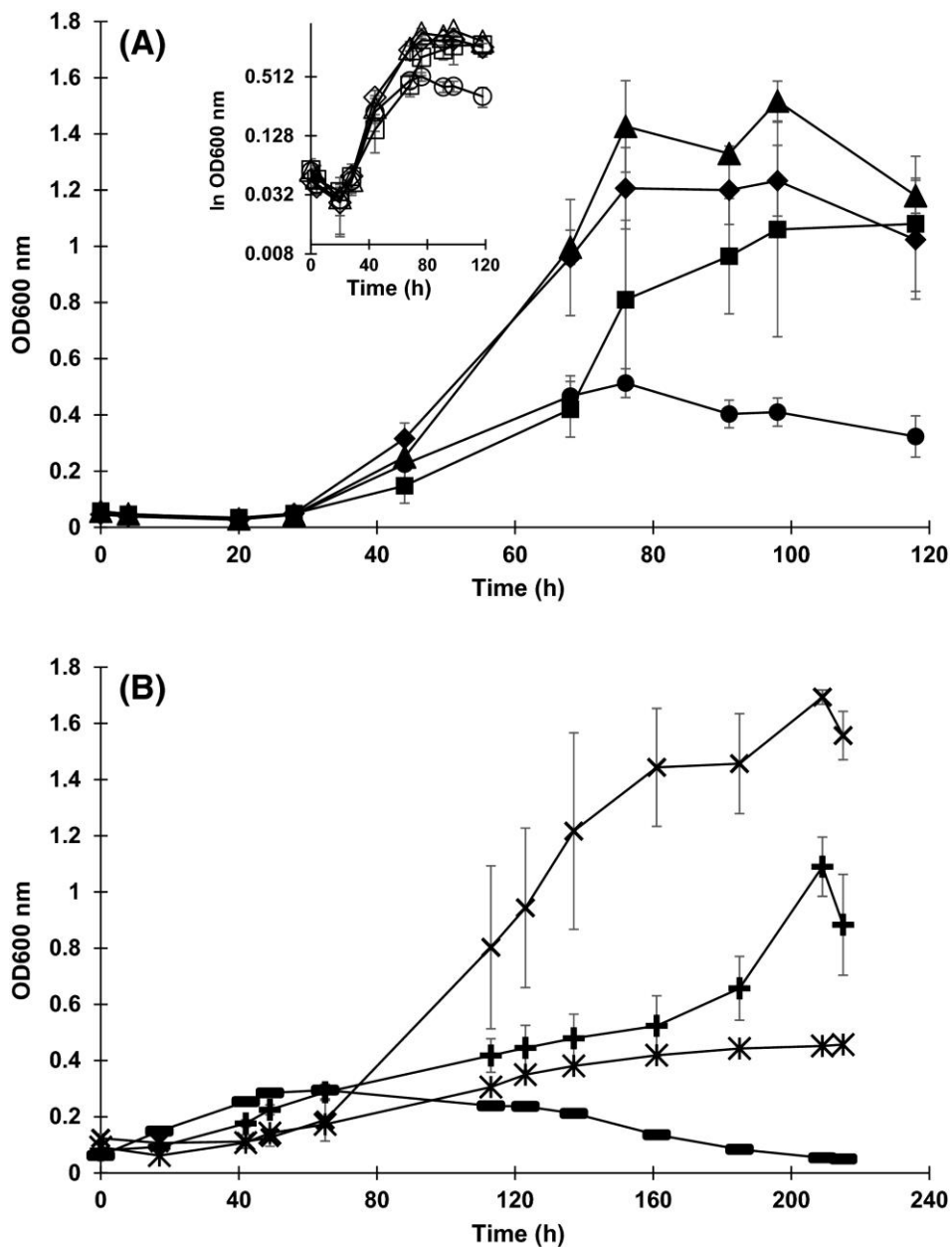


**Figure 1.** Growth of *Anaerobium acetethylicum* at different initial concentrations of glycerol incubated at 30°C for 118 h. Shown are mean values of triplicates  $\pm$  standard deviations, except for 1500 mM of glycerol ( $n = 2$ ). A. ● circles: 10 mM of glycerol, ◆ diamonds: 50 mM of glycerol, ▲ triangles: 100 mM of glycerol, ■ squares: 200 mM of glycerol. A inset. Half-logarithmic plot of the data presented in (A). Same symbols as in (A), but open symbols. B. X xes: 500 mM of glycerol, + crosses: 1000 mM of glycerol, \* asterisks: 1500 mM of replicate A, - minuses: 1500 mM of replicate B.

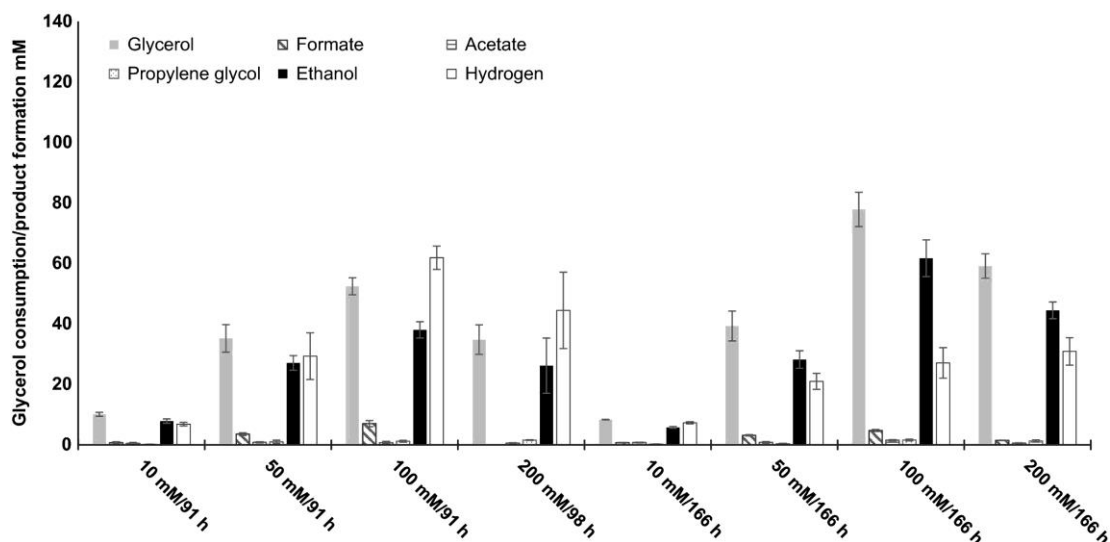


**Figure 2.** Glycerol consumption and product formation in cultures with varying initial glycerol concentrations. Products and substrate were analyzed after 91 h, 98 h or 166 hr as indicated. Headspace-to-culture volume ratio 1.5. Shown are mean values of triplicates  $\pm$  standard deviations, except for 200 mM/98 h ( $n = 2$ ). Order of bars in the respective category: first glycerol, second formate, third acetate, fourth propylene glycol, fifth ethanol, sixth hydrogen.

**Table 1.** Stoichiometry of glycerol fermentation and product formation by *Anaerobium acetethylicum* at different initial glycerol concentrations after 98 h. Shown are mean values of  $n = 3$  except for the growth experiment with 189.6 mM of glycerol ( $n = 2$ ).

Glycerol		Fermentation products (mM)							Yield		
Initial (mM)	Cell dry mass formed (mg/l)	Consumption (mM)	Assimilation (mM) <sup>1</sup>	Dissimilation (mM)	Ethanol	H <sub>2</sub>	Formate	Acetate	Propylene glycol	Electron recovery (%)	Growth yield (g dry mass /mol substrate)
10.8	114	10.1	1.3	8.8	7.9	6.9	0.7	0.5	0.1	93.8	11.3
48.7	304	35.2	3.6	31.6	27.1	29.3	3.6	0.8	1	93.4	8.6
97.4	327	52.4	3.9	48.5	38	61.9	7	0.7	1.2	91.1	6.2
189.6*	217*	34.8*	2.6*	32.2*	26.2*	44.5*	0*	0.6*	1.6*	96.9*	6.2*
506.1	284.9	71.3	3.4	67.9	57.9	69	0	0.5	2	91.4	4

<sup>1</sup>Glycerol assimilated was calculated assuming an OD<sub>600</sub> to dry mass correlation of 250 mg/l = OD<sub>600</sub> 1 and according to the following assimilation equation:  $17 \text{ C}_3\text{H}_8\text{O}_3 + 5 \text{ CO}_2 \rightarrow 14 \text{ C}_4\text{H}_7\text{O}_3 + 19 \text{ H}_2\text{O}$ , \*duplicate measurements, one culture with 189.6 mM glycerol did not grow, all other measurements done in triplicates.

---

At the end of the growth experiments, cultures were analysed for glycerol consumption and assimilation (maximum growth at late exponential phase) and dissimilation to different fermentation products. The electron recoveries obtained from the fermentation of 10, 50, 100, 200 and 500 mM of glycerol were found to be in a range of 91.1–96.9%, indicating that no major fermentation products beyond ethanol, hydrogen, and small amounts of formate, acetate and propylene glycol were formed (Table 1). However, at glycerol concentrations higher than 500 mM and when cultures were in late stationary to decline phase, the electron recoveries were lower than 90% (data not shown), indicating that part of the products or the amount of assimilated glycerol was not quantified correctly. At 10 mM of initial glycerol, the cells converted 8.8 mM of glycerol to 7.9 mM of ethanol and 6.9 mM of hydrogen; i.e., the glycerol- to- ethanol ratio was found to be about 1: 0.9 (Table 1). Growth yields decreased with increasing substrate concentrations and were 11.3 g dry mass mol<sup>-1</sup> substrate at 10 mM of initial glycerol and 4 g dry mass mol<sup>-1</sup> substrate at 500 mM of initial glycerol (Table 1). Another independent batch fermentation experiment with 100 mM of glycerol carried out in triplicates showed that the average pH value changed within 166 h from initially 7.2 to 6.3, probably due to the accumulation of CO<sub>2</sub> as no significant amounts of organic acids could be identified.

Although the fermentation of glycerol by *A. acetethylicum* yielded mainly ethanol and hydrogen and small amounts of acetate, formate and propylene glycol, another yet unidentified and unquantified compound was observed. This compound had a retention time of 21.1 min under our separation conditions and did not correspond to any of numerous compounds tested that could possibly arise as side products of glycerol fermentation, e.g. 1,3- propanediol, 3- hydroxypropionaldehyde synthesized from acrolein, 1- butanol, butyrate, succinate, 1,3- butanediol, acetaldehyde, 2- oxopropanal, 1- propanol and 2- propanol.

## **2.2 Growth of *A. acetethylicum* at elevated glycerol concentrations: solvent toxicity**

In order to investigate the maximum tolerable glycerol concentration, growth experiments with varying initial glycerol concentrations ranging from 500 to 3000 mM were performed. The strain showed longer lag phases when pre-cultures grown at lower glycerol concentrations were inoculated into medium containing higher initial glycerol concentrations. Therefore, a culture of *A. acetethylicum* was slowly adapted to higher concentrations by

subsequently transferring inocula from stationary- phase batch cultures with 10 mM of glycerol to 200 mM, to 500 mM, to 1000 mM and finally to 1500 mM of glycerol. Then, the growth experiments were repeated (Fig. 1B). At higher glycerol concentrations, growth was measurable at 500, 1000 and 1500 mM of glycerol. A maximum of 1500 mM of glycerol corresponding to  $138 \text{ g l}^{-1}$  was tolerated and growth was observed in two of three replicates with maximum optical densities at 600 nm of 0.46 and 0.3 at 1500 mM of initial glycerol concentration (Fig. 1B).

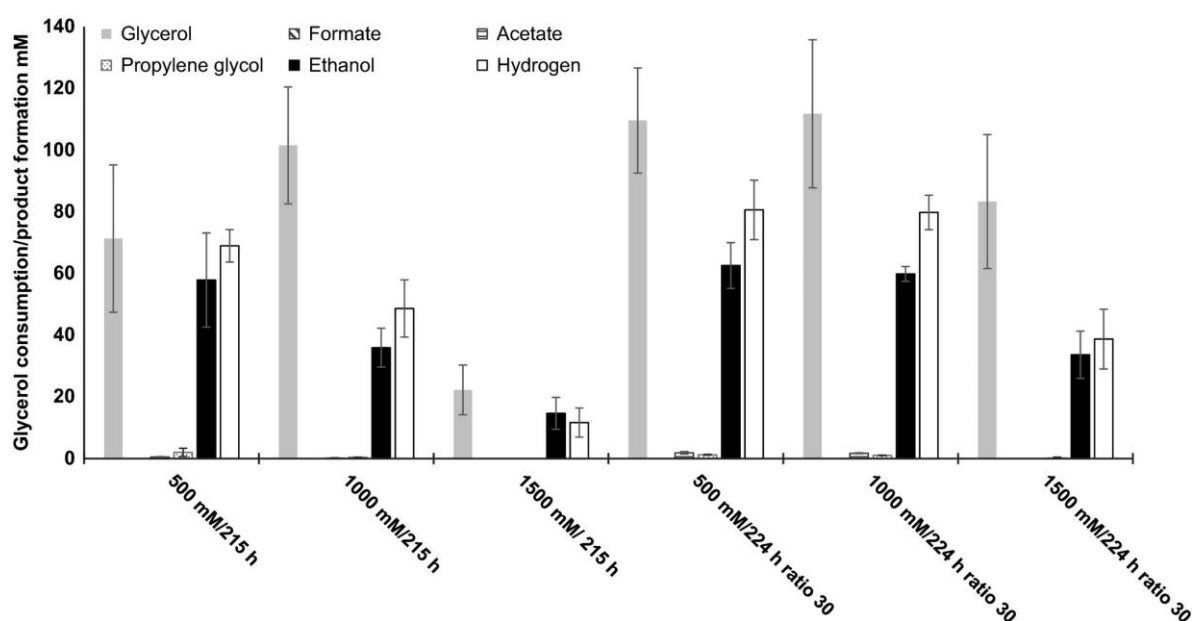


**Figure 3.** Glycerol consumption and product formation in cultures with varying initial glycerol concentrations. Products and substrate were analyzed after 215 h or 224 hr as indicated. Headspace- to- culture volume ratio 1.5 or 30 where indicated. Shown are mean values of triplicates  $\pm$  standard deviations, except for 1500 mM/215 h ( $n = 2$ ). Order of bars in the respective category: first glycerol, second formate, third acetate, fourth propylene glycol, fifth ethanol, sixth hydrogen.

Growth was completely inhibited at 2000 and 3000 mM of initial glycerol concentrations (data not shown). The growth tests were repeated and experimental conditions improved by the following modifications: cultivation was done in 600 ml infusion bottles with 20 ml of culture volume to increase the headspace- to- culture volume ratio to 30 thus allowing accumulation of higher amounts of hydrogen and subsequently ethanol, which is coproduced

---

with hydrogen in an approximately 1:1 ratio. The maximally accumulated average ethanol concentration was 63 mM ( $2.9 \text{ g l}^{-1}$ ) after 224 h of incubation when cultures were grown with 500 mM of initial glycerol in infusion bottles with a headspace- to- culture volume ratio of 30 (Fig. 3). Growth and glycerol degradation did not proceed further when the culture reached this ethanol concentration. In cultures with 500, 1000 and 1500 mM of initial glycerol concentrations with a headspace- to- culture volume ratio of 1.5, ethanol and hydrogen yields were generally slightly lower compared with cultures with the same initial glycerol concentrations and a headspace- to- culture volume ratio of 30 (Fig. 3).

### **2.3 Identification of genes encoding putative enzymes involved in glycerol fermentation by *A. acetethylicum***

Whole- proteome analysis of cell- free extracts of glycerol- grown cells of *A. acetethylicum* revealed that the genes coding for all putative enzymes involved in the proposed pathway shown in Fig. 4 were expressed during growth with glycerol. Glycerol is a small molecule that can diffuse slowly across the bacterial cell membrane. Facilitated diffusion is the least common type of energy- independent transport systems found in bacteria, e.g. the glycerol uniporter in *E. coli* (Sweet et al., 1990; Truninger and Boos, 1993). Although we could not detect the presence of a glycerol uptake facilitator protein (GlpF) in the total proteome analysis yet, we were able to identify the corresponding gene locus tag (Ga0116910\_10171) predicted to code for the GlpF protein in the genome of *A. acetethylicum*. According to the proposed glycerol fermentation pathway in *A. acetethylicum* (Fig. 4), after uptake (GlpF), glycerol is first converted to dihydroxyacetone (DHA) by glycerol dehydrogenase (GldA), which is subsequently phosphorylated to DHA- phosphate (DHAP) by dihydroxyacetone kinase (DhaK). Proteome analysis identified two putative genes that encode GldA (locus tag Ga011691\_101526 and 101551; in the following section, the prefix ‘Ga011691’ is omitted from the locus tag) and Dhak (101527; Table 2). DHAP is either partially metabolized to 1,2- propanediol via 2- oxopropanal, which involves a putative methylglyoxal synthase (Mgs; 1001113) or metabolized further by enzymes of the glycolytic pathway via acetyl- CoA as shown in Fig. 4. As expected, candidate genes coding for the putative enzymes triosephosphate isomerase (10001 and 101914), glyceraldehyde 3- phosphate dehydrogenase (1001392), phosphoglycerate kinase (1001391), phosphoglycerate mutase (1001389 and 103027), enolase (1001503), pyruvate kinase (1004153) and

---

ferredoxin- dependent putative pyruvate:ferredoxin oxidoreductase (103224) were expressed and identified in the proteome of glycerol- grown cells of *A. acetethylicum* (Table 2). However, pyruvate kinase (1004153) had a sequence coverage of only 12.2% with three identified peptides (Table 2).

Acetyl-CoA is partly utilized for assimilation or it is further metabolized either to acetate or ethanol. Conversion of acetyl-CoA to ethanol involves two enzyme reactions catalyzed by acetaldehyde dehydrogenase and alcohol dehydrogenase respectively (Fig. 4). Proteome analysis identified the putative candidates for both enzymes, acetaldehyde dehydrogenase (1004188) and alcohol dehydrogenase (101528 and 101313; Table 2). Similarly, conversion of acetyl-CoA to acetate involves two enzyme steps catalyzed by phosphate transacetylase and acetate kinase (Fig. 4), which were both expressed and identified (phosphate transacetylase (1001587) and acetate kinase (1001586; Table 2). During oxidative decarboxylation of pyruvate to acetyl- CoA by the ferredoxin- dependent pyruvate:ferredoxin oxidoreductase, carbon dioxide (CO<sub>2</sub>) and reduced ferredoxin are generated. The released CO<sub>2</sub> can be reduced to formate coupled to generation of oxidized ferredoxin by formate dehydrogenase (Fig. 4). Although glycerol fermentation by *A. acetethylicum* produced comparatively low amounts of formate (Table 1), proteome analysis did not confirm expression of candidate genes coding for putative formate dehydrogenases. Moreover, the draft genome sequence of *A. acetethylicum* does not contain candidate genes for formate dehydrogenases. Yet, a formate C- acetyltransferase (pyruvate: formate lyase) was identified in the proteome (Table 2). Likewise, ferredoxin could also be reoxidized coupled to hydrogen production as show in Fig. 4, but hydrogenase could not be reliably detected in the proteome. The only potential candidate was an iron- only hydrogenase (100543) with a sequence coverage of 12.2% and a score of 88.4 (Table 2). The coverage of most proteins identified were in the range of 31.9–89.9% (Table 2) and some identified proteins had coverages lower than 30% which makes it doubtful whether these were present in glycerol-grown cells.

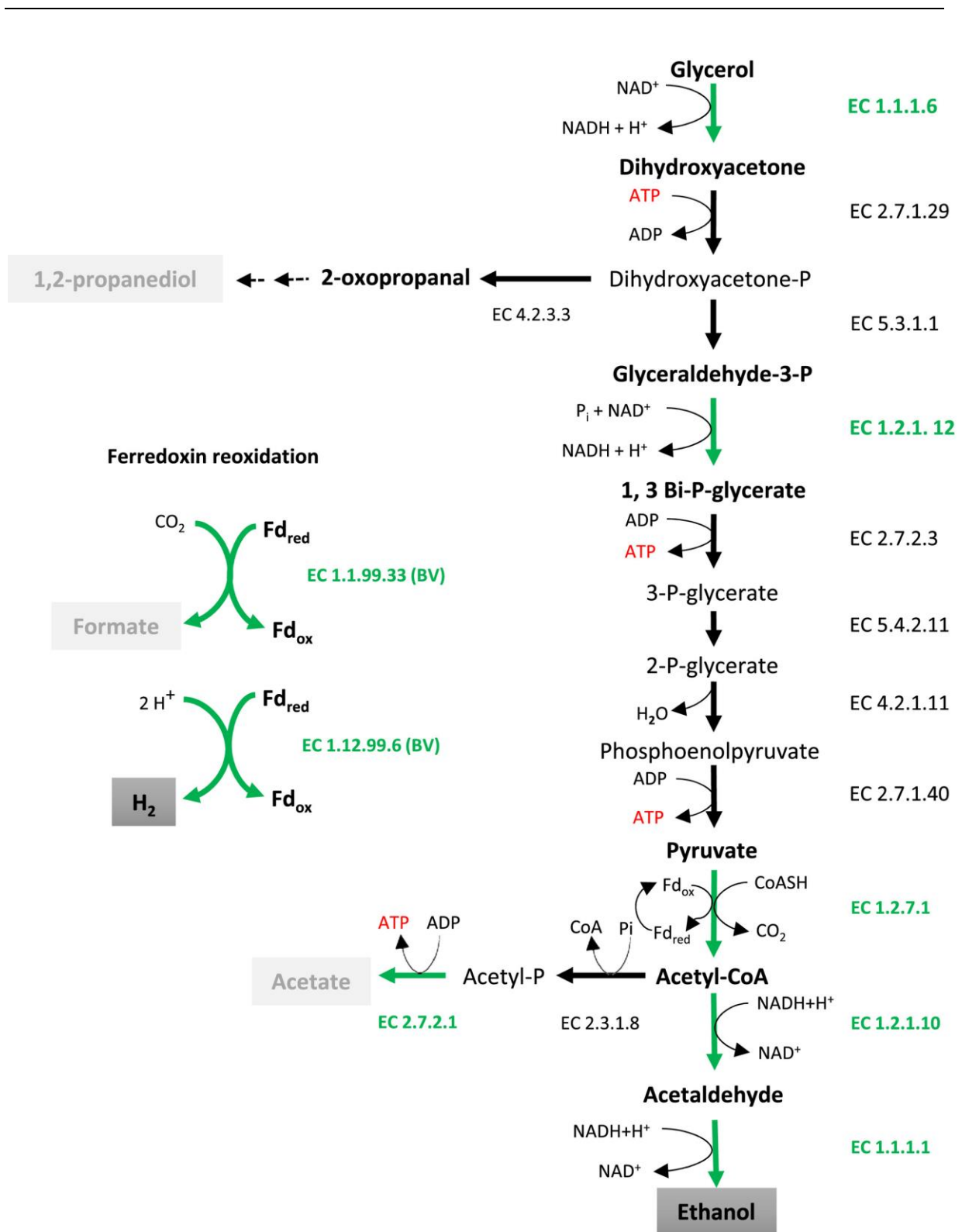


**Figure 4.** Anaerobic fermentative metabolism of glycerol by *Anaerobium acetethylicum* showing formation of the ethanol, acetate, formate and hydrogen. Green thick arrows indicate the activity of the respective enzyme confirmed by proteome analysis and enzyme assays with cell extract glycerol- grown cells. Bold black arrows represent enzymes confirmed by

---

total proteome analysis of glycerol- grown cells and dashed arrows show putative steps for 1, 2- propanediol production. The genes encoding (locus tag) for the respective enzymes involved in the glycerol metabolism are shown: glycerol dehydrogenase (EC 1.1.1.6; Ga0116910\_101526 and 101551); dihydroxyacetone kinase (EC 2.7.1.29; Ga0116910\_101527); triosephosphate isomerase (EC 5.3.1.1; Ga0116910\_10001 and 102914); glyceraldehyde 3- phosphate dehydrogenase (EC 1.2.1.12; Ga0116910\_1001391); phosphoglycerate kinase (EC 2.7.2.3; Ga0116910\_1001391); phosphoglycerate mutase (EC 5.4.2.11; Ga0116910\_1001389 and 103027); enolase (EC 4.2.1.11; Ga0116910\_1001503); pyruvate kinase (EC 2.7.1.40; Ga0116910\_1004153); pyruvate- ferredoxin oxidoreductase (EC 1.2.7.1; Ga0116910\_103224); CoA- dependent acetaldehyde dehydrogenase (EC 1.2.1.10; Ga0116910\_1004188); alcohol dehydrogenase (EC 1.1.1.1; Ga0116910\_101528 and 101313); phosphoacetyl transferase (EC 2.3.1.8; Ga0116910\_1001587); acetate kinase (EC 2.7.2.1; Ga0116910\_1001586); hydrogenase (EC 1.12.99.6; Ga0116910\_100543); formate dehydrogenase (EC 1.1.99.33); and methylglyoxal synthase (EC 4.2.3.3; Ga0116910\_1001113). BV – benzyl viologen and Fd – ferredoxin.

**Table 2.** Proteins that are likely to be involved in the proposed glycerol fermentation pathway identified by total proteomics (Orbitrap LC-MS analysis) from cell-free extract of *A. acetethylicum* cells grown with glycerol.

Gene loci <sup>a</sup>	IMG predicted function <sup>b</sup>	Coverage <sup>c</sup> (%)	Peptides <sup>d</sup>	Score <sup>e</sup>	Mass (kDa) <sup>f</sup>
101526	glycerol dehydrogenase	55.15	12	8982	40.0
101551	glycerol dehydrogenase	5.56	2	1894	40.5
101527	dihydroxyacetone kinase	58.83	24	4911	62.2
1001390	triosephosphate isomerase	89.92	11	4187	26.6
102914	triosephosphate isomerase	67.56	12	1509	29.7
1001392	glyceraldehyde 3-phosphate dehydrogenase	70.92	15	3876	35.4
1001391	phosphoglycerate kinase	78.34	20	5899	42.0
1001389	2,3-bisphosphoglycerate-independent phosphoglycerate mutase	31.91	11	861	56.6
103027	2,3-bisphosphoglycerate-independent phosphoglycerate mutase	14.68	4	176	44.5
1001503	enolase	22.88	6	305	47.6
1004153	pyruvate kinase	12.22	3	59	63.6
103224	pyruvate-ferredoxin/ferredoxin oxidoreductase	55,21	38	4261	127.9
1004188	acetaldehyde dehydrogenase / alcohol dehydrogenase	83.01	58	22648	95.2
101528	alcohol dehydrogenase	71.05	17	3608	39.8
101313	NAD(P)-dependent dehydrogenase, short-chain alcohol dehydrogenase family	10.63	2	158	27.4
1001587	phosphate acetyltransferase	27.49	5	165	35.1
1001586	acetate kinase	39.04	9	411	43.0
100543	iron only hydrogenase large subunit, C-terminal domain	12.24	5	88	64.9
1001113	methylglyoxal synthase	52.53	6	258	17.6
1004109	formate C-acetyltransferase	38.53	13	562	75.7

a, Integrated Microbial Genomes (IMG) (Markowitz et al., 2009) gene locus tag (Ga0116910\_); b, protein identification and function derived from IMG annotation; c, sequence coverage represents the extent of peptides obtained during MS-MS identification of the respective protein; d, number of peptides detected during MS-MS identification; e, mascot search score and f, peptide mass calculated by MS-MS identification.

---

## 2.4 Glycerol fermentation by *A. acetethylicum*: in-vitro enzyme activity measurements

Key enzymes of a hypothetical pathway of glycerol fermentation to ethanol and hydrogen were assayed in *in vitro* enzyme assays with cell-free extracts of glycerol- or glucose-grown cells (the latter as a control). In the first step, glycerol dehydrogenase (GldA) oxidizes glycerol to dihydroxyacetone (DHA) with  $\text{NAD}^+$  as electron acceptor. Glycerol-grown cells showed high specific activity for GldA ( $100 \text{ mU mg}^{-1}$  of protein) with glycerol and  $\text{NAD}^+$ . DHA is most likely phosphorylated to dihydroxyacetone phosphate (DHAP) by the activity of the enzymes dihydroxyacetone kinase and triose phosphate isomerase (Fig. 4). *In vitro* enzyme activities for methylglyoxal synthase, dihydroxyacetone kinase and triosephosphate isomerase were not assayed, but their involvement in the predicted glycerol fermentation pathway was evidenced by total proteome analysis (Table 2). Glyceraldehyde-3-phosphate was oxidized and phosphorylated to 1,3-bisphosphoglycerate in cell-free extract in the presence of  $\text{NAD}^+$  by glyceraldehyde-3-phosphate dehydrogenase, which showed an activity of  $282 \text{ mU mg}^{-1}$ . 1,3-bisphosphoglycerate is converted to pyruvate most likely by glycolytic enzymes which were not assayed but identified by whole-proteome analysis (Table 2). Pyruvate is oxidized and decarboxylated to acetyl-coenzyme A with ferredoxin by a putative pyruvate:ferredoxin oxidoreductase that could be measured using benzyl viologen ( $457 \text{ mU mg}^{-1}$ ) as an artificial electron acceptor and was also confirmed by measuring the reduction of native oxidized ferredoxin ( $17 \text{ mU mg}^{-1}$ ) prepared from *Clostridium pasteurianum* (Table 3).

**Table 3.** Measurement of key enzyme activities in the proposed pathway of glycerol fermentation by *A. acetethylicum* in cell-free extract of cells grown with glycerol.

Enzymes	Activity (mU/mg of protein)
Acetaldehyde dehydrogenase	37± 4.6
Alcohol dehydrogenase	513± 128
Glyceraldehyde 3-P dehydrogenase	282± 47
Glycerol dehydrogenase	100± 28
Pyruvate ferredoxin oxidoreductase	457 ± 11 (BV) 17 ± 4 (Fd)
Formate dehydrogenase	1.6 ± 0.11
Hydrogenase	3070 ± 779 (BV)
Acetase kinase	26 ± 2.44

Note: Enzyme activity measured with BV- benzylviologen and Fd- ferredoxin

Acetyl- CoA can be reduced to ethanol with NADH via acetaldehyde by acetaldehyde dehydrogenase and alcohol dehydrogenase respectively (Fig. 4). Enzyme assays with glycerol- grown cell- free extract showed activity for acetaldehyde dehydrogenase (37 mU mg<sup>-1</sup>) and alcohol dehydrogenase (513 mU mg<sup>-1</sup>) respectively. In addition to ethanol, glycerol fermentation by *A. acetethylicum* also produced small amounts of acetate and formate. However, no activity could be measured for the phosphate- dependent conversion of acetyl-CoA to acetyl- phosphate by phosphate acetyltransferase, but a comparatively lower activity of 26 mU mg<sup>-1</sup> was observed for an ADP- dependent acetate kinase in cell- free extract which converts acetyl- phosphate to acetate and generates ATP. Similar to acetate kinase, a very low activity (1.6 mU mg<sup>-1</sup>) was observed for formate dehydrogenase (Table 3) and a comparably very high activity of 3070 mU mg<sup>-1</sup> was observed for hydrogenase (BV).

According to the proposed pathway (Fig. 4), fermentation of glycerol needs reoxidation of NADH and ferredoxin. Reoxidation of ferredoxin occurs mainly through hydrogenase, but

---

also by formate dehydrogenase to a lower extent (Table 3). When glycerol, NADH and vitamin B<sub>12</sub> were combined in buffer along with cell- free extract of glycerol- grown cells, no activity was detectable for the assumed glycerol dehydratase and the combined 1,3- propanediol dehydrogenase, indicating that glycerol is unlikely to serve as an electron acceptor to produce 1,3- propanediol via 3- hydroxypropionaldehyde. Furthermore, no activity for glycerol dehydrogenase was observed in the cell- free extract of glucose- grown cells, indicating that the latter enzyme is specifically expressed during growth with glycerol.

#### 4. Discussion

Glycerol was studied as a substrate for biofuel production mainly because of its abundance, low price and its highly reduced state that makes it prone to generate reduced products like ethanol, hydrogen and also other industrially relevant compounds (Dharmadi et al., 2006; Clomburg and Gonzalez, 2013). In comparison with other glycerol- fermenting strains, *A. acetethylicum* has higher or at least similar glycerol tolerance, but a low ethanol tolerance. *Clostridium pasteurianum* converts 691 mM (63.6 g l<sup>-1</sup>) of glycerol to mixed fermentation products including butanol, 1,3- propanediol, ethanol, butyrate, acetate and lactate, when grown with 1250 mM (114.6 g l<sup>-1</sup>) of initial glycerol concentration (Biebl, 2001). Glycerol fermentation by *E. coli* at an initial glycerol concentration of 108 mM (10 g l<sup>-1</sup>) yields mainly ethanol, hydrogen and formate, similar to *A. acetethylicum* , but requires complex growth supplements such as yeast extract, tryptone or corn steep liquor (Dharmadi et al., 2006; Murarka et al., 2008). Similarly, *Paenibacillus macerans*, a glycerol- fermenting bacterium, produces ethanol and 1,2- propanediol but depends as well on tryptone as supplement in the growth medium ((Table 4); Gupta et al., 2009). In contrast to these reports, *Anaerobium acetethylicum* did not require additional organic supplements for fermentation of glycerol, except for the defined seven vitamins (Pfennig, 1978) present in the medium which include biotin. Biotin could replace yeast extract in cultures of *C. pasteurianum*, but the overall fermentation time was three times longer than with yeast extract (Biebl, 2001). When grown in defined mineral medium containing the seven vitamins and glycerol as substrate, *A. acetethylicum* had growth rates of 0.101–0.116 h<sup>-1</sup> which are about 2–3 times higher than those reported for *E. coli* (0.04 h<sup>-1</sup>) when grown with glycerol in the presence of tryptone

(Murarka et al., 2008), but about four times lower than those reported for *P. macerans* ((0.4 h<sup>-1</sup>); Gupta et al., 2009). However, growth of *A. acetethylicum* was not exponential any more after 44 h, indicating that growth is inhibited at this time point. Exponential growth in defined medium is basically possible when grown with gluconate at a growth rate of 0.693 h<sup>-1</sup>; therefore, the medium itself should allow exponential growth as well for cells grown with glycerol (Patil et al., 2015).

**Table 4.** Comparison of ethanol production and growth rates between *A. acetethylicum* and other anaerobic glycerol fermenting bacterial strains.

Organisms	Max. glycerol tolerated (M; (g/l))	Organic supplements required	Fermentation products	Max. growth rate observed (per hour)	References
<i>Anaerobium acetethylicum</i>	1.5 (138)	7-vitamins	E, H, a,f, pg, CO <sub>2</sub>	0.116	This study
<i>Escherichia coli</i> MG1655	0.108 (10)	CTS	E, (H, F) <sup>1</sup> , s, CO <sub>2</sub>	0.04	Dharmadi et al., 2006
<i>Escherichia coli</i> S1	0.375 (34.5)	T, YE	E, (H, F), <sup>1</sup> s, CO <sub>2</sub>	No data available	Adnan et al., 2014
<i>Paenibacillus macerans</i>	0.108 (10)	T	E, H, pg, f	0.4	Gupta et al., 2009
<i>Clostridium pasteurianum</i>	1.25 (115)	Biotin	E, 1,3-Pd, ButOH, B, A	0.37	Biebl et al., 2001

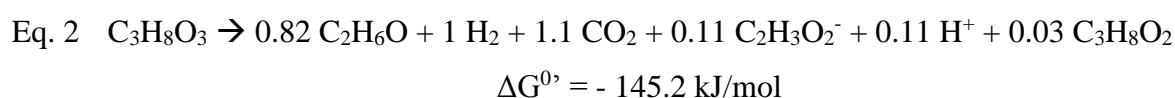
Fermentation products H=hydrogen, E=ethanol, F/f=formate, S/s=succinate, Pg/pg=propylene glycol, ButOH=butanol, 1,3-Pd=1,3-propanediol, B=butyrate, A/a=acetate (Capital letters- major products and small letter- minor products); complex supplements: CTS=corn steep liquor, T=tryptone, YE=yeast extract. <sup>1</sup>production of hydrogen or formate is pH-dependent.

---

In addition, the maximum glycerol concentration tolerable by *A. acetethylicum* was 1500 mM (138 g l<sup>-1</sup>), which is 13.8 times higher than the glycerol concentrations tested for *E. coli* (Dharmadi et al., 2006; Murarka et al., 2008). In a study aimed at optimizing glycerol utilization by *E. coli*, the optimal glycerol concentration was 375 mM (34.5 g l<sup>-1</sup>; Adnan et al., 2014). However, even though *A. acetethylicum* can grow at comparably high initial glycerol concentrations, maximally tolerable ethanol concentrations reached during glycerol fermentation were in the range of 60–70 mM, which is similar to the maximal concentrations observed for *E. coli* (Dharmadi et al., 2006; Murarka et al., 2008), but much lower than the observed maximum ethanol concentration of 342 mM (15.72 g l<sup>-1</sup>) for a growth- optimized *E. coli* strain (Adnan et al., 2014). However, it is unclear whether the ethanol concentrations accumulating in cultures of the latter two bacteria do not increase further due to lysis of the cells by ethanol or due to thermodynamic inhibition. This is, however, unlikely as the overall free reaction enthalpy of glycerol conversion to ethanol and hydrogen is negative enough to allow complete conversion of substrate into product (Eq. 1).



The free reaction enthalpy required to generate one ATP from phosphorylation of ADP to ATP is about -60 to -70 kJ mol<sup>-1</sup> (Schink, 1997). Therefore, equation 1 should allow the production of at least 1 mole of ATP per mole of glycerol. When considering the reaction of glycerol fermentation carried out by cultures of *A. acetethylicum*, which also produced small amounts of side products, the reaction becomes even more favourable allowing an overall ATP yield of 1–2 ATP per mole of glycerol (Eq. 2).



When Eq. 1 reaches its equilibrium ( $\Delta G' = 0$ ), including 60 kJ mol<sup>-1</sup> for formation of 1 ATP, the equilibrium constant has a value of about 10<sup>5</sup>, meaning that the reaction equilibrium is far on the side of the reaction products. Thus, thermodynamic inhibition can be ruled out as a

---

possible reason for the incomplete fermentation of glycerol to ethanol and hydrogen, and inhibition of growth by fermentation metabolites is very likely, i.e., via solvent toxicity. *A. acetethylicum* could ferment glycerol ranging from 10 to 1500 mM initial concentrations, but ethanol production did not exceed 63 mM (Fig. 3). Therefore, increased concentrations of glycerol in the growth medium did not increase ethanol production beyond this latter concentration and growth was most likely inhibited by the ethanol toxicity. Ethanol is known as a growth-inhibiting agent for bacteria as it acts as hydrophobic stressor, especially at concentrations higher than 25% (w/v; 5400 mM), and therefore destabilizes biological membranes by weakening hydrophobic interactions (reviewed in Cray et al., 2015; Ingram, 1990). This effect on hydrophobic interactions also causes a reduction of water activity, which was shown to induce water stress in fungi (Hallsworth et al., 1998). This could explain the higher ethanol concentration observed after 166 h of incubation in late stationary to decline phase (62 mM) compared with the ethanol concentration present after 91 h in early stationary phase (38 mM). Most likely, cells were partially lysed by ethanol after they reached stationary phase while still being metabolically active and continuing to ferment glycerol to ethanol and hydrogen. This lytic effect of ethanol might also be reflected by the fact that growth yields decreased with increasing substrate and ethanol concentrations.

Consequently, a certain proportion of assimilated substrate was possibly underestimated, which might explain the incomplete electron recoveries at glycerol concentrations higher than 500 mM. Growth could also be inhibited through acidification of the medium. At a substrate concentration of 100 mM of glycerol, the pH dropped from initial 7.2 to 6.3 at the end of growth and earlier investigations revealed a pH range of 6.5–8.5 of strain GluBS11T for growth with gluconate (Patil et al., 2015). Therefore, glycerol fermentation could possibly be improved by increasing the buffer strength.

In this study, the fermentation of glycerol to ethanol, CO<sub>2</sub> and hydrogen by *A. acetethylicum* was biochemically characterized (Fig. 4). Glycerol fermentation by *A. acetethylicum* also produced small amounts of 1,2-propanediol (Table 1). Clomburg and Gonzalez (2013) reported that 1,2-propanediol is derived from dihydroxyacetone phosphate. The enzyme methylglyoxal synthase which dephosphorylates dihydroxyacetone phosphate to methylglyoxal was identified in the proteome of *A. acetethylicum* (Table 3). Methylglyoxal (2-oxopropanal) could theoretically be reduced to 1,2-propanediol via acetol

---

(hydroxyacetone) or lactaldehyde (Clomburg and Gonzalez, 2011). Both pathways involve glycerol dehydratase and aldehyde oxidoreductase, of which one at least the gene for glycerol dehydratase could be identified in the genome of *A. acetethylicum* (glycerol dehydratase large subunit Ga0116910\_100557). 2- oxopropanal could therefore possibly be reduced to 1,2- propanediol by one or both of the aforementioned pathways (Fig. 4). 2- oxopropanal is also known as a highly toxic metabolite in bacterial cells and could therefore be inhibitory for growth of *A. acetethylicum* (Booth et al., 2003; Clomburg and Gonzalez, 2011). Despite the fact that HPLC chromatograms of culture supernatants of *A. acetethylicum* occasionally showed small peaks at the same retention time as 2- oxopropanal, accumulation of this metabolite could not be reliably verified and 2- oxopropanal did possibly not exceed concentrations higher than 1 mM (data not shown).

Interestingly, batch fermentation experiments with glycerol revealed that hydrogen accumulated at high concentrations, while almost no formate was produced (Table 1). This finding was supported by the approximately 2000- fold lower activity of formate dehydrogenase compared with hydrogenase (Table 3). In contrast to this, cultures grown with gluconate or glucose as substrates produced higher concentrations of formate than hydrogen at a ratio of hydrogen to formate of about 1:2 (Patil et al., 2015). Therefore, formate is a more prominent metabolite when cultures are grown with sugars, which might be due to the fact that twice as much CO<sub>2</sub> is released per mole of hexose oxidized compared with glycerol. Even though formate could be detected as a metabolite and formate:benzyl viologen oxidoreductase activity was detected in cell- free extracts, we were unable to find the corresponding formate dehydrogenase genes in the genome sequence. Possibly, the observed activity is a side reaction of formate C- acetyltransferase (pyruvate:formate lyase) which was identified in the proteome.

When *A. acetethylicum* was grown with a larger headspace- to- culture volume ratio, the maximum concentrations of ethanol and hydrogen were slightly higher compared with cultures with a low headspace- to- culture volume ratio, indicating that hydrogen is also inhibitory for glycerol degradation. Similar observations were also made for *E. coli* grown in a fermenter sparged with argon gas, which vastly increased the amount of glycerol degraded (Murarka et al., 2008). Although experiments with cultures of *A. acetethylicum* permanently

---

sparged with argon or nitrogen have not been done yet, it can be assumed that this might stimulate fermentation of glycerol as well.

Even though *A. acetethylicum* has certain advantages over other glycerol- fermenting organisms, the fact that side products are formed in batch cultures especially at higher glycerol concentrations might be disadvantageous for large- scale bioethanol production. Among acetate, formate and 1,2- propanediol frequently observed at small concentrations, a further product was released in cultures of *A. acetethylicum* that could not be identified by HPLC. It was previously reported that during fermentation of glycerol by *Clostridium pasteurianum*, 1,3- propanediol is produced via 3- hydroxypropionaldehyde (Dabrock et al., 1992). However, in this study we could detect neither 1,3- propanediol nor 3- hydroxypropionaldehyde as metabolites, and the activities of the respective enzymes were absent in *in vitro* assays, although we recently reported that occasionally very small amounts of 1,3- propanediol could be detected by HPLC in cultures of *A. acetethylicum* (Patil et al., 2015). Likewise, succinate, lactate, 1- butanol, 1- propanol, 2- propanol, butyrate, propionate and 1,3- butanediol were ruled out as possible side products and neither one of the corresponding metabolic pathways is present in the genome of *A. acetethylicum* with a complete set of genes (Patil et al., 2016). Interestingly, the percentage of ethanol produced per glycerol slightly increased with increasing substrate concentration, with an optimal initial glycerol concentration of 100 mM (9.2 g l<sup>-1</sup>) at which the strain showed maximal efficiency of glycerol- to- ethanol conversion (79% glycerol conversion to ethanol).

## 5. Conclusion

As *A. acetethylicum* strain GluBS11<sup>T</sup> naturally has a high tolerance towards elevated glycerol concentrations, it could be a potentially useful agent for treating glycerol- rich wastewaters coming from the biodiesel industries. Our study shows that the maximum initial glycerol concentration that did not inhibit growth and metabolic activity of the cells was 1500 mM of pure glycerol. However, 100 mM of initial glycerol concentration was optimal for efficient conversion of glycerol to ethanol (79% conversion efficiency) and hydrogen as compared to other tested initial concentration. Solvent toxicity tests of *A. acetethylicum* for glycerol and ethanol showed that ethanol is the key solvent that strongly inhibits growth and fermentation activity. Although the strain could produce about 61 mM of ethanol during growth with 100

---

mM of glycerol, addition of 50 mM of initial ethanol completely inhibited growth (Fig. S1). The inability to accumulate high concentrations of ethanol (more than 60 mM) during growth is possibly a drawback for large- scale applications. Moreover, pure glycerol was used as a substrate in this study and glycerol derived from biodiesel production might contain compounds that inhibit growth. Yet, due to its high tolerance for glycerol and its fermentation pattern to mainly ethanol and hydrogen, the strain has a high potential for future industrial application in biodiesel industries to convert crude glycerol to value- added biofuel. Future research should therefore focus on increasing the strain's ability to tolerate ethanol concentrations higher than 60 mM. This could be accomplished, e.g. by genetic engineering of the strain and introducing metabolic pathways for synthesis of oleic acid, which is believed to protect the cell membranes of yeast from the toxic effect of ethanol (You et al., 2003). This would, however, require the development of a genetic system for the strain. It is known that ethanol tolerance in yeast can also be increased by addition of Tween- 80 and oleic acid to growth media, which did not increase ethanol tolerance in *A. acetethylicum*, however, (data not presented) and probably led to inhibition of growth (Andreasen and Stier, 1954). Besides ethanol and hydrogen as main fermentation products, the strain produces very little amount of undesired fermentation products such as acetate and formate; therefore, future efforts in metabolically engineering the strain could aim at deleting the enzymes leading to acetate production, i.e., acetate kinase, and formate production, i.e., formate dehydrogenase, for the production of bioethanol.

## **6. Experimental procedures**

### **6.1 Source of strain and genome sequence**

*Anaerobium acetethylicum* strain GluBS11<sup>T</sup> was recently isolated in our laboratory and was characterized morphologically and taxonomically (Patil et al., 2015). Strain GluBS11<sup>T</sup> is available in public culture collections such as the German Collection of Microorganisms and Cell Cultures (DSMZ 29698) or the Korean Type Culture Collection (KCTC 15450). Recently, metabolic features and characteristics of the high- quality permanent draft genome sequence of *A. acetethylicum* strain GluBS11<sup>T</sup> are described (Patil et al., 2016). The draft genome of *A. acetethylicum* strain GluBS11<sup>T</sup> was sequenced as part of the Genomic Encyclopedia of Type Strains, Phase III (KMG- III): the genomes of soil and plant- associated and newly

---

described type strains (Whitman et al., 2015). The genome project is deposited in the Genomes OnLine Database under Project ID: Gp0139288 (Liolios et al., 2008).

## **6.2 Cultivations and glycerol fermentation experiment**

Pre-cultures of *A. acetethylicum* were cultured in a bicarbonate- buffered and sulfide- reduced mineral medium adjusted to pH 7.2 as described before (Patil et al., 2015) containing 10 mM of glycerol, at 30°C in 25 ml Hungate test tubes or 100 ml infusion bottles. The following seven vitamins were added to the medium after autoclaving from a concentrated, filter- sterilized stock solution: cyanocobalamine (50 µg l<sup>-1</sup>), p- aminobenzoic acid (50 µg l<sup>-1</sup>), biotin (10 µg l<sup>-1</sup>), nicotinic acid (100 µg l<sup>-1</sup>), pantothenate (25 µg l<sup>-1</sup>), pyridoxamine (250 µg l<sup>-1</sup>) and thiamine (50 µg l<sup>-1</sup>; Patil et al., 2015; Pfennig, 1978). For longer storage, the strain was maintained in culture medium at 4°C, and actively growing cultures were used as inoculum for inoculation of each experiment. Fermentation experiments were performed either in 25 ml glass tubes sealed with butyl rubber stoppers and closed with aluminium crimps under a N<sub>2</sub>/CO<sub>2</sub> (80:20) atmosphere filled with 10 ml of medium, or in infusion bottles sealed with butyl rubber stoppers under the same atmosphere filled with each of 50, 100 ml or 1 l of culture medium. Growth experiments with large headspace- to- culture volume ratio were performed in 600 ml infusion bottles sealed with butyl rubber stoppers. The gas phase of the bottles was exchanged to N<sub>2</sub>/CO<sub>2</sub> (80:20). Then, the bottles were autoclaved at 121°C and 1 bar overpressure for 25 min and thereafter filled with 20 ml of medium with syringes. Substrate stock solutions (glycerol and ethanol) were maintained under anoxic conditions (under N<sub>2</sub> gas) and filter- sterilized using cellulose acetate filters with 0.2 µm pore size. Stock solutions were added to the medium as sole source of carbon and energy with sterile disposable needles and syringes. To investigate the influence of different concentrations of glycerol on the fermentation pattern, glycerol was added to the culture medium at concentrations ranging from 10 to 200 mM. Growth was monitored by measuring optical densities directly in test tubes at 600 nm wavelength (OD<sub>600 nm</sub>) using a tube spectrophotometer M107 (Spectronic Camspec, Leeds, UK). When cultures reached optical densities higher than 0.7, samples were withdrawn with syringes and diluted 1:10 with medium and optical densities were measured in plastic cuvettes with a Jenway 6305 spectrophotometer (Jenway, Staffordshire, UK). Spectrophotometers were zeroed with sterile blank medium, and all experiments were performed in triplicates.

---

### 6.3 Alcohol (Glycerol and Ethanol) tolerance

To investigate the influence of glycerol and ethanol at different concentrations on glycerol fermentation by *A. acetethylicum*, various concentrations of glycerol (ranging from 10 mM to 3000 mM) and ethanol (10–100 mM) were added to the culture medium. *A. acetethylicum* cells were always grown and maintained in glycerol- containing medium and gradually adapted to higher concentrations of glycerol. Cultures were inoculated to an initial OD600 of about 0.02 in medium supplemented with different concentrations of glycerol. In the ethanol tolerance experiments, all culture tubes were supplemented with 10 mM of glycerol as growth substrate with varying concentrations of ethanol. All incubations were performed at 30°C in the dark, and growth was monitored spectrophotometrically at OD600 until the cultures reached the stationary phase. At the end of experiments (stationary phase), samples were collected from each culture tube and stored at –20°C until further use. Measurement of substrate consumption or fermentation product formation was taken by HPLC as described below. All fermentation experiments were performed in triplicates.

### 6.4 Preparation of cell-free extracts

Cultures of *A. acetethylicum* grown in 1 l medium with 20 mM of glycerol were grown until cells reached mid- to- late exponential growth phase (after 24–48 h). Cells were harvested by centrifugation at 7000 × g, for 20 min at 10°C in a Sorvall RC- 5B centrifuge (Du Pont de Nemours, Bad Homburg, Germany) under anoxic conditions using airtight polypropylene centrifuge bottles in an anaerobic chamber (Coy, Ann Arbor, MI, USA). Cell pellets were washed by resuspending them in approximately 200 ml of anoxic 50 mM of Tris–HCl buffer (pH 7.5) containing 3 mM of dithiothreitol (DTT) and centrifuged again. Cell pellets were stored at –20°C until further use. Finally, cell pellets were suspended in 4–5 ml of the same buffer and cells were disrupted by passing three times through an ice- cold MiniCell French pressure cell (SLM Aminco, Cat. No. FA003) operated at 137 MPa pressure as described recently (Junghare et al., 2016) or cells were opened by enzymatic lysis using lysozyme treatment. Lysis with lysozyme was performed by adding 2 mg ml<sup>-1</sup> of lysozyme and 0.1 mg ml<sup>-1</sup> of DNase I to cell suspensions, which were then incubated at 37°C for 1 h. Cell debris was removed by high- speed centrifugation (27,000 × g for 30 min at 4°C) using an

---

ultracentrifuge under anoxic conditions. The supernatant was transferred to 8 ml serum vials closed with butyl rubber stoppers and sealed with aluminium caps. The headspace was exchanged under a stream of 100% nitrogen gas. This supernatant was defined as crude cell- free extract and was stored on ice for enzyme activity measurements.

### **6.5 Total proteome analysis**

Cell- free extracts of glycerol- grown cells of *A. acetethylicum* were used for the identification of the total proteome to identify the putative proteins/enzyme involved in the anaerobic fermentation of glycerol. Proteins were reduced with 10 mM of DTT for 30 min and alkylated with iodoacetamide followed by overnight trypsin digestion. The resulting digested protein mixture was applied to reversed- phase liquid chromatography nanospray tandem mass spectrometry (LC- MS/MS) using an LTQ- Orbitrap mass spectrometer (Thermo Fisher) and an Eksigent nano- HPLC. The LC- MS/MS was equipped with the reversed- phase LC column measuring 5  $\mu\text{m}$ , 100  $\text{\AA}$  pore size C18 resin in a 75-  $\mu\text{m}$  i.d.  $\times$  10 cm long piece of fused silica capillary (Acclaim PepMap100; Thermo Scientific, Dreieich, Germany). After sample injection, the column was washed for 5 min with 95% mobile phase A (0.1% formic acid) and 5% mobile phase B (0.1% formic acid in acetonitrile), and peptides were eluted using a linear gradient of 5% mobile phase B to 50% mobile phase B in 205 min, then to 80% B in an additional 5 min at 300  $\text{nl min}^{-1}$ . The LTQ- Orbitrap mass spectrometer was operated in a data- dependent mode in which each full MS scan (30 000 resolving power) was followed by seven MS/MS scans where the seven most abundant molecular ions were dynamically selected and fragmented by collision- induced dissociation (CID) using a normalized collision energy of 35% in the LTQ ion trap. Dynamic exclusion was allowed. Tandem mass spectra were searched against a suitable protein database of the annotated genome sequence of *A. acetethylicum* using Mascot (Matrix Science) with trypsin enzyme cleavage, static cysteine alkylation by iodoacetamide and variable methionine oxidation. Search results were validated on the basis of top hits and scores obtained in the Mascot search engine.

### **4.6 In vitro enzyme activity measurements**

---

For measurement of *in vitro* enzyme activities, cell- free extract was prepared from cells grown with glycerol or glucose (the latter as control) as described above and used for enzyme assays. Enzyme activities were measured under anoxic conditions using 1.5 ml quartz cuvettes closed with rubber stoppers and gassed with N<sub>2</sub> gas (unless otherwise mentioned). All additions were performed with airtight Unimetrics microlitre syringes (Macherey- Nagel, Germany). Enzyme assays were performed at 30°C using a UV-vis spectrophotometer V- 630 (Jasco, Gross- Umstadt, Germany). One unit of specific enzyme activity (U) was defined as the amount of enzyme required to convert 1 μmole of substrate into the specific product per minute and per milligram of protein. Protein concentrations were estimated by the microprotein assay (Bradford, 1976) with bovine serum albumin as standard. All enzyme assays were performed at least in triplicates under anoxic conditions at 30°C.

i) **Glycerol dehydrogenase** (glycerol:NAD<sup>+</sup> oxidoreductase, EC 1.1.1.6) activity was assayed using 1.5 ml in quartz cuvettes containing 1 ml of reaction mixture containing 50 mM of Tris-HCl buffer, pH 7.5, 3 mM of dithiothreitol, 0.2 mM of NAD<sup>+</sup> and 20 μl of cell- free extract (approx. 0.1 mg of protein). Enzyme reactions were started by addition of 20 mM of glycerol. The reduction of NAD<sup>+</sup> to NADH in the presence of glycerol was monitored spectrophotometrically by the increase in absorbance due to NADH formation at 340 nm wavelength.

ii) **Glycerol dehydratase** (EC 4.2.1.30) **and 1, 3- propanediol dehydrogenase** (EC 1.1.1.202) activities were assayed together in a coupled enzyme assay containing 1 ml of reaction mixture of 50 mM of Tris-HCl, pH 7.6, with 3 mM of DTT, 0.3 mM of NADH, 24 μM of cyanocobalamine (vitamin B<sub>12</sub>) and 20 μl of cell- free extract. The reaction was started by addition of 2 mM of glycerol and decrease in the NADH concentration was determined at 340 nm in spectrophotometer.

iii) **Glyceraldehyde- 3- phosphate dehydrogenase** (EC 1.2.1.12) was measured following the increase in NADH concentration at 340 nm. The 1 ml of reaction mixture containing 50 mM of potassium phosphate buffer, pH 7.5, 0.2 mM of NAD<sup>+</sup> and 20 μl of cell- free extract. The reaction was started by addition of 0.3 mM of glyceraldehyde 3- phosphate.

iv) **Pyruvate synthase** (EC 1.2.7.1; also called pyruvate: ferredoxin oxidoreductase) was assayed as reduction of benzyl viologen monitored at 578 nm. The 1 ml of assay mixture

---

containing 50 mM of Tris–HCl buffer, pH 7.5, containing 3 mM of DTT, 2 mM of benzyl viologen, 0.3 mM of CoASH, and 20 µl of cell- free extract. The reaction was started by addition of 2 mM of pyruvate. Alternative to benzyl viologen, the enzyme activity was also determined with ferredoxin isolated from *Clostridium pasteurianum*. The reduction of ferredoxin was monitored spectrophotometrically as the increase in absorbance at 390 nm wavelength. Ferredoxin from *C. pasteurianum* was essentially prepared as previously described (Schönheit et al., 1978).

v) **Acetate kinase** (EC 2.7.2.1) was measured in a coupled enzyme assay. One millilitre of reaction mixture in 50 mM of Tris–HCl, pH 7.6, with 3 mM of DTT, 0.33 mM of NADH, 5 mM of phosphoenolpyruvate, 5 mM of MgCl<sub>2</sub>, 5 mM of ATP, 2 U of D- lactate dehydrogenase and 20 µl of cell- free extract. The reaction was started with 5 mM of acetate, and decrease in concentration of NADH was monitored at 340 nm.

vi) **Acetaldehyde dehydrogenase** (EC 1.2.1.10) activity was assayed in 1 ml of reaction mixture of 50 mM of Tris–HCl buffer, pH 7.5, containing 3 mM of DTT, 0.2 mM of NAD<sup>+</sup>, 0.3 mM of coenzyme A (CoASH) and 20 µl of cell- free extract. The reaction was started by addition of 0.5 mM of acetaldehyde. The reduction of NAD<sup>+</sup> to NADH was monitored spectrophotometrically by the increase in absorbance at 340 nm wavelength.

vii) **Alcohol dehydrogenases** (EC 1.1.1.1) activity was determined in 1 ml of reaction mixture containing 50 mM of Tris–HCl buffer, pH 7.5, 3 mM of dithiothreitol, 0.2 mM of NADH and 20 µl of cell- free extract. The enzyme reaction was started by addition of 0.5 mM of acetaldehyde, and the decrease in NADH absorbance was monitored spectrophotometrically at 340 nm wavelength.

viii) **Formate dehydrogenase** (EC 1.1.99.33) activity was assayed as reduction of benzyl viologen monitored at 578 nm. The 1 ml of assay mixture contained 50 mM of Tris–HCl buffer, pH 7.5, 3 mM of DTT, 2 mM of benzyl viologen and 20 µl of cell- free extract. The reaction was started by addition of 2 mM of formate.

ix) **Hydrogenase** (EC 1.12.99.6) activity was assayed in cuvettes gassed with hydrogen. The 1 ml of assay mixture containing 50 mM of Tris–HCl buffer, pH 7.5, containing 3 mM of DTT, 2 mM of benzyl viologen. The reaction was started by addition of 20 µl of cell extract, and reduction of benzyl viologen was monitored at 578 nm.

---

#### 4.7 Analytical methods

Ethanol, acetate, glycerol, propionate and formate were quantified by HPLC with a Rezex RHM- monosaccharide H<sup>+</sup> 300 × 7.80 mm 8 μm ion exchange column (Phenomenex, Aschaffenburg, Germany) using a method previously described (Dharmadi et al., 2006). The column was operated at 40°C and 30 mM of sulfuric acid was used as mobile phase at a flow rate of 0.6 ml min<sup>-1</sup> using a LC- 10ATvp pump (Shimadzu, Munich, Germany). The mobile phase was degassed with a DGU- 20A3R degassing unit (Shimadzu), and samples were injected with a 234 autosampler (Gilson, Limburg- Offheim, Germany). For analysis of the separated compounds, a refractive index detector RID- 10A (Shimadzu) was used and the signals obtained were analysed with the shimadzu lab solutions software version 5.81. When 5 mM of sulfuric acid was used as eluent with the column heated to 60°C, formate and glycerol could not be separated. Similar observations were made for the same separation problem before (Dharmadi and Gonzalez, 2005). Prior to HPLC analysis, samples and standards were prepared by mixing 200 μl of sample or standard with 20 μl of 1 M H<sub>2</sub>SO<sub>4</sub> to remove HCO<sub>3</sub><sup>-</sup>. Acrolein as a standard was measured with and without prior acidification. 3- hydroxypropionaldehyde is not commercially available and was prepared by acidification of acrolein (2- propenal) with sulfuric acid essentially as described before (Hall and Stern, 1950). Acrolein was added to an anoxic 1 M H<sub>2</sub>SO<sub>4</sub> solution to a final concentration of 100 mM. This solution was incubated at room temperature overnight (16 h) and directly used as a standard for HPLC analysis.

Hydrogen was quantified with a GC6000 Vega Series 2 GC (Carlo Erba, Italy) gas chromatograph equipped with a HWD 430 thermal conductivity detector. The steel column (45/60 Carboxen 1000, Supelco) was heated to 120°C. A comparable column was used as reference column. Nitrogen was used as carrier gas at a concentration of 100% and at a column pressure of 60 kPa. The manual injection port was heated to 150°C, and the detector and filament temperatures of the thermal conductivity detector were 180°C and 270°C respectively. Detector signals were analysed with a D- 2500 Chromato- Integrator (Merck Hitachi) set to a plot attenuation of 4 and a sensitivity of 250. Samples of 100 μl were withdrawn from culture vessels with a syringe mounted to a valve with needle and injected at atmospheric pressure.

---

#### 4.8 Thermodynamic calculations

The assimilation equation for glycerol fermentation was calculated assuming that glycerol is oxidized to biomass with CO<sub>2</sub>. Thermodynamic calculations were done according to method described (Thauer et al., 1977) and using the online  $\Delta G$  calculator tool available on our webpage (<https://cms.uni-konstanz.de/schink/dg-calculator/>). The free energy formation enthalpy for 1,2- propanediol is  $\Delta H_f^0$  liquid propylene glycol = 501.0  $\pm$  4.1 kJ mol<sup>-1</sup> (Knauth and Sabbah, 1990), which was not available in the list mentioned in Thauer et al., (1977) and was retrieved from the webpage of the National Institute of Standards and Technology webbook ( <http://webbook.nist.gov/cgi/inchi?ID=C4254142&Units=SI>).

#### 4.9 Source of chemicals

All biochemicals used in this study were purchased from Sigma- Aldrich (Munich, Germany) or Carl Roth (Karlsruhe, Germany) and were at least of reagent grade. All other chemicals were from Sigma- Aldrich and were of analytical grade. Acrolein was a kind gift from Christian Leitner from the group of Dr. Tanja Gaich at the University of Konstanz. Gases were obtained from Messer- Griesheim (Darmstadt, Germany) or Sauerstoffwerke Friedrichshafen (Friedrichshafen, Germany).

#### Acknowledgments

The authors thank Antje Wiese for technical help with medium preparations and Dr. Bernhard Schink for critically reading the manuscript and valuable suggestions. The publicly available annotated genome sequence of *A. Anaerobium* was provided on the Integrated Microbial Genomes system of the Joint Genome Institute (JGI) of the U.S. department of energy whose service is highly appreciated. The work conducted by the U.S. Department of Energy Joint Genome Institute, a DOE Office of Science User Facility, is supported by the Office of Science of the U.S. Department of Energy under Contract No. DE- AC02- 05CH11231.YP is indebted to the Landesgraduiertenförderungsgesetz (LGFG) scholarship programme of the University of Konstanz in accordance with the State Law on Graduate Funding for providing the scholarship during this research.

#### Author's contribution

---

YP and MJ contributed equally. Experiments were conducted by YP, MJ and NM. NM, YP and MJ designed experiments and wrote the manuscript.

**Conflict of Interest:** The authors declare no conflict of interest.

### Supplementary information

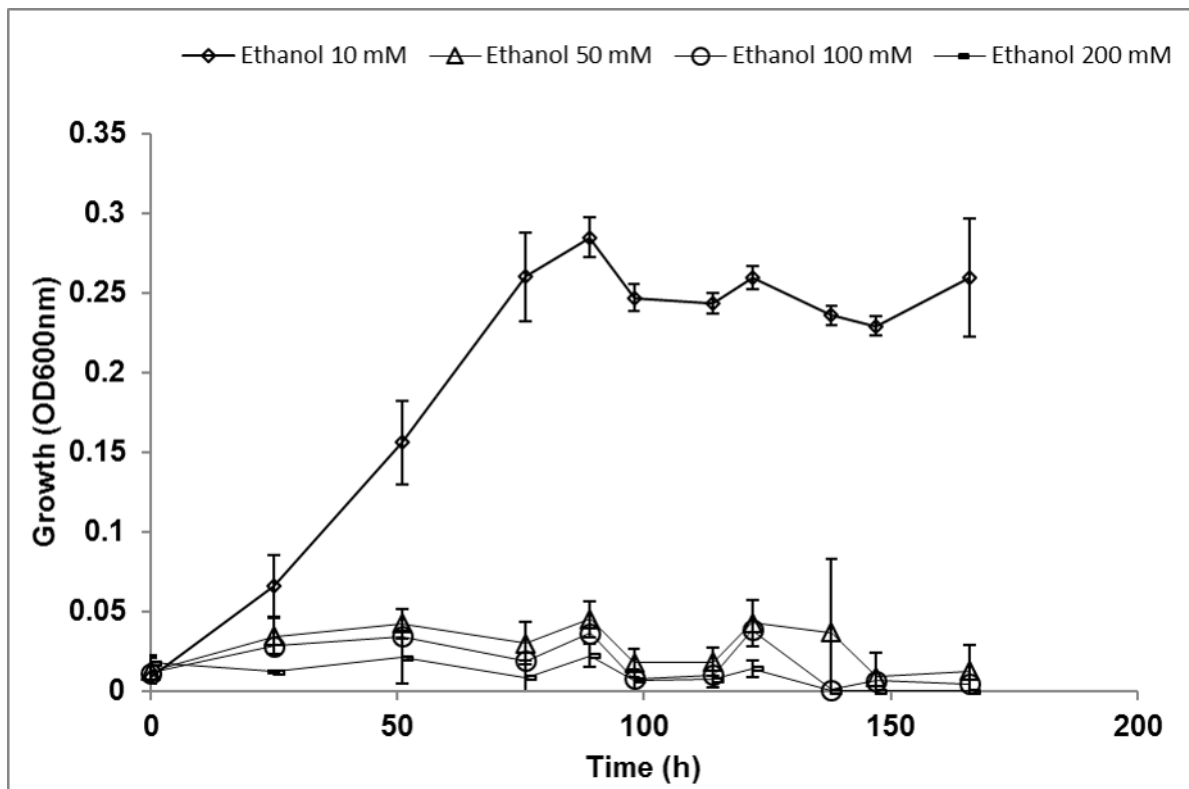


**Figure S1:** Growth of *A. acetethylicum* at different initial concentrations of glycerol and ethanol. Shown are mean values of triplicates  $\pm$  standard deviations.

# CHAPTER 4

---

## **Gluconate-fermentation by *Anaerobium acetethylicum*: an evidence for the involvement of modified Entner-Doudoroff pathway**

**Yogita Patil**, Madan Junghare, Nicolai Müller

(Submitted to Microbial Cell Factories: MICF-D-18-00366)

---

## 1. Abstract

**Background:** *Anaerobium acetethylicum* was isolated previously from an anaerobic enrichment culture from a methanogenic bioreactor sample, and groups phylogenetically within the family *Lachnospiraceae* within the order Clostridiales. Amongst a wide range of substrates, the strain mainly utilizes sugars, but also gluconate. For gluconate utilization, a modified Entner-Doudoroff (ED) pathway was found to be common in many *Clostridium* species in the past, e.g., in *C. formiaceticum*, *C. butyricum*, *C. acetobutylicum*, *C. pasteurianum*, *C. roseum*, and *C. tetanomorphum* (Bender et al., 1971). The objective of this study was to investigate the metabolic pathway of gluconate fermentation in *A. acetethylicum*.

**Results:** All possible enzyme activities of the initial pentose phosphate pathway, an ED pathway, and a modified ED pathway were tested by enzyme assays to investigate the mechanism of gluconate activation by *A. acetethylicum*. Total proteome analysis was done to support the presence of the respective enzyme systems. The genes responsible for gluconate fermentation stated in the proposed pathway were also identified in genome analysis. *Anaerobium acetethylicum* was found to use a modified Entner-Doudoroff pathway for gluconate degradation which is specifically induced during growth with this substrate. The main enzymes involved in the conversion of gluconate to acetate, formate, ethanol, and hydrogen are gluconate dehydratase, 2-keto-3-deoxy-gluconate (KDG) kinase, and 2-keto-3-deoxy-6-phospho-gluconate (KDPG) aldolase.

**Conclusions:** Gluconate is converted to KDG by gluconate dehydratase in a dehydration reaction. KDG is then converted into KDPG by KDG kinase and KDPG is split to pyruvate and glyceraldehyde-3-phosphate by KDPG aldolase. Further, glyceraldehyde-3-phosphate is converted to pyruvate by enzymes of the lower glycolysis pathway. From pyruvate, acetate, formate, ethanol, and hydrogen are formed as major fermentation products. The complete gluconate fermentation pathway is proposed based on the results of enzyme activity measurements, total proteome analysis, and genes identified by genome analysis.

**Key words:** *Anaerobium acetethylicum*, proteomics, enzyme assays, gluconate, modified ED pathway, acetate, ethanol, formate, carbon dioxide, proteome analysis.

---

## 2. Introduction

D-gluconic acid was discovered in 1870 by Hllasiwetz and Habermann (Röhr et al., 1983). It occurs naturally in plants, fruits, rice, meat, dairy products, honey, and wine (Ramchandran et al., 2006). Gluconic acid is derived from glucose by an oxidation reaction catalysed by microbial enzymes. It is a non-corrosive mild organic acid which is also responsible in part for the sour taste of wine and fruit juices (Ramachandran et al., 2006). Gluconic acid is produced from glucose by *Aspergillus niger* (Znad et al., 2004), and gluconic acid and its salts are applied in food, pharmaceutical, textile, detergent and leather industries.

The genus *Clostridium* is one of the largest and diverse genera known within the domain prokaryotes, and comprises anaerobic, Gram-positive, spore-forming bacteria that reside in diverse habitats such as soil, sediment, decomposing biological material and the lower gut of mammals (Suresh et al., 2007). In the past, studies reported on galacturonate and/or gluconate fermentation by *Clostridium* spp., e. g. *C. aceticum*, *C. pasteurianum*, *C. roseum*, *C. butyricum*, *C. rubrum*, and *C. acetobutylicum* (Andreesen and Gottschalk, 1969; Bender et al., 1971; Schink and Zeikus, 1983; Ng and Vaughn, 1963; Forsberg et al., 1987) but little is known about the degradation pathways and the associated genes in the solventogenic Clostridia (Servinsky et al., 2014). Johnson et al., (1931) showed that the product pattern in solventogenic fermentations depends on the degree of oxidation of substrates, e.g., gluconate degradation led to acetone as product, while glucose was mainly converted to butanol.

The first description of the so-called Entner-Doudoroff pathway (ED pathway) of glucose and gluconate degradation in *Pseudomonas saccharophila* dates back to 1952 (Entner and Doudoroff, 1952). Here, gluconate is initially phosphorylated by a kinase to 6-phosphogluconate which is then subsequently dehydrated to 2-keto-3-deoxy-6-phosphogluconate (KDPG). KDPG is then cleaved to pyruvate and glyceraldehyde-3-phosphate (GAP) by an aldolase (Entner and Doudoroff, 1952). Later, it was demonstrated that *Pseudomonas saccharophila* degrades galactose by a slightly different mechanism involving oxidation of galactose to its aldonic acid galactonic acid with subsequent dehydration to 2-keto-3-deoxy-galactonic acid. The latter compound is then phosphorylated and cleaved to pyruvate and GAP, which is often referred to as the De Ley-Doudoroff pathway (DD pathway) (De Ley and Doudoroff, 1957, Lamble et al., 2004). In the beginning exclusively known in *P. saccharophila*, the presence of the ED and DD pathways turned out

---

to be present also in other bacteria, most of them being aerobic (Kerstens and De Ley, 1968). While this pathway has become a famous textbook example describing a pathway of glucose utilization alternative to the Embden-Meyerhof-Parnas pathway of glycolysis, the term “ED pathway” was also used to describe microbial utilization of one of its intermediates, namely gluconate (Entner and Doudoroff, 1952). In contrast, the term “modified ED pathway” was used in numerous studies in the past addressing different variations of this pathway. The modified ED pathway in *Clostridium* species describes a set of enzyme reactions analogous to the ED pathway, with the only exception that gluconate is initially dehydrated to 3-keto-2-desoxy-gluconate and then phosphorylated to 2-keto-3- desoxy-6-phospho-gluconate analogous to the oxidation of galactonate in *Pseudomonas saccharophila* (Bender et al., 1971, DeLey and Doudoroff, 1957). Another modified Entner-Doudoroff pathway can be found in glucose degradation in the thermophilic archaeon *Sulfolobus solfataricus* (De Rosa et al., 1984). This organism uses a non-phosphorylative variation of the ED pathway (npED pathway) in which gluconate is dehydrated to 2-keto-3-deoxygluconate which is split to pyruvate and glyceraldehyde (De Rosa et al., 1984).

The early studies on *C. formicaceticum*, formerly classified as *C. aceticum* (Andreesen et al., 1970), reported that gluconate fermentation occurs via a modified Entner-Doudoroff (ED) pathway, also known as semi-phosphorylative ED pathway (Ahmed et al., 2005), i.e. breakdown of gluconate is initiated by a dehydration to yield 2-keto-3-deoxy-gluconate (KDG) which is subsequently phosphorylated by a specific kinase which yields 2-keto-3-deoxy-6-phosphogluconate (KDPG) as an intermediate (Andreesen and Gottschalk, 1969; Bender et al., 1971). However, more recently Servinsky et al., (2014) studied glucose, gluconate and galacturonate metabolism in *C. acetobutylicum* and provided the first experimental evidence that gluconate fermentation occurs via the Entner-Doudoroff (ED) pathway. On the contrary, many other bacterial species, e.g., *Escherichia coli* (Eisenberg and Dobrogosz, 1967), *Salmonella typhimurium* (Fraenkel and Horecker, 1964), *Pseudomonas natriegens* (Eagon and Wang, 1962), and *Streptococcus faecalis* (Sokatch and Gunsalus, 1957) ferment gluconate through the ED pathway. This pathway involves a gluconokinase that initially phosphorylates gluconate to 6-phosphogluconate, a dehydratase that converts 6-phosphogluconate to KDPG, and an aldolase which cleaves KDPG to pyruvate and glyceraldehyde-3-phosphate. Gluconic acid is degraded fermentatively also by lactic acid bacteria such as *Lactobacillus reuteri* and *L. mucosae*, and by acid-utilizing bacteria such as

---

*Megasphaera elsdenii* and *Mitsuokella multiacida*. Gluconic acid is fermented by lactic acid bacteria to lactate and acetate, which are subsequently used by acid-utilizing bacteria such as *M. elsdenii* to form butyrate (Tsukahara et al., 2002). The fermentation of gluconate (34.1 mM) by *E. coli* ML30 produces mainly ethanol (6.3 mM), acetate (36.6 mM), formate (11.9 mM), lactate (4.8 mM), and succinate (4.8 mM) (Eisenberg and Dobrogosz, 1967) while gluconate fermentation (28.2 mM) by *C. acetobutylicum* yields mainly acetate (29.2 mM) and butyrate (9 mM) (Servinsky et al., 2014). In contrast to this, the recently described *A. acetethylicum* ferments gluconate (8.4 mM) to mainly acetate (8.4 mM), formate (4.6 mM), ethanol (4.9 mM), and hydrogen (2.1 mM), but no butyrate (Patil et al., 2015). The results obtained favour former ideas about the involvement of a modified Entner-Doudoroff pathway in gluconate metabolism. In the present study, we describe the enzymes involved in the fermentation of gluconate by *A. acetethylicum*. Results of direct enzyme activity measurements as well as results from total proteome analysis and genes identified in genome analysis were used to propose the gluconate fermentation pathway in *A. acetethylicum*.

Fermentation of glycerol by *A. acetethylicum* and its potential use for the production of biofuel was recently described (Patil et al. 2017). This strain can use a wide range of sugars and gluconate while producing ethanol, hydrogen, formate and acetate as major fermentation products, thus rendering it a potential biotechnologically relevant organism. Elucidation of the underlying metabolic pathways is therefore crucial in order to understand and eventually manipulate the electron flow during substrate conversion for efficient production of chemicals or for wastewater treatment.

### 3. Results

The recent study of *A. acetethylicum* indicated that gluconate is fermented to acetate, ethanol, formate, and hydrogen as major fermentation products, however the degradation pathway was not known (Patil et al., 2015). Three pathways commonly used by bacteria for gluconate degradation were investigated for their presence in *Anaerobium acetethylicum* by enzyme assays. For a more structured overview, the proposed pathway is divided into a modified ED pathway and three branches according to the final fermentation products: the acetate, hydrogen, formate, and ethanol branches.

---

### **i) Gluconate degradation**

The activities of key enzymes detected in cell-free extracts included gluconate dehydratase (E. C. 4.2.1.39), 2-keto-3-deoxy-gluconate-kinase (KDG kinase, E. C. 2.7.1.45) and KDPG aldolase (E. C. 4.1.2.14). Low activities for gluconokinase or 6-phosphogluconate dehydrogenase were observed in cell-free extracts (0.011 and 0.012 U/mg respectively). The average specific activity of the dehydratase observed in gluconate grown cell-free extract was 0.115 U/mg (Table 1). Further, the KDG kinase and KDPG aldolase activities were confirmed to be present in cell-free extract and measured by a coupled assay with lactate dehydrogenase. KDPG aldolase cleaves KDG in two steps to 3-carbon compounds, i.e. pyruvate and glyceraldehyde-3-phosphate. The average activities of KDG kinase and KDPG aldolase were 0.25 U/mg and 1.35 U/mg. Glyceraldehyde-3-phosphate was further converted to pyruvate by glycolysis enzymes (table 1, figure 1).

### **ii) Acetate production by acetate kinase through substrate-level phosphorylation**

The acetate-forming branch is usually coupled to energy conservation by acetate kinase forming ATP and acetate. Pyruvate: ferredoxin oxidoreductase forms acetyl-CoA from pyruvate and coenzyme A. Pyruvate: ferredoxin oxidoreductase activity was higher when benzyl viologen or methyl viologen was used as artificial electron acceptor compared to activities with ferredoxin as electron acceptor (table 1). Acetyl-CoA is converted to acetyl phosphate by phosphotransferase, and the average activity was found to be 0.947 U/mg. Further from acetyl-phosphate, acetate is formed by acetate kinase. The average activity of acetate kinase was found to be 0.176 U/mg.

### **iii) Ethanol production**

An NADH-dependent alcohol dehydrogenase activity was detected which suggests that pyruvate is further metabolized to ethanol by *A. acetethylicum*. Part of the acetyl-CoA is most likely converted into acetaldehyde by acetaldehyde dehydrogenase, and acetaldehyde can be converted into ethanol by alcohol dehydrogenase. The average activities observed for aldehyde dehydrogenase and alcohol dehydrogenase were 0.011 U/mg and 0.012 U/mg, respectively.

#### iv) Production of formate and H<sub>2</sub>

Activities of formate dehydrogenase and hydrogenase were measured with benzyl viologen as artificial electron acceptor (maximum activities 0.024 U/mg and 4.3 U/mg and respectively). No activity was observed with NAD<sup>+</sup> as electron acceptor. Incubation times of 2 to 3 minutes were required to start the activity with benzyl viologen. With benzyl viologen as electron acceptor, the activity of hydrogenase was found to be higher than the activity of formate dehydrogenase.

**Table 1.** Enzyme activities in the proposed pathway of gluconate fermentation in cell-free extracts of *A. acetethylicum* grown with gluconate. (Average of three measurements  $\pm$  standard deviation in two independent cell free extracts CFE, BV = benzyl viologen, MV = methyl viologen, Fd = ferredoxin).

Enzyme assay	Average specific activities mU/mg	
	CFE-1	CFE-2
Gluconate dehydratase (E.C.4.2.1.39)	366 $\pm$ 25.4	321 $\pm$ 26.5
KDG kinase (E.C.2.7.1.45)	129 $\pm$ 22	29 $\pm$ 25
KDPG aldolase (E.C.4.1.2.14)	1351 $\pm$ 112	854 $\pm$ 61
Glyceraldehyde-3-phosphate dehydrogenase (E.C.1.2.1.12)	746 $\pm$ 20	630 $\pm$ 54
phosphoglycerate kinase (E.C.2.7.2.3)	728 $\pm$ 32	940 $\pm$ 140
Enolase (EC 4.2.1.11)	629 $\pm$ 29	1314 $\pm$ 29
Pyruvate kinase (E.C.2.7.1.40)	130 $\pm$ 84	107 $\pm$ 12
Formate dehydrogenase with BV (E.C.1.2.1.2)	10 $\pm$ 3	24.7 $\pm$ 3
Hydrogenase with BV (E.C.1.12.99.6)	4348 $\pm$ 691	2706 $\pm$ 58
Acetyl phosphotransferase (E.C.2.3.1.8)	947 $\pm$ 152	805 $\pm$ 8
Acetate kinase (E.C.2.7.2.1)	176 $\pm$ 29	144 $\pm$ 7.6
Alcohol dehydrogenase (E.C.1.1.1.1)	11 $\pm$ 1	4.6 $\pm$ 1.5
Acetaldehyde dehydrogenase (E.C.1.2.1.10)	11.2 $\pm$ 0.95	12.12 $\pm$ 0.81
Pyruvate: acceptor oxidoreductase with BV (E.C.1.2.7.1)	4941 $\pm$ 656	212 $\pm$ 4.4
Pyruvate: acceptor oxidoreductase with MV or Fd (E.C.1.2.7.1)	123 $\pm$ 50 (Fd)	1541 $\pm$ 7 (MV)
Glutamate dehydrogenase (E.C.1.4.1.4)	133 $\pm$ 5.4	43 $\pm$ 1.3
Gluconokinase (E.C.2.7.1.92)	11 $\pm$ 4	12.9 $\pm$ 0.6
6-phosphogluconate dehydrogenase (EC 1.1.1.44)	12 $\pm$ 8	12.4 $\pm$ 0.09

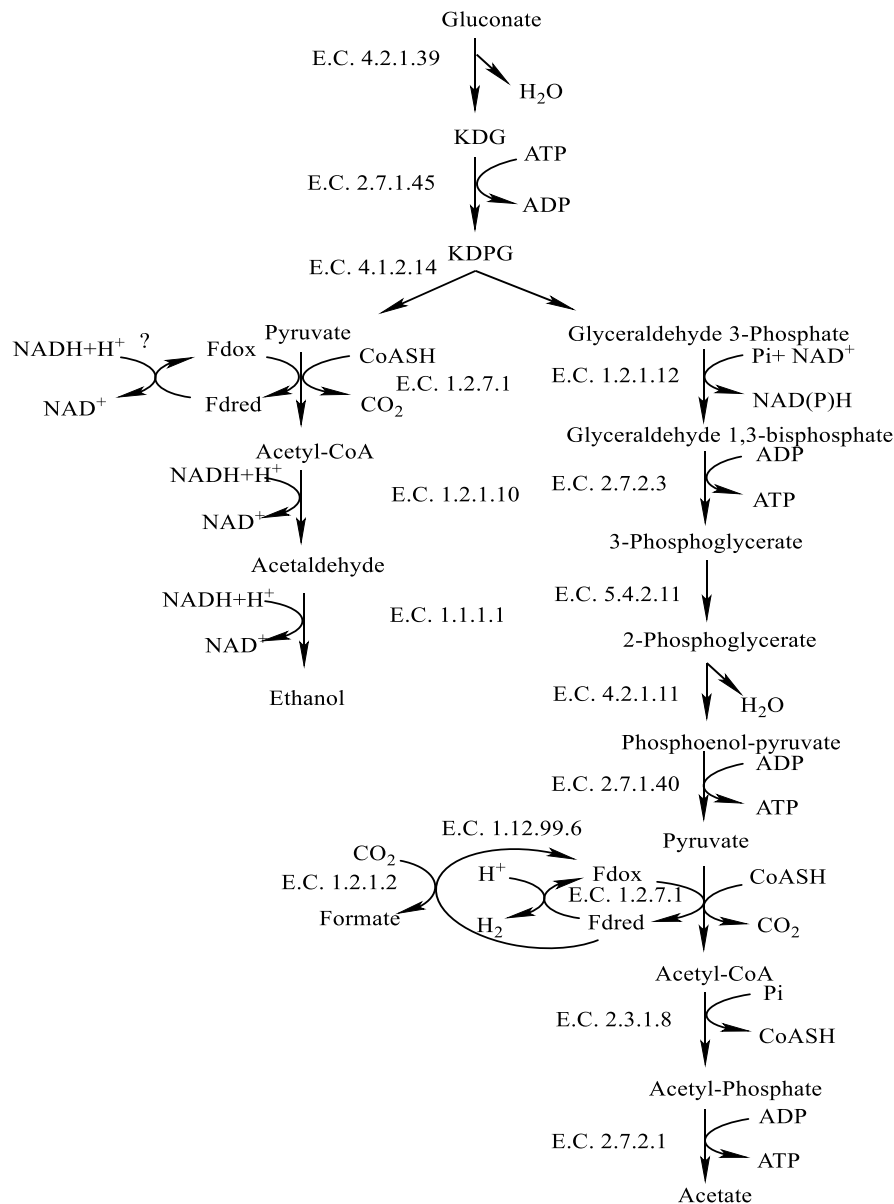


**Figure 1:** The proposed pathway for gluconate fermentation. Gluconate dehydratase (E. C. 4.2.1.39), 2-keto-3-deoxy-gluconate-kinase (KDG kinase, E. C. 2.7.1.45) and KDPG aldolase (E. C. 4.1.2.14, Ga0116910-101517). Glyceraldehyde-3-phosphate dehydrogenase (EC 1.2.1.12 Ga0116910-1001392), phosphoglycerate kinase (Ga0116910-1001391), phosphoglycerate mutase (Ga0116910-1001389). Pyruvate kinase (EC 2.7.1.40 Ga0116910-1004153), pyruvate:ferredoxin oxidoreductase (Ga0116910-103224). Acetate kinase (EC 2.7.2.1, Ga0116910-103636, 104214 and 1001586), phosphate acetyltransferase (EC 2.3.1.8, Ga0116910-1001587), pyruvate: acceptor oxidoreductase (pyruvate synthase; EC 1.2.7.1), acetaldehyde dehydrogenase (EC 1.2.1.10), and alcohol dehydrogenase (EC 1.1.1.1. Ga0116910-102016, 101528,102215, 1004154 and 1004188), formate dehydrogenase (E.C.1.2.1.2), hydrogen: acceptor oxidoreductase (hydrogenase; EC 1.12.99.6 Ga0116910-100543, 1001466, 1001467, 1001470, 1001473 and 1001507).

---

### 3.5. Identification of genes potentially involved in gluconate fermentation in the genome of *Anaerobium acetethylicum*

The genome sequence of *A. acetethylicum* revealed the presence of four gluconate: proton symporters which are likely to be involved in uptake of gluconate and are encoded by Ga0116910-10413, Ga0116910-10069, Ga0116910-100214, and Ga0116910-10418. The genes Ga0116910-101515 and 101516 encode a 2-dehydro-3-deoxyglucono-kinase, which is the enzyme involved in the semi-phosphorylative ED pathway that converts KDG into KDPG by phosphorylation. However, gluconate dehydratase, was not found which would be needed for activation of gluconate via KDG. Instead, a dihydroxy-acid dehydratase gene (locus tags Ga0116910-10068 and 101679) was identified which could be responsible for the observed gluconate dehydratase activity. The gene coding for KDPG aldolase (2-dehydro-3-deoxyphosphogluconate aldolase / (4S)-4-hydroxy-2-oxoglutarate aldolase) Ga0116910-101517 could be responsible for the conversion of KDPG to glyceraldehyde-3-phosphate and pyruvate. The glyceraldehyde-3-phosphate dehydrogenase Ga0116910-1001392, phosphoglycerate kinase Ga0116910-1001391, phosphoglycerate mutase Ga0116910-1001389 and pyruvate kinase Ga0116910-1004153 and 1001611 could further convert glyceraldehyde to one more molecule of pyruvate through the lower glycolysis pathway. The genes encoding pyruvate: ferredoxin / flavodoxin oxidoreductase are also present (locus tags Ga0116910-1005157, 101718 and 103224). Numerous genes encoding alcohol dehydrogenases were found during genome analysis, thus confirming the potential presence of enzymes responsible for the observed production of ethanol (Ga0116910-102016, 101528, 102215, 1004154 and 100149, 100152, 1001542, 101220, 100818, 1002131, 102038). A gene coding for acetaldehyde dehydrogenase (locus tag Ga0116910-1004188) was also identified. Also, the genes encoding acetate kinase (Ga0116910-103636, 104214 and 1001586) were identified in the genome. The formate C-acetyl transferase-activating enzyme with the gene loci Ga0116910-1004112, 100861, 102929, 103527, 103626, and formate C-acetyl transferase (Ga0116910-100860, 1004109 and 102934, 102935) were found which could be responsible for the production of formate during gluconate fermentation. The genes coding for enzymes that could produce hydrogen were also identified, i. e., putative iron-only hydrogenase subunits (Ga0116910-100467, 1001473, 1001507) and NADP<sup>+</sup>-reducing hydrogenase subunit D Ga0116910-1001466, subunit C Ga0116910-1001467, subunit B Ga0116910-1001468, and subunit A Ga0116910-1001470. Additionally, a ferredoxin-

---

dependent hydrogenase is present at gene locus Ga0116910-100545. Hence, all the genes for enzymes potentially involved in a Modified Entner-Doudoroff pathway were identified in the genome analysis.

The genes encoding enzymes for the other metabolic pathways such as transketolases and transaldolases for the pentose phosphate pathway, and kinases for the EMP pathway were also identified. Three genes for transaldolases (locus tag Ga0116910-101533, 101534, and 103542) could be involved in the pentose phosphate pathway. Transketolases (locus tags Ga0116910- 101529, 101530, 102021, 102022, 102026, 102027, 103543, 103630, 103631, 104022, 104023) were also identified in the genome. Also ribulokinases (Ga0116910-101326, 103624) and xylulokinases (Ga0116910-1002210, 101321, 102020, 102050, 102219, 102335, 10372, and 10419) are present. Two genes for glucokinase were identified (Ga0116910-101179, 102147) as well as the genes for fructokinase (Ga0116910-101026, 10296).

### **3.6. Gluconate-degrading enzymes identified by total proteome analysis**

Gluconate-degrading enzymes were identified by total proteome analysis according to the methods described before (Patil et. al., 2016). Two enzymes for the aforementioned dihydroxy acid dehydratase with locus tags Ga0116910\_10068, 10069, 101679 (the prefix has been omitted from the gene locus tag number in the following section) were identified in both glucose-grown and gluconate-grown cell-free extracts. In the gluconate-grown extract, the dehydratase gene 10068 is expressed twofold higher than in the glucose-grown extract (Figure 2). The above-mentioned genes carrying the annotation 2-dehydro-3-deoxygluconokinase (Ga0116910-101515 and 101516) were also expressed. This annotation is the synonymous name for KDG kinase (EC 2.7.1.45). 2-dehydro-3-deoxygluconokinase (locus tag 101516) was present in higher abundance in gluconate-grown cells compared to glucose-grown cells. The gene locus of 2-dehydro-3-deoxyphosphogluconate aldolase (KDPG aldolase) is 101517 which was expressed at a higher score (1643.62) in gluconate-grown cell-free extract compared to glucose-grown cell-free extract (161.27). The gene product for a gluco-kinase (locus tag 101179) was found as well. Further, glucose 6-phosphate isomerase was expressed at a slightly lower score in gluconate-grown cell-free extract (1393.75) than in glucose-grown cell-free extract (2076.28). 6-phosphofructo-kinase

---

(gene locus 100633) had a score of 819.25 in gluconate-grown cell-free extract and 834.56 in glucose-grown cell-free extract (Figure 2). 6-Phosphogluconolactonase (gene locus 1001376) was expressed at a score of 147.49 and 154.15. Enzymes of the lower glycolysis pathway (Glyceraldehyde-3-phosphate dehydrogenase (gene locus 1001392), phosphoglycerate kinase (gene locus 1001391), phosphoglycerate mutase (gene locus 1001389) were expressed under both growth conditions (Figure 2). Enolase (gene locus 1001503) was expressed at low levels during growth with gluconate, the respective peptides could not be identified during growth with glucose. Two gene products for pyruvate kinase (gene loci 1004153 and 1001611) were found. Further, pyruvate: ferredoxin oxidoreductases 103224 and 1005157 were found, as well as formate C-acetyl transferase (gene locus 1004109). Acetaldehyde dehydrogenase and alcohol dehydrogenase (gene loci 1004188 and 100149 respectively) and acetate kinase (gene locus 1001586) and phosphotransacetylase (gene locus 1001587) were identified. The gene loci for hydrogenases were NADP<sup>+</sup>-reducing hydrogenase subunits HndA 1001470, HndB 1001507, HndC 1001467, HndD 1001466; ferredoxin-reducing hydrogenase large subunit 100545, iron-only hydrogenase large subunit 100543 were also present in the proteome. The genes expressed for other enzymes of the pentose phosphate pathway were also found. Transaldolase having locus 103542 and transketolase having gene locus 103543 had high scores in glucose-grown cells. The gene locus for phosphoglucomutase was 10473 with a higher score in glucose-grown cells (1354.41) than in gluconate-grown cells (929.87). Two genes for phosphoglucomutase were present which catalyze the reversible transfer of the phosphate group of glucose 1-phosphate to glucose 6-phosphate. The compared proteomics data are shown in Figure 2.

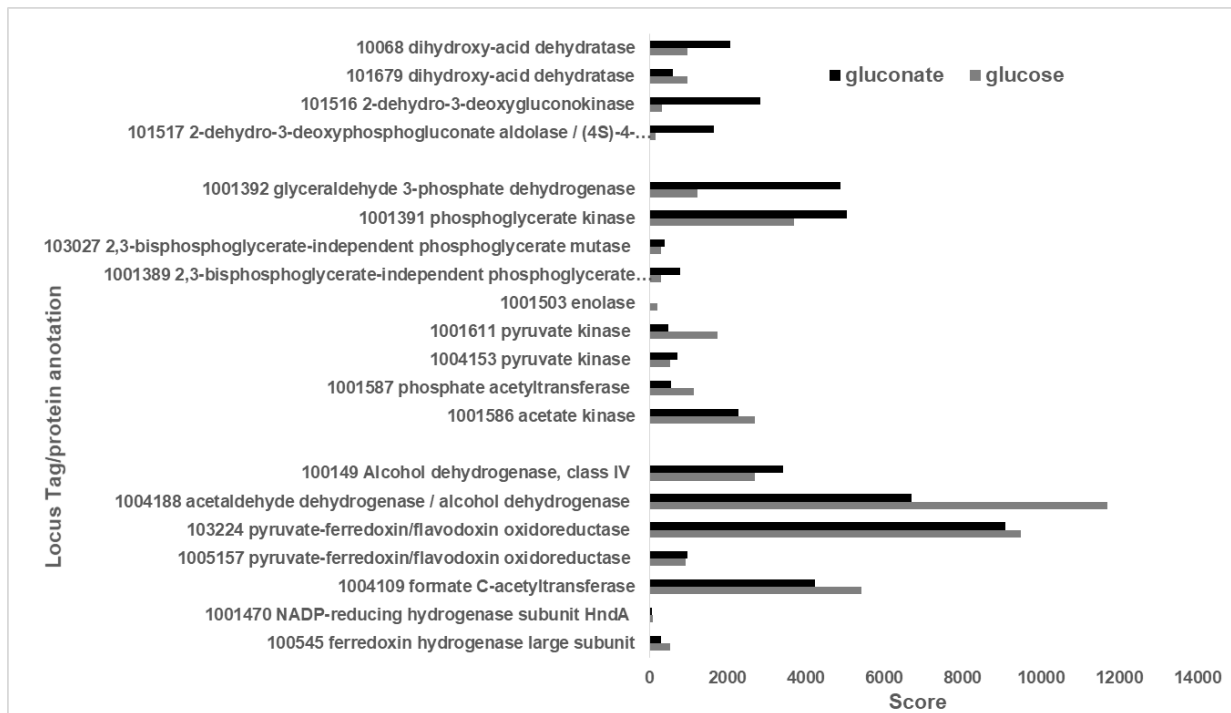


**Figure 2:** Comparative total proteome analysis of *A. acetithylicum* grown with glucose and gluconate. Shown are mascot scores as measures of protein expression levels.

**Table 2.** Proteins involved in the gluconate fermentation pathway were identified by total proteome analysis as described before (Patil et. al. 2016) in a cell-free extract of *A. acetethylicum* grown on gluconate.

Gene loci	IMG predicted function <sup>b</sup>	Coverage <sup>c</sup>	Peptides <sup>d</sup>	Score <sup>e</sup>	Mass (kDa) <sup>f</sup>
Ga011691 0_					
101517	2-dehydro-3-deoxyphosphogluconate aldolase	79.69	18	1643.62	34.2
1001	Triosephosphate isomerase	89.92	11	4187.80	26.6
102914	Triosephosphate isomerase	67.56	12	1509.70	29.7
1001392	Glyceraldehyde-3-phosphate dehydrogenase	70.92	15	3876.50	35.4
1001391	phosphoglycerate kinase	78.34	20	5899.78	42.0
1001389	2,3-bisphosphoglycerate-independent phosphoglycerate mutase	31.91	11	861.40	56.6
103027	2,3-bisphosphoglycerate-independent phosphoglycerate mutase	14.68	4	176.21	44.5
1001503	Enolase	22.88	6	305.88	47.6
1001300	Phosphoenolpyruvate carboxykinase	61.16	27	7345.10	61.1
1004153	Pyruvate kinase	12.22	3	59.73	63.6
1005167	Pyruvate, orthophosphate dikinase	68.65	42	7956.88	96.4
1002196	Indolepyruvate ferredoxin oxidoreductase alpha subunit	19.83	8	284.91	63.1
	Indolepyruvate ferredoxin oxidoreductase beta subunit	21.69	3	166.97	20.7
1004188	Acetaldehyde dehydrogenase / alcohol dehydrogenase	83.01	58	22648.12	95.2
101528	Alcohol dehydrogenase	71.05	17	3608.46	39.8
101313	NAD(P)-dependent dehydrogenase, short-chain alcohol dehydrogenase family	10.63	2	158.00	27.4
1001587	Phosphate acetyltransferase	27.49	5	165.14	35.1
1001586	Acetate kinase	39.04	9	411.45	43.0
1004109	Formate C-acetyl transferase	73.68	35	4216.88	75.7

a. Integrated microbial genomes (IMG, Markowitz et al., 2009) Gene locus tag (Ga0116910\_). b. Protein identification and function detection from the IMG annotation. c. Sequence coverage represents the extents of peptides obtained during MS-MS identification of the respective proteins. d. The number of proteins obtained during MS-MS identification. e. Mascot search score. f. Peptide mass calculated by MS-MS identification.

---

## 4. Discussion

Microorganisms running their energy metabolism through fermentation have to be efficient in converting the available energy into ATP. Anaerobic and aerobic microorganisms use various glycolytic pathways for the breakdown of sugars and sugar acids, yet the causes favouring one pathway over the other one might depend on the environmental conditions and are not clearly understood. It was hypothesized that various microorganisms use modifications of the EMP or ED – pathway to find an optimal balance between actual energy yield and metabolic cost for protein synthesis (Flamholz et al., 2013). The EMP pathway requires substantially more enzymes than the ED or modified ED pathway. The advantage of the modified ED pathway is that it requires less energy to activate the substrate gluconate. On the other hand, the ED pathway yields only one mole of ATP per mole of sugar as opposed to two mole of ATP per mole of sugar in the EMP pathway (Flamholz et. al 2013). The EMP pathway and ED pathway have unique enzymes in their upper parts, but they share the enzymes of the lower glycolysis pathway. The EMP pathway uses hexokinase and 6-phospho-fructokinase to activate the substrate, while the ED and modified ED pathway have the KDPG aldolase as key enzyme of the upper glycolytic part.

In the past, *Clostridium* spp., *Escherichia coli* and *Erwinia chrysanthemi* were reported to maintain pathways to metabolize galacturonate (Richard and Hilditch, 2009; van Rijssel et al., 1999; Ashwell, 1952; Peekhaus and Conway, 1998). The EMP is the major sugar degradation pathway in *Clostridium* spp. Here, gluconate is fermented through a modified ED pathway in *C. aceticum* (Andreesen et. al., 1969). In a similar study, it was shown in *Rhodopseudomonas spheroides* that gluconate degradation started with a dehydration reaction and not by initial phosphorylation (Szymona and Doudoroff, 1960). Also the number of bacteria known to metabolize compounds structurally similar to gluconate via the corresponding non-phosphorylated keto-deoxy acids, and the cofactor requirement of the above three enzymes has been studied in detail in gluconate fermentation by *C. aceticum* (Andreesen et. al., 1969).

The Embden-Meyerhof-Parnas (EMP) pathway is a very common glycolytic pathway in bacteria and other organisms (Kim and Gadd, 2008; Fraenkel, 1996), but also pathways like the Entner–Doudoroff (ED) and the phosphoketolase pathways are used by many types of organisms as alternative pathways for specific reasons. It was shown that there are

---

biologically multiple feasible routes for glucose metabolism (Kim and Gadd, 2008; Conway, 1992; Melendez-Hevia et al., 1997; Entner and Doudoroff, 1952; Bar-Even et al., 2012; Sung et al., 1988). Among these, the EMP and ED pathways are the most common bacterial glycolytic pathways, in which the substrate is phosphorylated and then cleaved into two molecules of three-carbon units (e.g. pyruvate and glyceraldehyde-3-phosphate) which are further metabolized to produce ATP through substrate-level phosphorylation (Fraenkel, 1996; Fuhrer et al., 2005). Specifically, hexokinase is unique to the EMP pathway while 6-phosphogluconate dehydratase (or pentose phosphate-pathway), and KDPG aldolase are unique to the ED pathway. However, the absence of enzyme activities for the two enzymes in cell-free extracts, e.g. hexokinase (catalyzing the conversion of gluconate to 6-phosphogluconate) and 6-phosphogluconate dehydratase (catalyzing the conversion of 6-phosphogluconate to KDPG), suggests that gluconate and/or glucose are metabolized by *A. acetethylicum* via the modified ED pathway (Ashwell pathway, Ashwell et. al., 1960). The complete gluconate fermentation pathway proposed on the basis of our results is shown in figure 1.

In order to identify the pathway of gluconate metabolism in *A. acetethylicum*, enzyme assays for the possible ED pathway and the modified ED pathway were performed. There are three possible pathways for gluconate fermentation: The first one is the combination of initial reactions of the pentose phosphate pathway and reactions of the lower part of glycolysis to produce pyruvate which in turn could be converted to acetate, formate, ethanol, and hydrogen as main products. Glucono-kinase could convert gluconate to 6-phosphogluconate and 6-phosphogluconate dehydrogenase could oxidize it to ribulose-5-phosphate. Further ribulose-5-phosphate could be metabolized by epimerase, transketolases and transaldolase into glyceraldehyde-3-phosphate. Glyceraldehyde-3-phosphate could be converted to pyruvate via lower glycolysis reactions. The respective enzyme activities were found to amount to few miliunits only (maximum 14 mU/mg) and were not reproducible. The second possible pathway of gluconate degradation is the Entner-Doudoroff pathway used by many microorganisms (Eisenberg and Dobrogosz, 1967). In this pathway, gluconate could be converted to 6-phosphogluconate by gluconokinase. Later dehydratase could convert 6-phosphogluconate to 2-keto-3-deoxy-6-phosphogluconate. The activity for gluconokinase was also very low (0.011 U/mg). Since gluconokinase, 6-phosphogluconate dehydrogenase and epimerase activities were not found in cell-free extract of *A. acetethylicum* the

---

involvement of the pentose phosphate pathway and the ED pathway as major sugar-degrading pathways could not be confirmed. The third possible pathway is the modified ED pathway analogous to the one in *C. aceticum* (Andreesen and Gottschalk, 1969). This system involves three main enzymes. Gluconate dehydratase converts gluconate to 2- keto-3-deoxy-gluconate (KDG). Then KDPG is formed from KDG by a kinase, and KDPG is converted to pyruvate and glyceraldehyde-3-phosphate by KDPG aldolase. This pathway was confirmed to be present in *A. acetethylicum* in this study. Pyruvate and glyceraldehyde-3-phosphate were produced by the activity of KDPG aldolase. Glyceraldehyde-3-phosphate was further converted to one more molecule of pyruvate by the lower part of glycolysis to form acetate, formate, ethanol, and hydrogen as final products of fermentation. The activities of gluconate dehydratase, KDG kinase, and KDPG aldolase were detected in cell-free extracts of *A. acetethylicum* and thus indicate the presence of a modified ED pathway of the DeLey-Doudoroff type, with initial sugar acid dehydration followed by phosphorylation as observed in *Clostridium* species before (Bender et al., 1971). Also all the genes coding for enzymes of the pathway were identified in the genome. Proteome analysis additionally verified the expression of all necessary enzymes. The enzyme for initial dehydration of gluconate was not identified in the genome or proteome at first sight, as no gene with the annotation “gluconate dehydratase” was found. Instead, three genes carrying the annotation “dihydroxy acid dehydratase” (Ga0116910\_10068, 10069, 101679) were found, of which gene locus Ga0116910\_10068 and Ga0116910\_101679 were identified in the proteome of both gluconate- and glucose-grown cells. Such an enzyme was described already in *Sulfolobus solfataricus* which uses a non-phosphorylative ED pathway for glucose oxidation (Kim and Lee, 2005). The catalytic promiscuity of this enzyme allows this organism to dehydrate a variety of different sugar acids with the same enzyme. This promiscuity was in part described as a general feature of evolutionarily undeveloped and inefficient enzyme systems, but could also be explained as an adaptation to extreme environments to maintain metabolic flexibility of the strain (Lamble et al., 2004). Maintaining one gene, i. e., enzyme for several purposes could also contribute to the overall robustness of the ED pathway in *S. solfataricus*, thus rendering the organism less sensitive to spontaneous gene mutations in a harsh environment (Figueiredo et al., 2017). Also in *A. acetethylicum*, a promiscuous dehydratase could contribute to keep metabolic expenditures low while being adaptable to rapidly changing environmental conditions at the same time as to be expected in a bioreactor, the source of this

---

organism. Moreover, expressing a small set of enzymes for multiple purposes could help the cell to reduce maintenance costs and to maintain a robust degradation pathway.

During growth with glucose or gluconate, all relevant enzymes of the pathway were identified in the proteome, some of them however at expression levels that are appropriate for housekeeping enzymes or enzymes in anabolic functions. For instance, the enolase catalyzing the conversion of 2-phosphoglycerate to phosphoenolpyruvate had a Mascot-score of around 206 in glucose-grown cells, while the enzyme was absent in gluconate-grown cells. Yet, the activity of enolase was detected by enzyme assays in the range of 0.629 U/mg. The highest observed Mascot-score was 14696 for pyruvate water dikinase observed in glucose-grown cells, and most other key glycolytic enzymes were expressed in the same order of magnitude. It is therefore surprising why enolase was detected at such a low Mascot score. A similarly low expression of enolase was observed before in *A. acetethylicum* grown with glycerol (Patil et al., 2017). As most other enzymes of the lower glycolytic pathway were expressed, a different yet unidentified enzyme might take over the function of enolase. It is conceivable that an enolase-like enzyme is located in the membrane, which was not covered by the proteome analysis in this study. Such a membrane-bound enolase was observed before in the pathogenic bacterium *Pseudomonas aeruginosa*, however, this enzyme did not exhibit catalytic activity (Ceremuga et al., 2014). Alternatively, GAP may be metabolized by enzymes different from the conventional glycolysis enzymes. Recently, involvement of the serine ammonium lyase system was proposed for anaerobic oxidation of acetate by *Syntrophaceticus schinkii* (Manzoor et al., 2016). Here, the reverse Wood-Ljungdahl-pathway of acetyl-CoA oxidation to formate and CO<sub>2</sub> was suggested to be bypassed by conversion of acetyl-CoA to pyruvate with subsequent conversion to serine which could be further converted to formate through the glycine cleavage system. The enzymes 3-phosphoglycerate dehydrogenase, phosphoserine aminotransferase, and glutamate dehydrogenase were identified in the proteome at comparably high scores (table 2, figure 2). A pathway leading from GAP to pyruvate could therefore work as follows: First, GAP is oxidized via 1,3-bisphosphoglycerate to 3-phosphoglycerate. The responsible enzymes GAP-dehydrogenase and phosphoglycerate kinase were identified in the proteome of *A. acetethylicum* (table 2, figure 2). Further, 3-phosphoglycerate is oxidized to 3-phosphohydroxypyruvate by 3-phosphoglycerate dehydrogenase. 3-phosphohydroxypyruvate is transaminated with glutamate to O-phosphoserine and 2-ketoglutarate by phosphoserine

---

aminotransferase. 2-ketoglutarate is reduced and aminated to glutamate with NADH and ammonium by glutamate dehydrogenase, thus completing the reaction cycle. Phosphoserine could be dephosphorylated to serine by a hydrolase and serine be deaminated to pyruvate. This pathway would form only one ATP from GAP to pyruvate, as opposed to the lower glycolysis pathway which forms two, which would be clearly a disadvantage for a fermenting bacterium. Moreover, enzymes that could catalyze the latter two reactions were not detected in the proteome. It remains open what might be the cause of the comparably high expression of 3-phosphoglycerate dehydrogenase, phosphoserine ammonium-transferase and glutamate dehydrogenase. Possibly, these enzymes are responsible for fast amino acid synthesis and thus the fast growth of this bacterium (doubling time 1 hour, Patil et al., 2015).

## 5. Conclusions

The present study shows that *A. acetethylicum* uses a modified Entner-Doudoroff (ED) pathway for gluconate fermentation, similar to the pathway found previously in *Clostridium* species. All putative genes for the enzymes of a modified ED pathway were identified in genome analysis. Also genes coding for a pentose phosphate pathway are present in the genome. Proteome analysis of cell-free extracts prepared from gluconate-grown cells confirmed the presence of the main enzymes of the modified ED pathway. Further support for the hypothesis of a modified ED pathway is provided by results of enzyme assays. This study presents the complete proposed pathway for gluconate fermentation by *A. acetethylicum*.

## 6. Materials and methods

### 6.1. Strain and growth conditions

*Anaerobium acetethylicum* (DSM 29698) was routinely grown with gluconate as sole source of carbon and energy using a sulfide-reduced freshwater medium as described (Patil et al., 2015), with modified trace element solution SL-13. Resazurin was used as a redox indicator. The medium was prepared in Widdel flasks and autoclaved at 121°C for 25 min. The pH was adjusted to 7.3 and the medium was distributed to 500 ml bottles, sealed with butyl rubber stoppers under a continuous stream of N<sub>2</sub>/CO<sub>2</sub> (80/20). Substrates were added from filter-

---

sterilized stock solutions as described before (Patil et al., 2015). Cultures were incubated in the dark at 30° C and growth was monitored by measuring turbidity at 600 nm in a spectrophotometer (Jenway 6300). The metabolic features and characteristics of *A. acetethylicum* were described before in an investigation on the draft genome sequence (Patil et al., 2016).

## **6.2. Preparation of cell-free extracts**

For preparation of cell-free extracts, 500 ml cultures of *A. acetethylicum* were grown anaerobically with gluconate (10 mM). Cells were harvested in the late exponential growth phase by centrifugation at 7,500 g for 20 minutes in a Sorvall RC5B centrifuge (Du Pont de Nemours, Bad Homburg, Germany) at 4°C. The cell pellet was washed with 50 ml of a 50 mM Tris-HCl buffer, pH 7.6, and centrifuged again. The cell pellet was finally suspended in 4 ml of 50 mM Tris-HCl containing 3 mM dithiothreitol (DTT), 5-10 mg protease inhibitor cocktail (cOmplete ULTRA Tablet, Mini, EDTA-free, EASY pack, Roche Diagnostics GmbH, Mannheim, Germany), 2 µl DNase I and 2 µl RNase. The suspended pellet was passed through a cooled French Pressure cell (SLM AMINCO) operated at 137 MPa as described (Junghare et al., 2016). The resulting cell suspension was centrifuged at 30,373 g for 30 min (BECKMAN optima TL Ultracentrifuge, TLA-110.4 rotor, Beckman, München, Germany) to remove intact cells and cell debris. The supernatant was used for enzyme activity measurements either directly or was stored at -20°C until use.

## **6.3. *In vitro* measurement of enzyme activities**

For investigation of the gluconate fermentation pathway in *A. acetethylicum*, enzyme activities were measured in cell-free extracts prepared from cultures grown with gluconate as substrate. Enzyme activities were measured under anoxic conditions in 1.5 ml quartz or glass cuvettes sealed with rubber septa. For addition of liquids, airtight Unimetrics microliter syringes were used (Macherey-Nagel, Germany). A spectrophotometer (Jasco V-630, Jasco, Gross-Umstadt, Germany) was used for the measurement of change in absorbance of the respective compounds (NADH, NAD<sup>+</sup>, benzyl viologen and methyl viologen, derivatized acetyl phosphate, ferredoxin, esters of coenzyme A). To confirm the gluconate fermentation pathway in *A. acetethylicum*, enzyme assays for the pentose phosphate pathway, an ED

---

pathway, and a modified ED pathway were performed at 30°C under anoxic conditions. One unit of specific enzyme activity (U/mg) was defined as one  $\mu$ mole of substrate consumed or product formed per minute and per milligram of protein. Specific enzyme activities were calculated from the average of three replicates of at least two separate cell-free extracts. Protein concentrations were determined using the Bradford assay as described (Bradford, 1976). Bovine serum albumin was used as a standard, and standard curves were prepared from the average values of three replicates of different concentrations ranging from 0 to 150  $\mu$ g /ml of standard. Samples were diluted according to the range of the calibration curve.

**Gluconate dehydratase** (E.C.4.2.1.39) activity was measured in cell-free extracts that catalyzed the conversion of gluconate to 2-keto-3-deoxy-gluconate (KDG) most similar to gluconate-fermentation by *Clostridium* species (Andreesen and Gottschalk, 1969). The 2 ml total reaction mixture contained potassium phosphate buffer of pH 7.6, 3 mM cysteine, 10 mM gluconate, 200  $\mu$ l of cell-free extract, 2 mM MgCl<sub>2</sub>, and 2 mM FeSO<sub>4</sub>. The mixture was incubated in a water bath at 30°C in anoxic serum vials. Samples were collected after specific time intervals and the resulting KDG formation was assayed with the thiobarbituric acid test (Weissbach and Hurwitz, 1959).

**KDG kinase** (E. C. 2.7.1.45). KDG kinase converts KDG into KDPG. The assay mixture for gluconate dehydratase was used as a source of KDG. The activity was measured in a coupled reaction with KDPG aldolase and lactate dehydrogenase. Pyruvate released by KDPG aldolase was thus converted to lactate while NADH was oxidized in the same reaction. The 1 ml assay mixture contained 50 mM potassium phosphate buffer, pH 7.6, 3 mM cysteine, 100  $\mu$ l of KDG, 0.25 mM NADH, 2 mM MnCl<sub>2</sub>, 5 mM ATP, 0.5 U lactate dehydrogenase, and 100  $\mu$ l cell-free extract. The decrease in NADH absorption was measured at 340 nm.

**KDPG aldolase** (E. C. 4.1.2.14) activity was assayed in a 1 ml reaction mixture containing 50 mM potassium phosphate buffer, pH 7.6, with 3 mM cysteine, 0.12 mM NADH, 0.5 U lactate dehydrogenase, and 10- 20  $\mu$ l of cell-free extract. The reaction was started by addition of 0.1- 0.2 mM KDPG. The decrease in NADH absorption was observed at 340 nm.

**Glyceraldehyde-3-phosphate dehydrogenase** (EC 1.2.1.12) activity was measured in 1 ml of a reaction mixture containing 50 mM potassium-phosphate buffer, pH 7.6, with 3 mM DTT, 0.2 mM NAD<sup>+</sup> and 10–50  $\mu$ l of cell-free extract. The reaction was initiated by addition

---

of 4 mM glyceraldehyde-3-phosphate. The increase of NADH absorption was measured at 340 nm ( $\epsilon_{340 \text{ nm}} = 6.22 \text{ mM}^{-1} \text{ cm}^{-1}$ , Ziegenhorn et al., 1976)

**Phosphoglycerate kinase** (E.C. 2.7.2.3) activity was measured in 1 ml of reaction mixture containing 50 mM Tris-HCl buffer, pH 7.6, 3 mM DTT, 0.2 mM NADH, 1 mM MgCl<sub>2</sub>, ATP 2.5 mM, and 10-20  $\mu\text{l}$  cell-free extract. The decrease of absorption of NADH at 340 nm was observed after addition of 10 mM 3-phosphoglycerate.

**Enolase** (E.C. 4.2.1.11) activity was measured in a reaction mixture containing 50 mM Tris-HCl buffer, pH 7.6, 3 mM DTT, 0.2 mM NADH, 1 mM MgCl<sub>2</sub>, 0.5 mM ADP, 0.5 U of D-lactate dehydrogenase, and 10-20  $\mu\text{l}$  cell-free extract. The reaction was initiated by the addition of 2 mM 2-phosphoglycerate.

**Pyruvate kinase** (EC 2.7.1.40) activity was measured coupled to the activity of lactate dehydrogenase. The 1 ml reaction mixture contained 50 mM Tris-HCl buffer, pH 7.6, with 3 mM DTT, 0.2 mM NADH, 10 mM phosphoenolpyruvate, 0.5 U of D-lactate dehydrogenase, 20–100  $\mu\text{l}$  of cell-free extract, and 0.5 mM ATP. The decrease in NADH absorption was measured at 340 nm.

**Acetate kinase** (EC 2.7.2.1) activity was measured discontinuously by measuring the decrease in acetyl phosphate concentration at 535 nm (Müller et. al., 2008, Nishimura and Griffith, 1981). A reaction mixture of 3 ml total volume was used and contained 50 mM Tris-HCl, pH 7.6, 3 mM DTT, 3 mM acetyl phosphate, 5 mM ADP, 5 mM MgCl<sub>2</sub> and 150  $\mu\text{l}$  of cell-free extract. Serum bottles were made anoxic by flushing with 100% N<sub>2</sub>. After all additions were made, bottles were incubated at 30<sup>o</sup> C in a water bath and 400  $\mu\text{l}$  samples were taken at specific time intervals with syringes. Then 300  $\mu\text{l}$  of a 1.6 M hydroxylamine solution adjusted to pH 7.0 was added. After incubation for 5 minutes at room temperature, 300  $\mu\text{l}$  of a 10% FeCl<sub>3</sub> solution in 1.36 M HCl / 0.4 M trichloroacetic acid was added. The mixture was incubated for 5 minutes at room temperature and absorption at 535 nm was measured. The concentration of acetyl phosphate was detected by preparing a standard calibration curve from 0 to 7 mM.

**Pyruvate: acceptor oxidoreductase/pyruvate synthase** (EC 1.2.7.1) activity was measured by the change of absorption of benzyl viologen (11-dibenzyl-4, 4-bipyridinium-dichloride) at 578 nm ( $\epsilon_{578 \text{ nm}} = 8.65 \text{ mM}^{-1} \text{ cm}^{-1}$ ) (Diekert and Thauer, 1978) or oxidized ferredoxin at

---

390 nm ( $\epsilon_{390} = 30 \text{ mM}^{-1} \text{ cm}^{-1}$ ) (Gersonde, Trittelvitz et al., 1971). The 1 ml reaction mixture contained 50 mM Tris-HCl, pH 7.6, with 3 mM DTT, 0.5 mM coenzyme A, 2 mM benzyl viologen and 10–100  $\mu\text{l}$  of cell-free extract and 10 mM sodium pyruvate (Müller et al., 2008, Williams et al., 1987, Uyeda and Rabinowitz, 1971).

**Phosphate acetyltransferase** (EC 2.3.1.8) activity was assayed as the formation of acetyl-coenzyme A at 233 nm ( $\epsilon_{233} = 4.44 \text{ mM}^{-1} \text{ cm}^{-1}$ ) from acetyl phosphate and coenzyme A (Müller et al., 2008., Bergmeyer, 1974). The 1 ml reaction mixture contained 50 mM Tris-HCl, pH 7.6 with 3 mM DTT, 3 mM acetyl phosphate, 0.5 mM coenzyme A and 10  $\mu\text{l}$  cell-free extract.

**Acetaldehyde dehydrogenase** (EC 1.2.1.10) enzyme activity was measured in 1 ml reaction mixture containing 50 mM Tris-HCl, pH 7.6, with 3 mM DTT, 0.5 mM CoA-SH, 2 mM NAD<sup>+</sup>, 10-50  $\mu\text{l}$  cell-free extract, and 0.5 mM acetaldehyde. The increase in NADH absorption was measured at 340 nm.

**Alcohol dehydrogenase** (EC 1.1.1.1.) activity was measured in 1 ml reaction mixture containing 50 mM Tris-HCl, pH 7.6, with 3 mM DTT, 0.2 mM NAD<sup>+</sup>, 10-50  $\mu\text{l}$  cell-free extract and 10 mM ethanol. The increase in NADH absorption was measured at 340 nm.

**Pyruvate-formate-lyase/ formate C-acetyltransferase** (E.C. 2.3.1.54) activity was assayed by measuring the formation of formate from pyruvate and coenzyme A as substrates. The 1 ml reaction mixture contained 50 mM potassium phosphate buffer, pH 7.6 with 3 mM cysteine as reducing agent, 20 mM pyruvate, 0.5-1 mM CoA and 50  $\mu\text{l}$  of cell-free extract. Samples were withdrawn from the reaction mixture at time intervals and production of formate was measured by HPLC.

**Formate dehydrogenase** (E.C.1.2.1.2) activity was measured by using benzyl-viologen or NAD<sup>+</sup> as electron acceptors. The 1 ml reaction mixture contained 50 mM Tris-HCl, pH 7.6, 3 mM DTT, 2 mM benzyl viologen or 0.25 mM NAD<sup>+</sup>, 10-100  $\mu\text{l}$  cell-free extract and 10 mM sodium formate (Müller et. al 2008). The reduction of benzyl viologen was observed at 578 nm ( $\epsilon_{578} = 8.65 \text{ mM}^{-1} \text{ cm}^{-1}$ , Diekert and Thauer, 1978).

**Hydrogen: acceptor oxidoreductase / hydrogenase** (EC 1.12.99.6) enzyme activity was measured in a reaction mixture containing 50 mM Tris-HCl, pH 7.6, 3 mM DTT, 10-50  $\mu\text{l}$  cell-free extract, and 2 mM benzyl viologen. The headspace of the cuvette was filled with

---

hydrogen (Müller et. al. 2008, Diekert and Thauer, 1978). The reduction of benzyl viologen was observed at 578 nm.

**Gluconokinase** (EC 2.7.1.92) activity was measured as increase in NADH absorption in a coupled reaction using internal phosphogluconate dehydrogenase activity. The 1 ml assay mixture contained 50 mM Tris-HCl, pH 7.6, 3 mM DTT, 0.5 mM ATP, 3.5 mM MgCl<sub>2</sub>, 0.25 mM NAD<sup>+</sup>, 10 mM gluconate, and 50 µl of cell-free extract. The increase in NADH absorption was measured at 340 nm ( $\epsilon = 6.22 \text{ mM}^{-1} \text{ cm}^{-1}$ ).

**6-phosphogluconate dehydrogenase** (EC 1.1.1.44) activity was measured as increase in NADH absorption coupled to 6-phosphogluconate decarboxylation and dehydrogenation. The 1 ml assay mixture consisted of 50 mM Tris-HCl, pH 7.6, with 3 mM DTT, 0.2 mM NAD<sup>+</sup>, 3.5 mM MgCl<sub>2</sub>, 1 mM ADP, and 10–50 µl cell-free extract. The reaction was initiated by addition of 2 mM 6-phosphogluconic acid.

**Glutamate dehydrogenase** (E.C.1.4.1.4) activity was measured as increase in NADPH absorption in a buffer containing 50 mM Tris-HCl, pH 7.5, 3 mM DTT, 0.25 mM NADP<sup>+</sup>, and 20–40 µl cell-free extract. The reaction was started by addition of 2 mM glutamic acid.

#### **6.4. Analytical methods**

Growth was observed by measuring optical density at 600 nm with a Jenway 6300 spectrophotometer. Gluconate and fermentation products (acetate, formate, ethanol) were measured using an HPLC system fitted with a RID-10A detector (Shimadzu, Munich, Germany) and an Aminex HPX-87H ion exchange column (Bio-Rad, Munich, Germany) operated at 60°C. Separation of analytes was done with 5 mM H<sub>2</sub>SO<sub>4</sub> as mobile phase at a flow rate of 0.6 ml per min using a LC-10ATvp pump (Shimadzu, Munich, Germany) as described before (Müller et. al., 2008). Data were analyzed with the Shimadzu Lab Solution software package version 5.81. The proteins expressed during growth on gluconate and glucose were identified by mass spectrometry at the proteomics facility of the University of Konstanz as described before (Patil et.al 2017).

---

## 6.5. Sources of Chemicals and Gases

All chemicals/reagents used in this study were of analytical grade and were purchased from Merck / Sigma-Aldrich (Munich, Germany), Carl Roth (Karlsruhe, Germany), Roche diagnostics GmbH (Mannheim, Germany), Serva, Fluka chemicals, or Emsure. Gases were from Messer-Griesheim (Darmstadt, Germany) and Sauerstoffwerke Friedrichshafen (Friedrichshafen, Germany).

## List of Abbreviations

KDG: keto-deoxy-gluconate, KDPG: 2-keto-3-deoxy-6-phosphogluconate, POR: pyruvate oxidoreductase, ALDH: aldehyde dehydrogenase, ADH: alcohol dehydrogenase, APT: acetyl-phosphate transferase. PFO: pyruvate ferredoxin oxidoreductase, FDH: Formate dehydrogenase.

## Availability of data and material

All data presented in this work are included in the main article. The genome sequence of *Anaerobium acetethylicum* GluBS11 (DSM 29698) and its gene annotations are available in the Integrated Microbial Genomes database under the IMG genome ID 2675903067.

## Authors' contributions

YP, MJ, and NM designed experiments which were conducted by YP. YP, MJ, and NM analyzed the data and wrote the manuscript. All authors read and approved the final version of the manuscript.

## Acknowledgements

The authors are thankful to Antje Wiese for her technical support in the lab during the experimental work, and to Bernhard Schink for critically reading the manuscript. The authors also acknowledge the LGFG scholarship program of the University of Konstanz in accordance with the state law on Graduate Funding of Baden-Wuerttemberg for providing a scholarship to YP during this research.

---

# CHAPTER 5

---

## Enzymes involved in re-oxidation of reducing equivalents in fermenting bacteria

Yogita Patil, Nicolai Müller

(Draft manuscript)

---

## 1. Abstract

In fermentative metabolism a low amount of energy is conserved *via* substrate-level phosphorylation but it is also accompanied with the production of reducing equivalents such as NADPH, NADH and reduced ferredoxin (Fd<sup>red</sup>) which can be further exploited for energy conservation. However, very little is known about the biochemistry of such reactions in anaerobic bacteria. Here, we investigated the re-oxidizing enzymes systems involved in regeneration of redox balances in glucose- and gluconate-fermenting bacteria. *Anaerobium acetethylicum* ferments gluconate *via* a modified Entner-Doudoroff pathway. Results of *in vitro* enzyme assays indicated that generation of Fd<sup>red</sup> and NADPH occurs by a set of enzymes includes Fd-hydrogenase, Fd-NADP reductase and NADP-dependent hydrogenase, respectively. Furthermore, proteome analysis also confirmed the expression of genes encoding these enzymes. On the other hand, *Bacillus stamsii* that ferments glucose *via* the glycolysis was found to contain subunits of an EtfAB complex, and encoding genes were placed in single operon along with the genes for pyruvate-ferredoxin oxidoreductase and NADH dehydrogenase suggesting the presence of a comproportionating pyruvate dehydrogenase complex system for recycling reducing equivalents. *In vitro* assays performed with cell-free extracts revealed the presence of electron bifurcating enzyme activities that either require riboflavin, flavin mononucleotide (FMN) or flavin adenine dinucleotide (FAD) as cofactor (flavin-based electron bifurcation). Furthermore, genes encoding pyruvate:oxoglutarate dehydrogenase alpha- and beta-subunit were also found along with pyruvate-Fd-oxidoreductase putatively involved in pyruvate oxidation. In cell-free extract high activity of formate dehydrogenase could be observed specifically with Fd and riboflavin compared with NAD and NADP. FAD-dependent NADH dehydrogenase activity with Fd and riboflavin as an electron acceptors were detected. In the genome genes encoding pyruvate formate lyase and formate dehydrogenase were identified after proteome analysis.

### Keywords:

*B. stamsii*, *A. acetethylicum*, glucose fermentation, ferredoxin re-oxidation, pyruvate dehydrogenase, formate dehydrogenase, NADH oxidoreductase. Ferredoxin NADP reductase, ferredoxin hydrogenase, NADP dependent hydrogenase, pyruvate formate lyase.

---

## 2. Introduction

In the last decades, studies reported fermentation of glucose and/or gluconate with several *Clostridium* spp. (Andreesen and Gottschalk, 1969; Bender et al., 1971; Schink and Zeikus, 1983; Ng and Vaughn, 1963; Forsberg et al., 1987). *Anaerobium acetethylicum* and *Bacillus stamsii* are sugar degrading anaerobic bacteria that ferment glucose/gluconate to various fermentation end-products includes acetate, formate, lactate, ethanol, CO<sub>2</sub> or H<sub>2</sub> depending on type of metabolism (Patil et al., 2015; Müller et al., 2008). Fermentation end-products are produced from the central intermediate pyruvate (Murarka et al., 2010). Acetogens are able to produce pyruvate from acetyl-CoA and CO<sub>2</sub> by a reaction catalyzed by pyruvate:ferredoxin oxidoreductase (PFOR) (Fuchs, 2011; Furdui and Ragsdale, 2000).

In *E. coli*, pyruvate:formate-lyase (PFL) and the pyruvate dehydrogenase (PDH) are the key enzymes involved in pyruvate oxidation (Sawers and Clark, 2004). During fermentation, PFL replaces PDH which converts pyruvate to formate and acetyl-CoA, and the latter can be further metabolized to end-products such as acetate and ethanol, which contribute to ATP generation and also maintaining reducing equivalents, respectively (Murarka et al., 2010). In *Enterobacteria* (family *Enterobacteriaceae*) the PFL oxidizes pyruvate to acetyl-CoA and formate, and formate is then cleaved to H<sub>2</sub> and CO<sub>2</sub> by a formate:hydrogen lyase (McDowall et al., 2014). In strict anaerobe, like *Clostridia* (family *Clostridiaceae*), the PFOR oxidizes pyruvate to acetyl-CoA, CO<sub>2</sub> and reduced ferredoxin (Fd<sup>red</sup>). In this case, the electrons released from pyruvate oxidation have low redox potential that allows the transfer of electron to protons (H<sup>+</sup>) to form H<sub>2</sub> (E<sub>0</sub>' CO<sub>2</sub>/HCOOH= -432 mV; E<sub>0</sub>' Fd<sup>ox</sup>/Fd<sup>red</sup> = -400 mV; E<sub>0</sub>' H<sup>+</sup>/H<sub>2</sub>= -414 mV). Thus, electron released during oxidation of reducing equivalents by PFL and PFOR are utilized to form H<sub>2</sub> (Müller, 2001).

Glucose metabolism through the classical Embden-Meyerhof-Parnas (EMP) pathway generates NADH and Fd<sup>red</sup>. Some bacteria contain an enzyme NADH:ferredoxin oxidoreductase that can oxidize reducing equivalents to reduce protons to H<sub>2</sub> (Jungerman et al., 1973). However, thermodynamic point of view the redox potential of the NAD<sup>+</sup>/NADH pair (E<sub>0</sub>'= -320 mV) is not low enough to reduce protons to H<sub>2</sub> (E<sub>0</sub>' H<sup>+</sup>/H<sub>2</sub>= -414 mV). Nonetheless, anaerobic bacteria do produce H<sub>2</sub> from low-potential electron carriers such as Fd (E<sub>0</sub>' = -410 mV to -500 mV), but the question of how Fd is reduced with NADH remained poorly understood in many anaerobic bacteria (Müller et al., 2018). *Thermotoga*

---

*maritima* is sugar fermenting bacterium that reported to contain electron confurcating iron hydrogenase catalyzing oxidation of  $\text{Fd}^{\text{red}}$  with concomitant reduction of  $\text{H}^+$  to  $\text{H}_2$ , and thus drives the production of  $\text{H}_2$  from NADH (Schut et al., 2009).

Although, the fermentation of glucose to acetate,  $\text{CO}_2$ , and  $\text{H}_2$  is an exergonic reaction, but it is strongly inhibited by accumulation of  $\text{H}_2$ , and becomes feasible only if the partial pressure of formed  $\text{H}_2$  is kept below  $10^{-5}$  atm by  $\text{H}_2$ -consuming partner organism (a process called ‘interspecies hydrogen transfer’) that establish a syntrophic cooperation with fermenting bacterium (Schink, 1997; Thauer et al., 1977). By producing  $\text{H}_2$  (or formate) from electrons gained during acetyl-CoA intermediate oxidation, energy is required for the re-oxidation of reduced electron transfer flavoprotein (ETF) and NADH (Müller et al., 2009) a process called reverse electron transport (McInerney et al., 2007). Syntrophically fermenting bacteria that live at the thermodynamic energy limit of growth, a minimum of -20 to -15  $\text{kJ mol}^{-1}$  of energy is required for the synthesis of one ATP (Schink, 1997; McInerney et al., 2008). Syntrophic bacteria use different pathways to conserve energy (Stams et al., 2006), however, the biochemical mechanism remained largely unknown.

In recent years, several studies discovered novel energy conservation reactions in anaerobic bacteria that couple endergonic to exergonic redox reactions through a flavin-based electron bifurcation involving multi-enzymes complex (Herrmann et al., 2008; Li et al., 2008; Thauer et al., 2008; Schut et al., 2009). The lactate dehydrogenase of *Acetobacterium woodii* is an electron transferring flavoprotein (Etf) that couple  $\text{NAD}^+$  reduction in the presence of  $\text{Fd}^{\text{red}}$  through electron bifurcation mechanism and electrons are transferred from  $\text{Fd}^{\text{red}}$  to  $\text{NAD}^+$  together with oxidation of lactate to pyruvate:  $\text{lactate} + \text{Fd}^{\text{red}2-} + 2 \text{NAD}^+ \rightarrow \text{pyruvate} + \text{Fd}^{\text{ox}} + 2 \text{NADH}$  (Weghoff et al., 2015; Buckel and Thauer, 2013). Similarly, *C. kluyveri* that ferments ethanol and acetate to butyrate and hydrogen, reported to contain the electron bifurcating butyryl-CoA dehydrogenase/Etf complex (FAD-containing) enzyme shown to couple the endergonic reduction of ferredoxin ( $E_0' = -410$  mV) with NADH ( $E_0' = -320$  mV) to the exergonic reduction of crotonyl-CoA to butyryl-CoA ( $E_0' = -10$  mV) with NADH (Herrmann et al. 2008; Li et al., 2008).

In 2008, a novel glucose fermenting *B. stamsii* strain BoGlc83 was isolated from deep lake sediment (Lake Constance) using a  $\text{H}_2$ -consuming methanogenic partner organism (Müller et al., 2008). Interestingly, the strain has the ability to switch syntrophic glucose metabolism to

---

classical fermentation pathway in pure culture only if pyruvate was given as a co-substrate, and produces acetate and formate as end-products, but no ethanol (Müller et al., 2015). By contrast, sugar-fermenting bacteria, e.g., *Clostridium* spp. or *Ruminococcus albus* growing without H<sub>2</sub>-consuming organism shifts the fermentation metabolism and produce more reduced end-products such as butyrate, ethanol, or lactate (Iannotti et al., 1973; Thauer et al., 1977; Tewes and Thauer, 1980; Zeikus, 1983). *A. acetethylicum* strain GluBS11 which is closely related to the genus *Clostridium* belonging to family *Lachnospiraceae* (Patil et al., 2015) ferments glucose/gluconate to acetate, formate, ethanol and H<sub>2</sub>, but no butyrate was produced (usually butyrate is one of the main fermentation end-product in the genus *Clostridium*). Anaerobic degradation of glucose and gluconate by the strain BoGlc83 and strain GluBS11 occurs through the classical EMP pathway and modified ED pathway, respectively (Müller et al., 2008; Patil et al., 2015), generating 2 NAD(P)H and 2 Fd<sup>red</sup> that need to recycle to either produce H<sub>2</sub> and/or formate. However, oxidation of NAD(P)H or ferredoxin with H<sup>+</sup> to H<sub>2</sub> and/or H<sup>+</sup>/CO<sub>2</sub> (formate) is endergonic reaction and the enzymes involved remained unknown. In this study, we focused on the investigation of redox enzymes involved in balancing the reducing equivalents during fermentative sugar-based substrates degradation by metabolically two different anaerobic bacteria: strain BoGlc83 and strain GluBS11. *In vitro* enzyme assays were performed to investigate redox enzymes involved in re-oxidation of reducing equivalents and energy conservation, and findings were combined together with proteomic and genomic analysis.

### 3. Results and Discussion

#### 3.1 Genome-based model system for re-oxidation of NADH and ferredoxin in *B. stamsii*

Syntrophic glucose degradation by strain BoGlc83 is able to support the growth of the H<sub>2</sub>-consuming organism that indicate there must be a route for re-oxidation of the ferredoxin with the formation of H<sub>2</sub> with the concomitant NADH oxidation. We analyzed the draft genome sequence of *B. stamsii* in order to identify potential genes encoding redox enzymes involved in balancing reducing equivalents. After inspecting genome sequence, we have found the presence of genes in a single operon potentially encoding redox enzymes putatively involved in balancing reducing equivalence and energy metabolism (Figure 1). These genes include the Bsta\_03143 and Bsta\_03144 genes predicted to encode similar proteins

---

homologous to pyruvate:ferredoxin oxidoreductase (PFOR, also called pyruvate:ferredoxin dehydrogenase, PDH). The deduced amino acid sequence of both genes (Bsta\_03143 and Bsta\_03144) shared about 31% and 23% identity to experimentally characterized  $\alpha$ - $\delta$ -subunits of oxalate:oxidoreductase (OOR) of *Moorella thermoacetica* that oxidize oxalate to 2 CO<sub>2</sub> and generates two low-potential electrons (Gibson et al., 2015). The gene Bsta\_03143 encoding 84 kDa protein belongs to pyruvate synthase family protein, and possess binding domain for thiamin pyrophosphate (TPP). Whereas gene Bsta\_03144 encoding 38 kDa protein shown to contain the presence of [4Fe-4S] iron-sulfur cluster and a binding domain for ferredoxin, respectively.

The genome of *B. stamsii* also contain additional genes encoding proteins that were homologous to electron-transferring flavoprotein A (EtfA; locus tag Bsta\_03137) and EtfB (Bsta\_03138). Etf is an electron transferring flavoprotein that has been shown to catalyze simultaneous NADH/NAD<sup>+</sup> oxidation together with Fd<sup>ox</sup>/Fd<sup>red</sup> reduction through electron bifurcation reactions (Weghoff et al., 2015; Buckel and Thauer, 2013). Thus, in *B. stamsii* these two genes predicted to encode the homologous enzymes that are putatively involved in simultaneous oxidation of NADH/NAD<sup>+</sup> together with Fd reduction (Figure 1). Since the redox potential of NAD<sup>+</sup>/NADH ( $E_0' = -320$  mV) is not negative enough to catalyze simultaneous ferredoxin reduction Fd<sup>ox</sup>/Fd<sup>red</sup> ( $E_0' = -400$  mV) and it possible only if the reaction is coupled to the exergonic oxidation of pyruvate to acetyl-CoA (-500 mV) that releases two high potential electrons (Figure 1). A recent study on structure analysis of OOR allowed to gain mechanistic understanding and confirmed that TPP and [4Fe-4S] clusters are involved in substrate oxidation, which releases high potential electrons (-500 mV) that can catalyze low-potential redox reactions such as reduction of N<sub>2</sub>, H<sup>+</sup> or CO<sub>2</sub> (Gibson et al., 2015).

The deduced amino acid sequence of genes Bsta\_03137 (EtfA, 37 kDa) and Bsta\_03138 (EtfB, 30 kDa) exhibited high identity (48% and 45%) with experimentally characterized FAD containing EtfAB subunits of electron-bifurcating caffeyl-CoA reductase of *A. woodii* (Demmer et al., 2015). This enzyme catalyzes the reduction of caffeyl-CoA and ferredoxin by simultaneous oxidation of NADH (caffeyl-CoA + 2 NADH + 2 Fd<sup>ox</sup> = 2Fd<sup>red</sup> + 2 NAD<sup>+</sup> + dihydrocaffeyl-CoA). In a recent study, PFOR has been shown to catalyze oxidation of pyruvate to acetyl-CoA and CO<sub>2</sub>, with the release of two high potential electrons to reduce

low potential ferredoxin (Chen et al., 2018). Therefore, in analogy with the above mentioned examples in anaerobic bacteria the presence of homologous genes in *B. stamsii* encoding EtfAB and pyruvate:ferredoxin oxidoreductase (PFOR) strongly indicate that similar metabolic scenario may also apply for the re-oxidation of NADH and Fd together with pyruvate oxidation by comproportionating PFOR enzyme complex catalyzing reaction:  $\text{NADH} + \text{Fd}^{\text{ox}} + \text{pyruvate} + \text{CoA-SH} = \text{NAD}^+ + \text{Fd}^{\text{red-2}} + \text{acetyl-CoA} + \text{CO}_2$  (Figure 1).

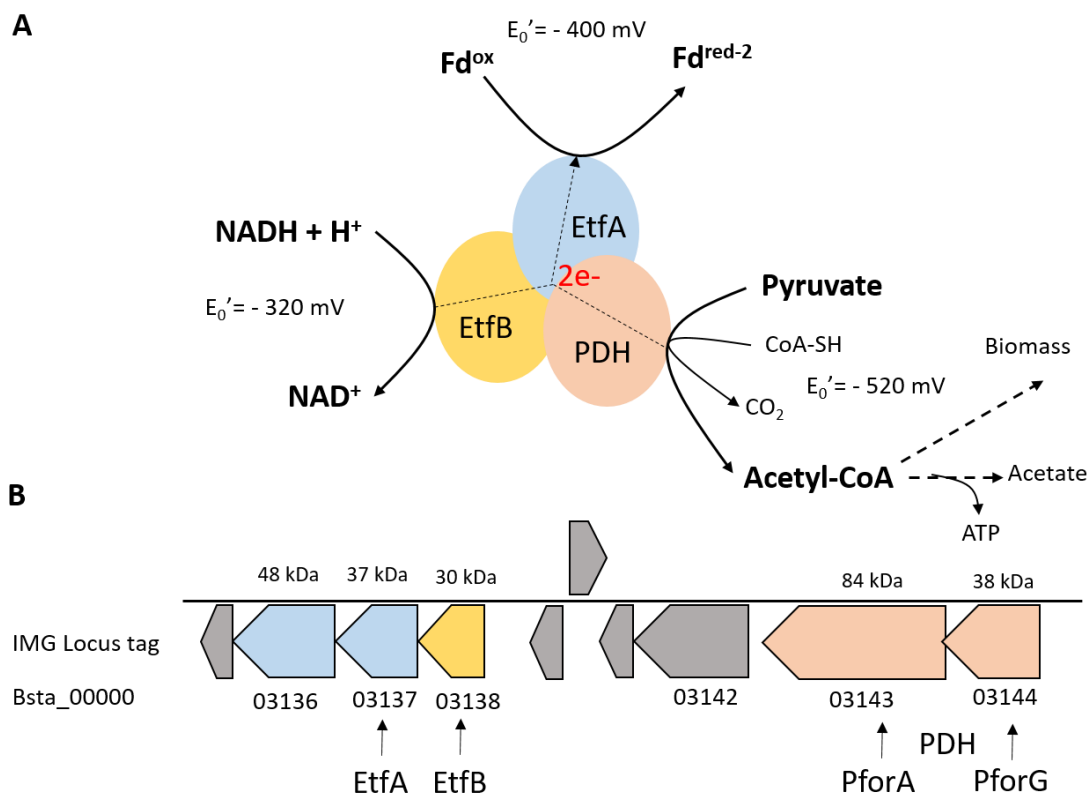


**Figure 1.** A) Genome-based proposed model of comproportionating pyruvate:ferredoxin oxidoreductase (PFOR) enzyme complex in *B. stamsii* strain BoGlc83. Composition of enzymes is based on homology of encoding proteins to known enzymes. B) The organization of the genes in a gene cluster encoding enzymes involved in NADH re-oxidation. IMG predicted functions of the genes: Bsta\_03136, electron transfer flavoprotein-quinone oxidoreductase; Bsta\_03137, electron-transferring flavoprotein A (EtfA); EtfB, Bsta\_03138, and PDH: Bsta\_03143, PFOR  $\alpha$ -subunit (PforA) and Bsta\_03145, PFOR  $\gamma$ -subunit (PforG). The genes shown in gray color are either hypothetical proteins or they do not have function in proposed enzyme system. The ferredoxin is assumed to accept two electrons.

### 3.2 *In vitro* assays for redox enzyme in cell-free extracts of *B. stamsii*

In order to provide a biochemical basis for redox enzymes particularly, enzymes from proposed model of comproportionating PFOR involved in re-oxidation of NADH and ferredoxin (Figure 1), *in vitro* enzyme assays were performed with cell-free extracts prepared from *B. stamsii* cells grown with glucose. For the investigation of comproportionating PFOR and differentiate it from associated individual activities, assay were performed in three ways: i) NADH acceptor oxidoreductase ( $\text{NADH} + \text{H}^+ + \text{acceptor}^{\text{ox}} = \text{NAD}^+ + \text{acceptor}^{\text{red}}$ ); ii) pyruvate:ferredoxin/riboflavin oxidoreductase ( $\text{pyruvate} + \text{CoA-SH} + \text{Fd}^{\text{ox}}/\text{Rb}^{\text{ox}} = \text{acetyl-CoA} + \text{Fd}^{\text{red}}/\text{Rb}^{\text{red}} + \text{CO}_2$ ); and iii) comproportionating pyruvate:ferredoxin/riboflavin dehydrogenase ( $\text{pyruvate} + \text{CoA-SH} + \text{Fd}^{\text{ox}}/\text{Rb}^{\text{ox}} + \text{NADH} = \text{acetyl-CoA} + \text{CO}_2 + \text{Fd}^{\text{red}}/\text{Rb}^{\text{red}} + \text{NAD}^+$ ), respectively. In addition to ferredoxin (prepared from *C. pasterianum*) as a substrate for the low potential electron acceptor, riboflavin (0.2 - 0.5  $\mu\text{M}$ ) was used as an alternative substrate.

**Table 1.** Summary of specific enzyme activities measured using cell-free extracts prepared from glucose grown cells of *B. stamsii*. Assays were performed either with riboflavin or ferredoxin. Enzyme tests were performed with two different cell-free extracts (CFE).

Enzyme test	Specific activity (mU/mg)			
	Riboflavin		Ferredoxin	
	CFE-1	CFE-2	CFE-1	CFE-2
NADH dehydrogenase	26.3 $\pm$ 5.6	20 $\pm$ 3.6	16.33 $\pm$ 3.0	28 $\pm$ 3
Comproportionating PDH	116.6 $\pm$ 11.8	181 $\pm$ 5.2	69.33 $\pm$ 12.5	128 $\pm$ 6.9
Pyruvate dehydrogenase	86.33 $\pm$ 2.0	137.6 $\pm$ 2	62.66 $\pm$ 4.7	106 $\pm$ 9
Comproportionating PDH	112.7 $\pm$ 7.8	151 $\pm$ 17.7	83.66 $\pm$ 6.02	131 $\pm$ 14

In cell-free extract, individual activity for NADH:acceptor oxidoreductase (dehydrogenase) with riboflavin (20-26.3 mU/mg) and ferredoxin (28-16 mU/mg) were detected in the same range (Table 1). To measure the activity of comproportionating pyruvate:ferredoxin oxidoreductase (pyruvate/acetyl-CoA + CO<sub>2</sub>: E<sub>0</sub>'= -500mV), NADH:acceptor oxidoreductase assay was combined with the addition of pyruvate and CoA-SH. After adding a pyruvate expected increase in activity was observed by 10 fold (116.6 - 181 mU/mg). When reaction was performed by the sequential addition of pyruvate, CoA-SH plus riboflavin, activity for

---

PFOR was found to be in the range of 86 mU/mg - 137 mU/mg, which is comparatively lower than the measured comproportionating PFOR activity. Activity increased (112 mU/mg and 151 mU/mg) following the addition of NADH (Table 1) as a strong indication of comproportionating PFOR activity (Table 1). The enzyme activities of pyruvate dehydrogenase (PDH) were found to be always overlapping with comproportionating PFOR activities only if PDH activity was started with ferredoxin or riboflavin followed by NADH addition. However, it was observed that the cell-free extract prepared by the addition of the 0.01 mM FAD in the buffer could stabilize the enzyme activities and background activities were not observed in this case. Similarly the electron bifurcating LDH/Etf enzyme complex also reported to requires FAD for stability and activity (Weghoff et al., 2015).

Upon replacing riboflavin with ferredoxin (in presence of FAD as cofactor), pyruvate:ferredoxin oxidoreductase and NADH:acceptor dehydrogenase activities could be measured, but only after long incubation of reaction mixture. It has been reported that ferredoxins from other anaerobic microorganisms may have different redox potential than with testing organism (Boll et al., 2000), which indicate that ferredoxin of *C. pasturianum* might not be suitable for *B. stamsii*. The average activity of NADH:ferredoxin oxidoreductase was found to be in the range of 16.33 and 28 mU/mg, and activity increased after addition of pyruvate and CoA-SH to 69 and 128 mU/mg, respectively (Table 1). Individual specific activity of PFOR with ferredoxin was in the range of 62 and 106 mU/mg. A similar increase in activity was detected after the addition of NADH. In the summary comproportionating activity of PFOR could be observed only if substrates were added in a specific order. For convenience the starting activities were referred to as controls to differentiate the increase in overall activities after the addition of remaining substrates (Figure 2).

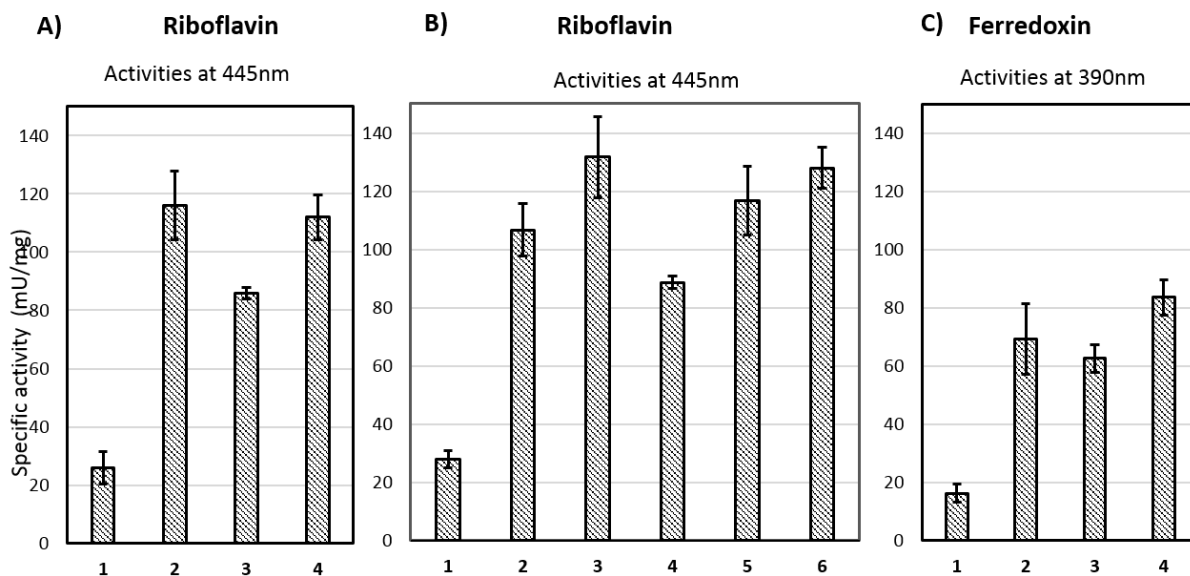


**Figure 2.** Comparison of comproportionating pyruvate dehydrogenase (PFOR) enzyme activities in extract of glucose grown cells of *B. stamsii* performed either with riboflavin or ferredoxin. **(A) 1:** (control) CFE + NADH; 2: CFE + NADH + pyruvate + CoA-SH; 3: (control) CFE + pyruvate + CoA-SH; and 4: CFE + pyruvate + CoA-SH + NADH. **(B) 1:** (control) CFE + NADH; 2: CFE + NADH + pyruvate + CoA-SH; 3: CFE + NADH + pyruvate + CoA-SH + Fd; 4: (control) CFE + pyruvate + CoA-SH; 5: CFE + pyruvate + CoA-SH + NADH; and 6: CFE + pyruvate + CoA-SH + NADH + Fd. **(C) 1:** (control) CFE + NADH + Fd + FAD; 2: CFE + NADH + Fd + FAD + pyruvate + CoA-SH; and 3: (control) CFE + Fd + FAD + pyruvate + CoA-SH; and 4: CFE + Fd + pyruvate + CoA-SH + NADH.

### 3.3 Riboflavin and ferredoxin based system in *B. stamsii*

The presence of a flavin containing EtfAB proteins and reproducible activity with FAD (riboflavin) was strong reason to consider that *B. stamsii* likely uses a flavin-dependent electron bifurcation system to drive endergonic oxidation of NADH coupled with ferredoxin reduction. The findings of *in vitro* activities in cell-free extracts of *B. stamsii* also indicated the presence of such enzymes system that mainly includes: ferredoxin oxidoreductase (PFOR), pyruvate dehydrogenase (PDH) and additional one pyruvate formate lyase (PFL; Bsta\_02393).

The PFL enzyme is proposed to catalyze a reaction:  $\text{NADH} + \text{pyruvate} + \text{CoASH} + \text{flavodoxin} \rightarrow \text{acetyl-CoA} + \text{flavodoxin}^{\text{red}}/\text{Fd}^{\text{red}} + \text{NAD}^+ + \text{formate}$  that regenerate  $\text{NAD}^+$ . Furthermore formate dehydrogenase alpha subunit was identified from partially

---

purified fraction from DEAE-sepharose. In anaerobic bacteria formate dehydrogenase catalyzes the reduction of CO<sub>2</sub> to formate (Bryan et al., 2011). The formate acetyl transferase/pyruvate formate lyase (PFL) enzymes are used by anaerobic bacteria to avoid the formation of more highly reduced products like NADH and reduced ferredoxin by acetylating pyruvate dehydrogenase complex and pyruvate ferredoxin oxidoreductase. Previously studies has shown the formation of formate by PFL (Thauer et al., 1972). Furthermore, formate dehydrogenase alpha subunit was also identified from partially purified fraction from DEAE-sepharose (in an attempt to purify the redox enzymes). In anaerobic bacteria formate dehydrogenase catalyzes the reduction of CO<sub>2</sub> to formate (Bryan et al., 2011). Enzyme for pyruvate oxidation (PFL and PFOR) derived from enzyme activities and two more interfering enzymes might interfere with activities is shown in Figure 3. Under such condition PFOR can reduce ferredoxin/flavins together with simultaneous oxidation of NADH with pyruvate oxidation generating NAD, acetyl-CoA and CO<sub>2</sub>. The PFL enzyme can generate formate and oxidize NAD<sup>+</sup> and flavins.

Confurcating enzyme activities reproducibly observed when riboflavin was used as an electron acceptor, suggests the flavin-based electron transfer reactions are involved in *B. stamsii* during recycling of reducing equivalents. The redox potential of NADH is -320 mV, pyruvate to acetyl CoA is -500 mV and the oxidation of NADH with riboflavin occurs at nearly the same redox potential. The presence of electron transferring flavoprotein (EtfAB) is again strong indication that the electron bifurcation reaction is performed by comproportionating PFOR enzyme complex analogous to LDH of *A. woodii* which also contains Etf subunits that uses the flavin-based electron bifurcation reaction for energy conservation (Buckel and Thauer, 2012). In *B. stamsii*, our hypothesis is that FAD/riboflavin is reduced together with the oxidation of NADH and pyruvate by NADH:oxidoreductase and pyruvate oxidoreductase, respectively. During this reaction free flavins ( $E_0' = -220$  mV) can accept electron from an electron donor like NADH ( $E_0' = -320$  mV) and transform to semiquinone radical form that possess more electronegative potential in the range of -500 to 520 mV. In this state, flavin is ready to accept two high potential electrons resulted from the oxidation of pyruvate to acetyl-CoA (-500 mV) and flavin is then fully reduced.

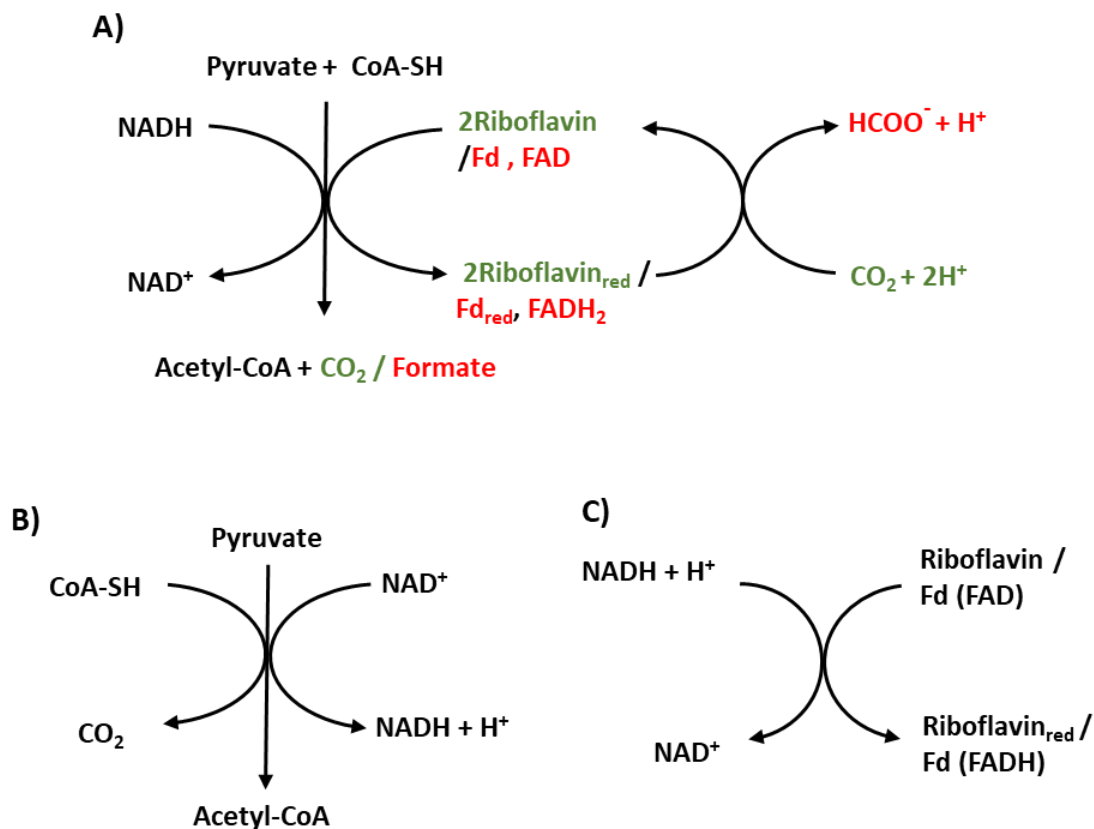


**Figure 3.** *In vitro* enzyme based potential NADH re-oxidation enzyme systems involved in *B. stamsii* for catalyzing redox reactions: A) The exergonic oxidation of pyruvate with riboflavin drives the endergonic oxidation of NADH with riboflavin. Riboflavin accepts 2e from pyruvate as well as 2e from NADH. B) Acetyl transferring pyruvate dehydrogenase complex C) Uncharacterized NADH dehydrogenase.

### 3.4 Enzymes involved in NAD(P)H and ferredoxin re-oxidation in *A. acetethylicum*

To identify the proteins/enzymes potentially involved in the re-oxidation of NAD(P)H and  $\text{Fd}^{\text{red}}$  during gluconate fermentation by *A. acetethylicum*, protein analysis was performed using soluble protein fraction prepared from cell-free extract of gluconate grown cells. Among the list of identified proteins, 7 proteins were suspected to be involved in the re-oxidation of reducing equivalents based on their annotated functions (Table 2). These include mainly four enzyme entities that were homologous to pyruvate:ferredoxin/flavodoxin oxidoreductase (PFOR), a ferredoxin hydrogenase (HydA1), ferredoxin:NADP reductase (NfnI) and NADP-reducing hydrogenase (HndDCA). In *A. acetethylicum*, these proteins were

encoded by genes constituting a different gene cluster located elsewhere in the genome (Figure 4).

**Table 2.** Proteins putatively involved in the re-oxidation of ferredoxin and NADPH identified from gluconate grown cell-free extract of *A. acetethylicum*.

Gene loci Ga0116910_	IMG predicted function	Enzyme name	Coverage	Score	Size (KDa)
1005157	Pyruvate:ferredoxin/ flavodoxin oxidoreductase	PFOR	8.06	192	127
103224	Pyruvate:ferredoxin/ flavodoxin oxidoreductase		66.30	9085	127
100545	Ferredoxin hydrogenase	HydA1	20	301	52
1001164	Ferredoxin:NADP reductase	NfnI	15.2	63	32
1001466	NADP-reducing hydrogenase subunit HndD	HndABCD	33.45	1275	63
1001467	NADP-reducing hydrogenase subunit HndC		35.29	838	64
1001470	NADP-reducing hydrogenase subunit HndA		16.46	74	18

The deduced amino acid sequence of the genes Ga0116910\_1005157 and Ga0116910\_103224 (59% identical to each other) showed sequence identity (57 - 55%) with recently characterized PFOR enzyme from *Moorella thermoacetica* (previously known as *Clostridium thermoaceticum*) that uses thiamine pyrophosphate (TPP), three [4Fe-4S] clusters, and CoA in reversible oxidation of pyruvate to acetyl-CoA and CO<sub>2</sub> with the releases two high potential electrons (-500 mV) that are enough to reduce ferredoxin (Chen et al., 2018). Both the genes shared only about 28 - 31% amino acid sequence identity with a gene (Bsta\_03143) predicted to encode PFOR alpha subunit in *B. stamsii*. In addition, proteome analysis of gluconate grown culture of *A. acetethylicum* allowed the identification of more proteins that were annotated as ferredoxin-dependent hydrogenase (Ga0116910\_100545) and shared about 28% identity with known iron only hydrogenase 1 (HydA1) from *C. pasteurianum* (Duan et al., 2018). A gene encoding ferredoxin:NADP reductase (Ga0116910\_1001164) was about 50% identical with ferredoxin:NADP oxidoreductase (NfnI) from *Pyrococcus furiosus*. NfnI is a FAD-dependent bifurcating

enzymes that couples the NADPH oxidation together with the reduction of NAD and ferredoxin (Lubner, et al., 2017). The deduced amino acid sequence of the gene (Ga0116910\_1001164) encoding ferredoxin: NADP reductase also indicated the presence of binding domain for FAD and ferredoxin.

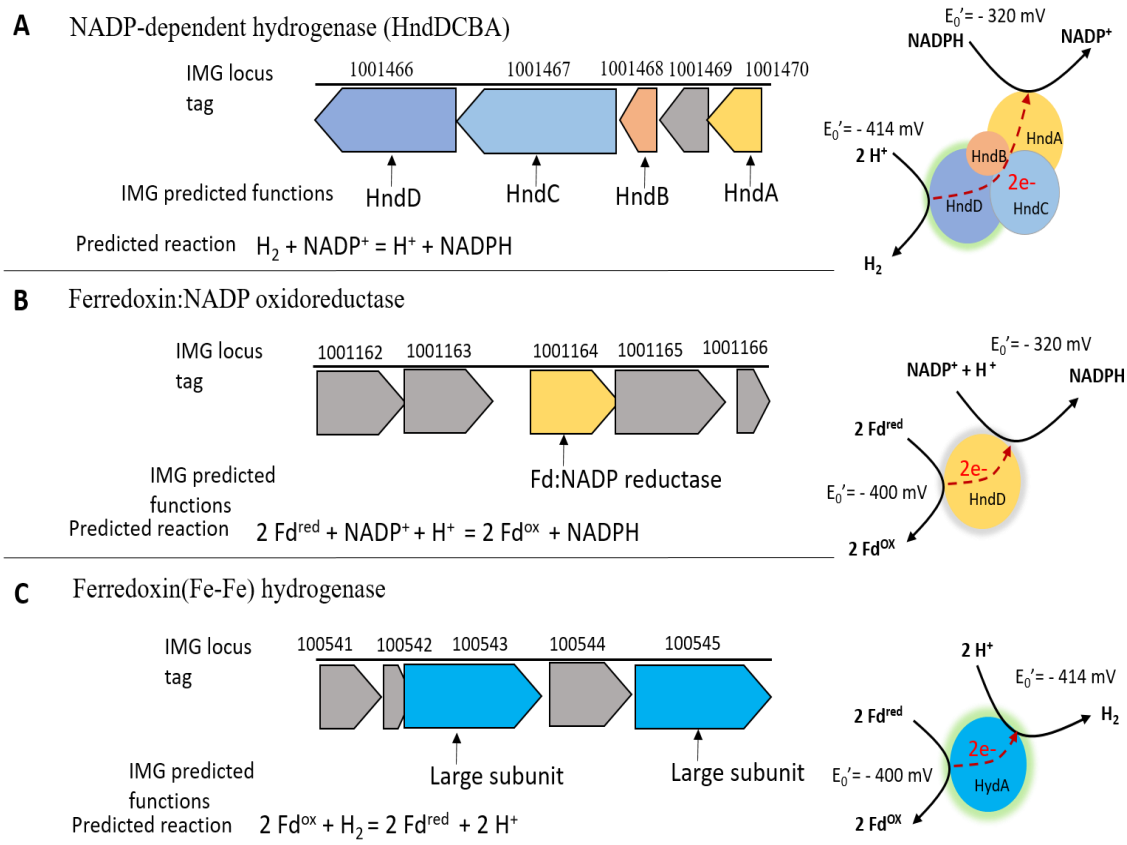


**Figure 4.** Organization of genes in the gene clusters encoding putative enzymes involved in balancing reducing equivalents in *A. acetithylicum* strain GluBS11. **A)** NADP-dependent hydrogenase (HndDCBA) complex is encoded by genes: HndD (1001466), HndC (1001467), HndB (1001468), DNA gyrase (1001469, and HndA (1001470). **B)** The ferredoxin:NADP dependent oxidoreductase encoded by a gene annotated as ferredoxin:NADP reductase (1001164). **C)** Cluster of the gene encoding iron only ferredoxin hydrogenase: iron only hydrogenase large subunit (100543) and ferredoxin hydrogenase large subunit (100545). The genes shown in grey color either annotated as hypothetical proteins or they have no function in the proposed gene cluster. Each gene locus tag is prefixed with Ga0116910\_.

---

In the protein analysis, we also identified a cluster of genes encoding the NADP-reducing hydrogenase (HndACD) that is highly homologous with a novel class of [Fe] hydrogenase encoded by *hndABCD* operon in *Desulfovibrio fructosovorans* (Dermoun et al., 2002). In the same gene cluster encoding HndACD, also contained a gene encoding HndB that together constitute a complete HndABCD hydrogenase complex (Figure 3A). In NADP-reducing hydrogenase complex active site of HndD is responsible for splitting H<sub>2</sub> and electrons would then transfer electron to HndA through the N-terminal [2Fe-2S] cluster towards HndC or HndB which harbors the NADP<sup>+</sup> binding domain (Dermoun et al., 2002). Thus, a cluster of genes encoding NADP-dependent hydrogenase (HndABCD) in *A. acetethylicum* likely one of three enzymes complex responsible for catalyzing the reversible oxidation of H<sub>2</sub> to two protons to carry out the reduction of NADP<sup>+</sup> to NADPH (Figure 3).

### 3.5 Specific activities of enzymes in cell-free extracts of *A. acetethylicum*

In the cell-free extract of gluconate grown cells of *A. acetethylicum*, PFOR activity with ferredoxin was observed (76 mU/mg) (Table 3). By contrast, *in vitro* enzyme test for PFOR in *B. stamsii* showed rather low or no activity with NADP, and activity was measurable only with NAD<sup>+</sup>. Furthermore, ferredoxin-dependent hydrogenase activity could be measured in cell-free extract with ferredoxin (28 mU/mg). Again, when ferredoxin was replaced with benzyl viologen, considerably high hydrogenase activity could be obtained (Table 3). In the presence of NADP, the average specific activity for bifurcating ferredoxin:NADP hydrogenase was found to be 42 mU/mg, and activity was decreased (20 ± 2.8 mU/mg) after the addition of ferredoxin (Table 3). The decrease in activity was proportional to the addition of ferredoxin. An enzyme test performed for bifurcating enzyme showed no hydrogen production in cell-free extract in a reaction mixture containing NADPH and sodium dithionite. However, this activity was performed with low concentration of NADPH (2.5 mM). Notably, low activity was detected for formate dehydrogenase with ferredoxin. Similarly, in the cell extract of *C. autoethanogenum* the specific activities of NADP- and ferredoxin-dependent hydrogenase and of NADP- and ferredoxin-dependent formate dehydrogenase were reported to be almost identical (Wang et al., 2013). Based on the *in vitro* enzyme assays results obtained with cell-free extracts, it can be speculated that the strain GluBS11 contain, Fd-NADP reductase, Fd-hydrogenase and NADP-dependent hydrogenase

as key redox enzyme system potentially involved in the re-oxidation of reducing equivalents and energy conservation mechanism (Table 3 and Figure 3).

**Table 3.** Average of specific activities of *Anaerobium acetethylicum* involved in the re-oxidation of NADPH and ferredoxin.

Enzyme	Avg. spec. activity mU/mg	
	CFE-1	CFE-2
Pyruvate:ferredoxin oxidoreductase	76 ± 6.7(Fd)	212 ± 4.4(BV)
Ferredoxin hydrogenase	28 ± 4.6(Fd)	346 ± 2.0(BV)
NADP-dependent hydrogenase	32.33 ± 3.0	43.3 ± 3.2
Formate dehydrogenase	9.9 ± 0.1(Fd)	17.3 ± 1.2(BV)
Ferredoxin:NADP reductase	25.5 ± 7	25 ± 6.0
NADP-Hydrogenase	42 ± 3.2 and 20 ± 2.8	00

In anaerobic bacteria, hydrogenases mainly function to dispose the excess of electrons produced during fermentation. There are three main types of hydrogenases named according to the composition of their active sites as Ni-Fe, Fe-Fe and Fe only hydrogenase (Vignais et al., 2007). The Ni-Fe hydrogenases generally occur in H<sub>2</sub> oxidizing organisms while Fe only hydrogenases are found in H<sub>2</sub> producing fermenting bacteria (Adams et al., 1990, Menon et al., 1994). The NADH-dependent multimeric hydrogenase (Fe-Fe) has been well studied in *S. wolfei* for its role in the re-oxidation of NADH (Losey et al., 2017). Based on previous findings, in *A. acetethylicum* NADPH is likely oxidized by NADP-dependent hydrogenase similar to sugar-degrading *Desulfovibrio fructosivorans* that possess 4 different hydrogenases (Casalot et al., 2002), and one of these is an NADP-dependent, that couples NADP (but no NAD) reduction to H<sub>2</sub> oxidation (Malki, 1995). In the genome of *A. acetethylicum* a single gene cluster encoding NADP-reducing hydrogenase complex (HndABCD) was detected (Figure 4A). Total proteome analysis revealed the presence of ferredoxin NADP-reductase (locus tag Ga0116910-1001164), ferredoxin hydrogenase large subunit (Ga0116910-100545) and the iron only hydrogenase large subunit (Ga0116910-100543) that are known to function in the fermentative hydrogen production to balance reducing equivalents.

### 3.6 Activity staining and protein identification for *A. acetethylicum*

In gluconate grown cells of *A. acetethylicum*, native gel protein electrophoresis was performed by using soluble protein fraction and solubilized membrane proteins. The native protein gel used for activity staining contained proteins obtained from a soluble protein fraction of cell-free extract. After putting sliced gel in small anoxic staining box and incubated for activity staining for ferredoxin-dependent hydrogenase and NADP-dependent hydrogenase that resulted in the staining of specific bands on the native protein gel (Figure 5). The native gel stained with benzyl viologen and H<sub>2</sub> displayed a single dark color reddish brown stained protein band running approximately at 65 kDa (Figure 5B). After analyzing the sliced protein band by peptide-mass fingerprinting revealed the identification of 32 kDa size ferredoxin:NADP reductase (1001164). These results indicate that ferredoxin-dependent hydrogenase enzyme is a dimer enzyme of 32 kDa and it is a 64 kDa size in its active state.

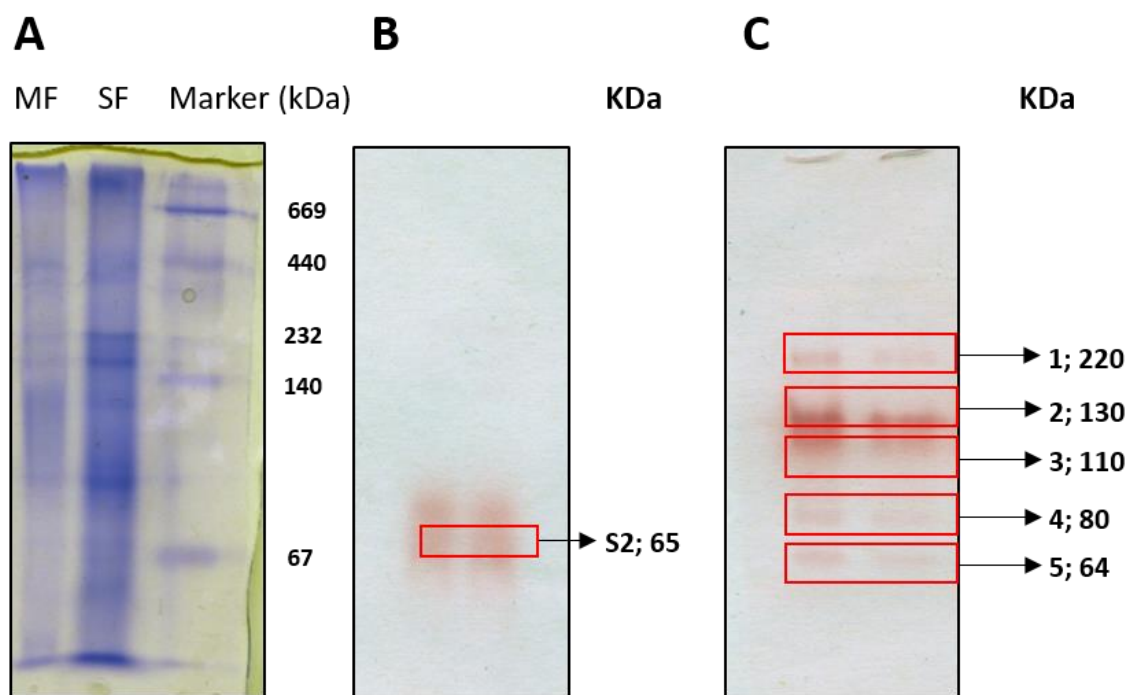


**Figure 5.** **A)** Native protein electrophoresis performed with soluble fraction (SF), dissolved membrane protein fraction (MF) of gluconate grown cells of *A. acetethylicum* and protein bands were visualized with Coomassie stain. **B)** Native protein gel stained for hydrogenase activity using benzyl viologen, H<sub>2</sub> plus TTC in a solution containing 50 mM Tris-HCl buffer pH 7.6 containing 3 mM DTT. **C)** Native protein gel stained for NDHP-dependent hydrogenase activity stained with benzyl viologen, TTC, NADPH in 50 mM Tris-HCl pH 7.6 with 3 mM DTT.

Furthermore, after staining a gel with benzyl viologen plus NADPH, 5 different protein bands were stained on gel that are labeled as 1 to 5 running approximately between 64 to 220 kDa (Figure 5C). These protein bands were stained as a result of activity of NADP-dependent hydrogenase. No bands could be developed for activity staining performed for formate dehydrogenase using benzyl viologen and TTC. Among five protein bands, protein band running approximate at 110 kDa size (band no. 3) revealed the identification of two protein species, a NADP-reducing hydrogenase (HndD, 63 kDa) and NADP-reducing hydrogenase subunit (HndC, 64 kDa) encoded by the genes that were located adjacent to each other (Table 4, Figure 4). These results again indicate that the HndDC occur together constitute about 130 kDa protein complex. Identification of proteins from remaining bands contains mainly NADH quinone oxidoreductases (Table 4).

**Table 4.** List of proteins identified from activity stained bands in *A. acetethylicum* by mass spectroscopy

Figure	Band	Band size (kDa)	Identified proteins	Coverage	Score	Mass (kDa)
B	S2	65	Ga0116910_1001164 Ferredoxin:NADP reductase	11.8	172	32.1
C	1	220	Ga0116910_1001508 NADH-quinone oxidoreductase subunit E	20.25	66	17
			Ga0116910_1001506 NADH-quinone oxidoreductase subunit F	25.63	883	64
	2	130	Ga0116910_1001505 NADH-quinone oxidoreductase subunit G	41.38	1002	64
			Ga0116910_1001506 NADH-quinone oxidoreductase subunit F	25.63	883	64
	3	110	Ga0116910_1001466 NADP-reducing hydrogenase subunit HndD	4	103	63
			Ga0116910_1001467 NADP-reducing hydrogenase subunit HndC	6.72	101	64
4	80	Ga0116910_1001164 ferredoxin--NADP+ reductase	14.19	104	32	
5	64	Ga0116910_1001164 ferredoxin--NADP+ reductase	14.19	87	32	

### 3.7 NADH(FAD)-dehydrogenase and formate dehydrogenase of *B. stamsii*

In addition to comproportionating PFOR activities, NADH dehydrogenase activity was detected in cell-free extracts using both the riboflavin and ferredoxin. The average specific activities of NADH dehydrogenase with riboflavin was in the range 26 and 20 mU/mg (Figure 5A). Activity for NADH dehydrogenase with ferredoxin in the presence of the 0.01 mM FAD as cofactor was slightly higher (28 to 38 mU/mg). These activities could result from a separate NADH dehydrogenases. Proteome analysis of glucose grown cells identified the presence of genes encoding proteins that annotated as uncharacterized NADH-dehydrogenase (Bsta\_01029; CoA-disulfide reductase), NADH dehydrogenase (01904; FAD-containing subunit) and a NADH dehydrogenase (Bsta\_03136; FAD/ NAD(P)-binding domain). The later enzyme is also a part of proposed comproportionating pyruvate dehydrogenase complex system (Figure 1). It indicates that the ferredoxin and flavin re-oxidation could mainly occur through the activities of formate dehydrogenase (Figure 5B) and NADH dehydrogenase (PFL will directly produce oxidize riboflavin and formate).

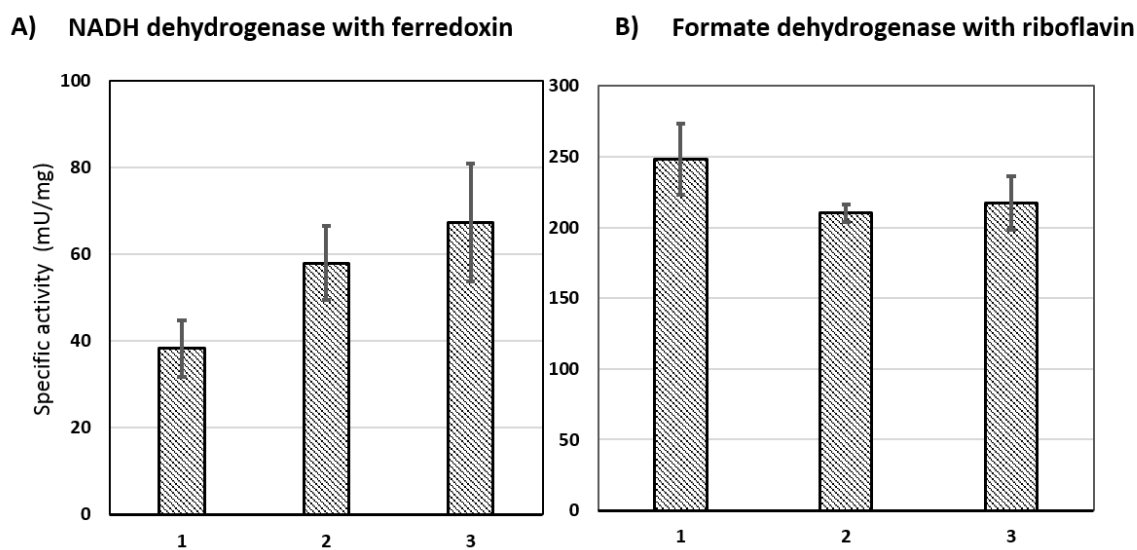


**Figure 6.** Comparison of specific enzyme activities measured in cell-free extracts of glucose grown cell of *B. stamsii*: **A)** NADH dehydrogenase was measured either with ferredoxin, or riboflavin (data not shown); and **B)** specific activities of formate dehydrogenase with riboflavin at 445 nm.

---

Blastp analysis of the deduced amino acid sequence of gene Bsta\_01029 displayed about 65% sequence identity with the experimentally characterized NADH (FAD)-dependent oxidoreductase from *Shewanella loihica* (Lee et al., 2014). In cell-free extract reproducible activity could be measured for NADH-dependent dehydrogenase (35 to 65 mU/mg) in the presence of ferredoxin and 0.01 mM FAD as a cofactor (Figure 6A). For the re-oxidation of ferredoxin, high activities of formate dehydrogenase were observed with riboflavin as well as ferredoxin, and specific activities were 244 mU/mg with riboflavin and 215 mU/mg with ferredoxin, respectively (Figure 6B). The additional activities of NAD-dependent pyruvate dehydrogenase activities were also detected in cell-free extract (14 mU/mg). The oxidation of reduced riboflavin (-400 mV) by formate/ CO<sub>2</sub> (-420) is a slightly endergonic reaction. But it seems it is the dominant process occurring in *B. stamsii* as it was also shown by activity measured with riboflavin in the presence of FAD. Formate dehydrogenase activity was observed with ferredoxin in the presence of FAD as cofactor suggesting formate is removed from the system to avoid reversible reaction process to keep riboflavin in oxidized state. These findings suggest that flavins and ferredoxin are oxidized through formate dehydrogenase.

### **3.8 Activity staining in cell free extracts of *B. stamsii***

Activity staining for NADH dehydrogenase (Figure 7E) resulted in mainly two bands on the native gel which were analyzed by Peptide-Mass-fingerprinting analysis. The activity staining for pyruvate dehydrogenase (Figure 7C) activity showed one single band. The comproportionating pyruvate dehydrogenase with NADH and FAD in addition to pyruvate and CoA-SH resulted two bands similar to NADH dehydrogenase (Figure 7B), but one was more intense at the same position in both controls (Figure 7D). The activity staining performed for formate dehydrogenase with the FAD resulted appearance of a very prominent pink color band which was developed within 5 minutes. Similar results obtained even without anoxic conditions (Figure 7E). The hydrogenase activity staining resulted in two bands without FAD and hydrogen. The Coomassie staining was also performed by using native PAGE marker as a standard (Figure 7A). During the writing results of activity stained bands for protein identification were unavailable.

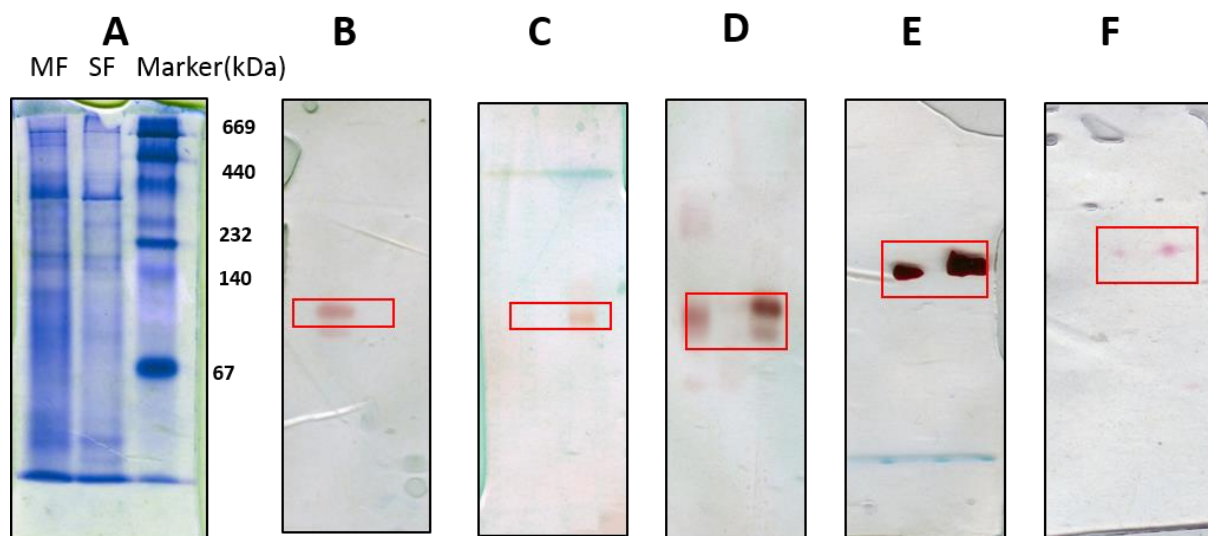


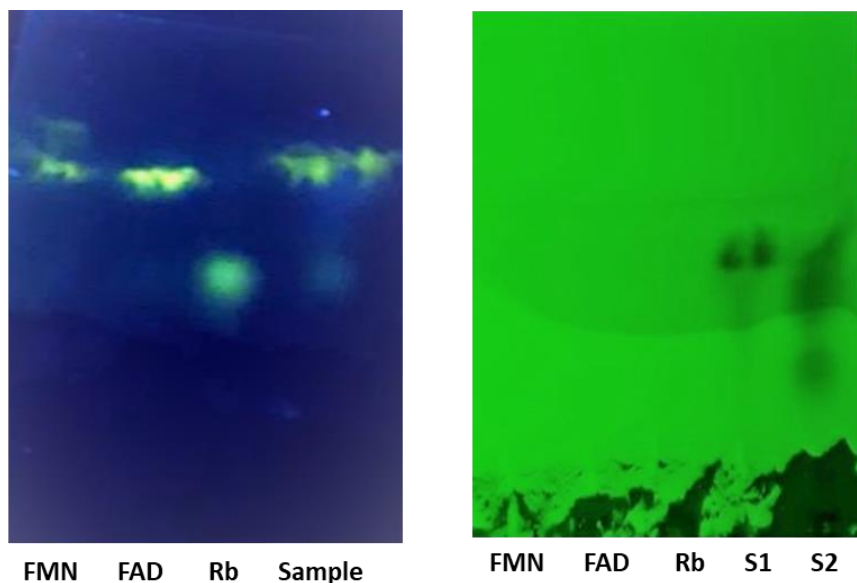
**Figure 7.** **A)** Coomassie staining of cell-free extracts membrane fraction (MF), soluble fraction (SF) and standard native protein PAGE marker. **B)** NADH dehydrogenase activity staining (50 mM Tris-HCl + 3 mM DTT + 2 mM benzyl viologen + 0.2 mM TTC + 0.2 mM NADH). **C)** Pyruvate dehydrogenase activity staining (50 mM Tris-HCl + 3 mM DTT + 10 mM pyruvate + 1 mM CoA-SH + 2 mM benzyl viologen + 0.2 mM TTC). **D)** comproportionating pyruvate dehydrogenase (50 mM Tris-HCl + 3 mM DTT + 0.1 mM FAD + 2 mM benzyl viologen + 0.2 mM TTC + 0.2 mM NADH). **E)** Formate dehydrogenase activity staining (50 mM Tris-HCl + 3 mM DTT + 2 mM benzyl viologen + 0.2 mM TTC + 10 mM formate + 0.2 mM FAD). **F)** activity staining for ferredoxin hydrogenase (50 mM Tris-HCl + 3 mM DTT + 2 mM benzyl viologen + 0.2 mM TTC + Hydrogen as gas phase).

### 3.9 Isolation of flavin like cofactor in *B. stamsii*

Most microorganisms synthesize riboflavin by riboflavin biosynthetic pathway (RBP) that produces one molecule of riboflavin from two molecules of ribulose-5-phosphate and one molecule of guanidine triphosphate by the combined activities of five enzymes (Jemenez et al., 2005, Guttierrez et al., 2015). Some bacteria do not possess RBP genes, but they contain genes encoding for the transporter proteins for riboflavin uptake from the extracellular environment (Vitreschak et al., 2002, Deka et al, 2013). Our results suggest that, *B. stamsii* has the ability to produce FAD (growth medium contains little amount of vitamin B1-riboflavin) and alternatively strain could also accumulate riboflavin from medium when supplemented with yeast extract. After extracting flavin-like compounds from glucose grown

---

cells of *B. stamsii*, the presence of FAD and/or riboflavin could be identified by thin-layer chromatography (TLC, Figure 8). In TLC, the isolated flavin compound was running at the same retention time as standard FMN or FAD. However, there was also a small band which appeared close to the retention time of standard riboflavin (Figure 7). In bacteria, the catalytically active form of riboflavin is FMN (flavin mononucleotide) or FAD (flavin adenine dinucleotide) which occurs in different redox states such as oxidized, reduced by one electron or reduced by two electrons. FMN or FADs are known to be involved in a broad range of redox reactions or electrons transfer reactions catalyzed by flavin based-enzymes where it serve as electron carriers such as in electron bifurcation reactions (Edward, 2014), (Weghoff et al., 2012; Hasse et al., 2014, Buckel and Thauer, 2018). Therefore, in *B. stamsii* it can be assumed that it acts as a natural electron acceptor in various flavin-based redox reactions catalyzed by flavin-based enzymes that are most probably involved in electron bifurcation reactions. Furthermore, the reproducible enzyme activities measured with ferredoxin, riboflavin or FAD strongly indicate these are alternate electron acceptors to each other. Earlier studies have shown that ferredoxin ( $E_0 = -400$  mV) and flavodoxin ( $E_0 = -420$  mV) can alternate to catalyze the dehydration reactions during the fermentation of glutamate (Thamer et al., 2003).



---

**Figure 8:** Chromatogram of standards of FMN, FAD, riboflavin and isolated samples from *B. stamsii* under UV irradiation.

## 4. Conclusion

The results of enzyme activity strongly indicate that the redox enzymes involved in the re-oxidation of NADPH and ferredoxin in *A. acetethylicum* are ferredoxin hydrogenase, ferredoxin NADP reductase and NADP-dependent hydrogenase. In consistent with these observations, activity staining for ferredoxin hydrogenase and NADP-dependent hydrogenase also showed the involvement of these enzymes for re-oxidation of NADPH and ferredoxin. By contrast, in *B. stamsii* the three main enzyme systems that seems to play key role in ferredoxin and NADH re-oxidation. The first, comproportionating pyruvate dehydrogenase for which activity with riboflavin as well as ferredoxin was observed could be observed as stated in the proposed model. Furthermore, in the genome of *B. stamsii* we have found two genes encoding uncharacterized NADH dehydrogenase (Bsta\_01029), NAD(FAD)-dependent dehydrogenase (Bsta\_01904) which are potential candidate enzymes for re-oxidation of NADH, independent of comproportionating pyruvate dehydrogenase complex. In third system pyruvate formate lyase converts pyruvate into Acetyl-CoA and formate by oxidizing NADH and flavins most similar ways of flavodoxin. Further formate dehydrogenase could cycle reduced riboflavin and ferredoxin produced by PFOR by formate dehydrogenase, and high activity was observed with riboflavin.

## 5. Materials and Methods

### 5.1 Cultivation of strains

*Anaerobium acetethylicum* was grown in sulfide-reduced freshwater medium by supplementing either gluconate (10mM) or glucose (10mM) as a substrate as described before (Patil et al., 2015). *Bacillus stamsii* (DSM 19598) was available in our lab was cultivated in freshwater reduced medium either as a pure culture (using glucose plus pyruvate) and in co-culture (glucose) with *Methanospirillum hungatei* (DSM 13809). Substrates were added to growth medium from the filter sterilized stock solutions. All cultivation experiments were performed at 30° C. The growth of the strain was determined by using change in optical densities taken at 600nm.

---

## 5.2 Preparation of cell-free extracts

For the production of cell-free extracts, *A. acetethylicum* was grown in a 1 liter medium by using gluconate or glucose as a growth substrate. After 2-3 day of incubation growth, culture was harvested anoxically in log-phase by centrifugation (7000 rpm x 30 min at 8° C; Sorvall RC-5B centrifuge with GS-3 rotor). The resulting cell pellet was washed and finally re-suspended in 50 mM Tris-HCl buffer (pH 7.5) containing 3 mM DTT, 1 mg DNase, and 5 mg of protease inhibitor cocktail. For the preparation of cell-free extract, cells were opened by passing through pre-cooled French Pressure cell (SLM AMINCO) operated at pressure 137 MPa. To remove cell debris, cell lysate was centrifuged at 27000 rpm for 30 minute. Resulting supernatant was referred as crude extract. In order to obtain soluble protein fraction, crude extract centrifuged at 50000 rpm for 1 hour and the supernatant was stored on ice or directly used for the enzyme assays. Similarly, coculture of *Bacillus stamsii* with *M. hungatei* was harvested anoxically by centrifugation (7000 rpm x 30 minutes). The resulted cell pellet was washed and finally re-suspended in 50 mM Tris-HCl buffer (pH 7.6 containing 3 mM DTT), 1 mg DNase (Fermentas), 1 mg RNase (Fermentas), 5 mg protease inhibitor cocktail (P 8465 Sigma Aldarich), 100 µl mutanolysin (1 U/ µl) and 0.01 mM FAD. For the preparation of cell-free extract of cells of *B. stamsii*, selective cell lysis of bacterial cells was performed by the action of mutanolysin incubated at 37° C for about 1 h (Wallrabenstein and Schink, 1994). The lysis of *Bacillus* cells was confirmed microscopically. The suspension was then centrifuged at 27000 rpm for about 30 minutes (Optima TL ultracentrifuge, Beckmann, Munich). The resulting supernatant was termed as cell-free extract and stored on ice for enzyme activity measurements and stored at -20 C for proteomic analysis.

## 5.3 *In vitro* enzyme assays with cell-free extracts

All spectrophotometric enzyme activities were performed at 30° C and measured by using spectrophotometer (Jasco V-630 or V-730, Gross-Umstadt, Germany). The standard enzyme assays were performed using 1 ml quartz or glass cuvettes. Cuvettes were made anoxic using N<sub>2</sub> gas and closed with butyl-rubber septum. All the stock solutions and buffers used for the enzyme activity measurements were made anoxic. All the additions were performed using gas-tight microliter syringes (Macherey-Nagel, Germany).

---

**A) *In vitro* enzyme activity measurements of *Bacillus stamsii***

**i) NADH-oxidoreductase** (EC 1.6.99.3): activity was measured in 1 ml reaction mixture containing 50 mM Tris-HCl buffer pH 7.5 with 3 mM DTT, 0.1 mM NADH, 0.01 mM FAD, 50  $\mu$ M ferredoxin ( $\epsilon$  390nm = 2.9) or 0.1  $\mu$ M riboflavin ( $\epsilon$  445nm = 13.1). Enzyme reactions were started by the addition of 20  $\mu$ l cell-free extract. The decrease in absorbance was detected at 390nm or at 445nm.

**ii) Pyruvate dehydrogenase** (EC 1.2.4.1) activity was measured in 1 ml reaction mixture containing 50 mM Tris-HCl buffer pH 7.6 with 3 mM DTT, 0.1 mM NAD / NADP / benzyl viologen/ Fd / Riboflavin , 10 mM pyruvate, 0.1 mM CoA-SH. The reaction was started by addition of 20  $\mu$ l cell-free extract and increase of absorbance was measured at respective wavelengths.

**iii) Comproportionating pyruvate dehydrogenase** activity was measured in 1 ml reaction mixture containing 50 mM Tris-HCl buffer pH 7.5 with 3 mM DTT, and 0.01 mM FAD, 10 mM pyruvate, 0.1 mM CoA-SH, 50  $\mu$ M ferredoxin or riboflavin 0.1  $\mu$ M and 20  $\mu$ l of cell free extract. After starting pyruvate dehydrogenase activity 0.1 mM NADH was added and increase in activity was measured at 390 or 445 nm. Alternatively, the background NADH dehydrogenase activity was started followed by the addition of pyruvate and CoA-SH to see the expected increase in activity.

**iv) Formate dehydrogenase** (EC 1.2.1.2) activity was measured in 1 ml of reaction mixture containing 50 mM Tris-HCl buffer pH 7.5 with 3 mM DTT, 0.01 mM FAD, 50  $\mu$ M ferredoxin / 0.1  $\mu$ M riboflavin/ 0.1 mM NAD/ 0.1 mM NADP, 10 mM formate and 20  $\mu$ l cell free extract.

**B) *Enzyme activity measurements of A. acetethylicum***

**i) Ferredoxin hydrogenase** (EC 1.12.7.2) activity was measured at 390 nm in 1 ml of reaction mixture containing 50 mM Tris-HCl buffer pH 7.6 with 3 mM DTT, 20  $\mu$ l of cell free extract, 1 mM NAD or NADP or benzyl viologen or ferredoxin. The cuvette was flushed with hydrogen and the activity was started by the addition of cell free extract.

---

**ii) Formate dehydrogenase** (EC 1.2.1.2) activity was measured in 1 ml of reaction mixture containing Tris-HCl buffer pH 7.6 with 3 mM DTT, 20 µl of cell free extract, 0.2 mM NAD/NADP/ or 50 µM of ferredoxin. The activity was started by the addition of 10 mM formate.

**iii) Pyruvate: ferredoxin oxidoreductase** (EC 1.2.7.1) activity was measured at 390 nm in 1 ml reaction mixture containing 50 mM Tris-HCl pH 7.6 with 3 mM DTT, 20 µl cell free extract, 50 µM ferredoxin or 0.2 mM NAD/NADP, 10 mM pyruvate, 0.1 mM of CoA-SH. The reduction of ferredoxin was observed at 390 nm.

**iv) NADP dependent hydrogenase** (EC 1.12.1.3) NADP-dependent hydrogenase activity was measured at 340 nm in 1 ml reaction mixture containing 50 mM Tris -Cl pH 7.6 with 3 mM DTT, 20 µl of cell free extract, 0.1 mM NADP. Hydrogen was used in the gas phase.

**v) Bifurcating NADP dependent hydrogenase** activity was measured with NADP at 340 nm in reaction mixture containing 50 mM Tris-HCl buffer of pH 7.6 with 3 mM DTT, 0.1 mM NADP, 20 µl CFE and 50 µM ferredoxin. Hydrogen was used in the gas phase.

**vi) Ferredoxin NADP reductase** (EC 1.18.1.2) activity was measured at 340 nm in 1 ml total reaction mixture containing 50 mM Tris-HCl buffer pH 7.6 with 3 mM DTT, 0.1 mM NADPH and 50 µM ferredoxin. The reaction was started by addition of 20 µl CFE.

**vii) Determination of NADPH stimulated hydrogenase**

The activity of NADPH dependent hydrogenase or confurcating hydrogenase was tested in physiological direction for the formation of hydrogen. The assay was performed as describe before (Müller et al., 2010) in small serum bottles closed with butyl-rubber stoppers and flushed with 100% N<sub>2</sub>. The 1 ml reaction assay mixture contained 100 mM potassium phosphate buffer pH 7.5, with 3 mM DTT, 2.5 mM NADPH, 5 mM sodium dithionite (Freshly prepared), and 100 µl of soluble fraction. The reaction mixture was incubated at 30°C in water-bath and after 60 minutes the gas sample of 200 µl was removed from the headspace of the bottle by airtight syringe and hydrogen was measured by GAS chromatography (Carlo Erba, GC-4300 as describe before (Müller et al., 2010). The control reactions were contained without NADH or dithionite or CFE. The specific enzyme activities were calculated from the amount of hydrogen produced per minute per mg of protein.

---

## 5.4 Protein electrophoresis and activity staining

### *i) SDS-PAGE electrophoresis*

Sodium-dodecyl-sulfate (SDS) polyacrylamide gel electrophoresis was done according to Laemmli method (1970). The resolving gel of 12% polyacrylamide and stacking gel of 4% polyacrylamide concentration was prepared. Protein samples were mixed with sample loading buffer in 1:1 proportion and heated at 95°C for 5-10 minutes. The samples were loaded on gel using micropipette tips along with prestained standard protein molecular weight marker (range 180 kDa -15 kDa). Electrophoresis was done by applying current of 100V for about 90 min until the marker front had reached to the bottom. Protein band on SDS-gels were visualized by staining the gels with Coomassie staining solution. Gel images were scanned by using HP gel scanner.

### *ii) Native PAGE electrophoresis*

Native polyacrylamide gels were prepared containing 10% polyacrylamide in resolving gel and 4% polyacrylamide in stacking gel. The samples were mixed with the sample buffer in 1:1 ratio and directly loaded on gel without any treatments. The gel was allowed to run at 90 V for 90 minutes. The native marker was used as a standard for comparing the molecular weights. The gel was carefully sliced into half and transferred into the solution for the respective activity staining as well as Coomassie staining. Bands were sliced after activity staining and submitted for analysis by peptide Mass-Fingerprinting spectrophotometry.

### *iii) Activity staining and Coomassie staining of the native gels*

For the activity staining of hydrogenase enzyme activity of *A. acetethylicum* the gel was cut and washed with 50 mM Tris-HCl buffer pH 7.6. After washing the gel was submerged in into the same buffer solution in anoxic box containing 2 mM benzyl viologen, 0.2 mM TTC, and 0.1 mM NADPH or gel was purged by using hydrogen gas or 5 mM formate with N<sub>2</sub> gas phase until the stained bands appeared for activity staining. The gel was stained in 40 ml of colloidal Coomassie staining solution mixed with 10 ml methanol (Neuhoff et al., 1988). The stained protein bands in activity staining were excised and submitted for protein identification by peptide mass fingerprinting spectrophotometry.

---

For activity staining of comproportionating pyruvate-dehydrogenase complex the cell-free extract of *B. stamsii* were run on native gel and the gel was cut into three replicates. Controls experiment for activity staining were made using different combination: control 1 contained 2 mM benzyl viologen, 0.2 mM NADH and 0.02 mM TTC in 20 ml of 50 mM Tris-HCl pH 7.6 with 3 mM DTT; control 2 contained 20 ml 50 mM Tris-HCl pH 7.6 with 3 mM DTT, 10 mM pyruvate, 2 mM benzyl viologen, 0.02 mM TTC and 0.5 mM CoA-SH. The mixture for enzyme assay test contained 20 ml 50 mM Tris-HCl pH 7.6 with 3 mM DTT, 0.2 mM NADH, 10 mM pyruvate, 0.5 mM CoA-SH, 0.02 mM TTC, 2 mM benzyl viologen and 0.05 mM FAD. The gel was allowed to stain in the mixture separately in different plates which were in anoxic staining box under the N<sub>2</sub> atmosphere. For formate dehydrogenase activity staining the same reaction mixture with TTC and benzyl viologen was used and formate was used as a substrate instead of NADH or pyruvate.

### **5.5 Protein identification by mass spectrometry**

The stained protein bands were excised from the gel and analyzed by peptide fingerprinting-mass spectrometry at the Proteomics Facility of University of Konstanz. After destaining protein bands, protein bands were treated overnight with trypsin for protein digestion to form individual peptide fragments. Then fragments were analyzed via reversed phase liquid chromatography (LC-MS) and Nano tandem Mass Spectrometry (MS) by using LTQ-Orbitap mass spectrometer (Thermo Fischer) and an Exsigent nano-HPLC. The samples were injected and for the first 5 minutes mixture of 90 % mobile phase A (0.1% formic acid) and 10 % mobile phase B (0.1% formic acid in acetonitrile) was allowed to run through the column. The peptide was eluted with specific gradient of mobile phase B. The LTQ-Orbitap spectrometer was operated in data mode. The five most abandoned molecular ions in the MS scans were selected and fragmented by CID. With Matrix Science (Mascot) the tandem mass spectra of analyzed peptides compared with *B. stamsii* database and proteins of *B. stamsii* were identified.

---

## 5.6 Isolation of riboflavin from *B. stamsii* and ferredoxin from *C. pasterianum*

The riboflavin isolation was performed for the identification of the cofactors present in cell extracts of *B. stamsii*. The aerobically grown pure culture of *B. stamsii* was used to produce large amount of cell mass for the isolation. The presence of FAD and riboflavin was identified in cell extracts of *B. stamsii* by thin layer chromatography using thin silica gel as stationary phase and water as a mobile phase. The standard FMN, FAD and riboflavin were run as standards with the sample. After development of the chromatogram the paper was dried and observed in the UV light at 254 and 345 wavelength in dark. Ferredoxin was isolated and prepared for enzyme activity measurements from the *C. pasterianum* (Schonheit et al, 1978). Protein concentration was determined by using Bradford assay (Bradford, 1976). Bovine serum albumin was used to prepare standard curve.

### Chemicals

All the chemicals were of analytical grade and were purchased from Sigma-Aldrich (Munich, Germany), Merk, Carl Roth (Karlsruhe, Germany), Roche diagnostics GmbH (Mannheim, Germany, Fluka chemicals, Serva or Emsure etc. The gases were purchased from the Messer-Grieseheim (Darmstadt, Germany) and Sauerstoffwerke Friedrichshafen (Friedrichshafen, Germany).

### List of Abbreviations

SDS: sodium dodecyl sulfate, CID: collision induced dissociation, DTT: Dithiothreitol, FAD: Flavin Adenine Dinucleotide, Fd: ferredoxin, CoA: Coenzyme-A. IMG/M: Integrated Microbial Genome and Microbiomes, HPLC: High Performance Liquid Chromatograph, TTC: Triphenyl Tetrazolium Chloride, BV: benzyl viologen, MS: Mass spectrometry. PDH: pyruvate dehydrogenase, FDH: formate dehydrogenase, NAD: nicotinamide adenine dinucleotide, NADP: nicotinamide adenine dinucleotide phosphate.

### Acknowledgment

The authors are thankful to LGFG scholarship program for providing scholarship to YP. The authors are also acknowledging the Proteomics Facility Center of University of Konstanz for proteomics analysis. The authors are thankful to Antje Wiese for helping in preparation of growth media and Julia Schmidt for preparation of ferredoxin from *C. pasterianum* for enzyme assays.

---

# CHAPTER 6

---

## General Discussion/Conclusions

---

## 1. Fermentation of glycerol and gluconate by *A. acetethylicum*

The fermentation of glucose and gluconate occurs in anaerobic bacteria in the absence of oxygen. During fermentations, the substrate serves not only as an electron donor, but also as a terminal electron acceptor, since oxygen, nitrate, fumarate, etc. are absent (Thauer et al., 1977). Therefore, such anaerobic bacteria do not use an electron transport chain to oxidize NADH to NAD<sup>+</sup> and must adapt to an alternative method for balancing reducing equivalents, e.g., NADH and maintain a supply of NAD<sup>+</sup> for the proper functioning of normal metabolic pathways (e.g. glycolysis) and energy conservation metabolism (Stadtman, 1966).

The study in chapter 2 described the draft genome sequence of *A. acetethylicum* which allowed us to gain detailed insight into its physiological and metabolic features. The strain GluBS11 belong to the family *Lachnospiraceae* within the order of *Clostridiales* (Rainey et al., 2009). The annotated genome contained putative genes coding for pentose phosphate pathway, the Embden-Meyerhof-Parnas pathway, the Entner-Doudoroff pathway and the tricarboxylic acid cycle. The identified genes in the genome indicated fermentation of glucose and gluconate to end products acetate, ethanol, and hydrogen. However, no genes for formate dehydrogenase were found in the genome. The draft genome sequence expands our views on the metabolic capabilities of strain GluBS11. Glycerol and gluconate fermentation has been studied in details for *A. acetethylicum* (Patil et al., 2017) and pathways were proposed based on biochemical assays, proteome analysis, and identification of genes in the draft genome.

The fermentation of glycerol resulted into ethanol, hydrogen, CO<sub>2</sub> as the major fermentation end-products. The glycerol fermentation was started by glycerol oxidation to dihydroxyacetone (DHA) by NAD dependent glycerol dehydrogenase enzyme. Then by the activity of dihydroxy acetone kinase and triose phosphate isomerase produced glyceraldehyde-3-phosphate. Pyruvate is produced via lower glycolysis part. The pyruvate is most likely oxidized by PFOR (pyruvate ferredoxin oxidoreductase) into acetyl-CoA. Acetyl-CoA is reduced into ethanol by acetaldehyde dehydrogenase and alcohol dehydrogenase enzymes. Acetate and formate was also produced in lower amounts. The total proteome analysis was performed to identify the proteins expressed after growing with glycerol as a growth substrate.

---

The studies on gluconate fermentation pathway in the strain *A. acetethylicum* showed that the gluconate fermentation found to occur through a modified ED pathway. In chapter 4 of this study the complete gluconate fermentation pathway based on results of enzyme activities, total proteome analysis as well as genome analysis is proposed which confirms the presence of a modified ED pathway in strain *Anaerobium acetethylicum*. Gluconate was found to be degraded by three main enzymes into pyruvate which differs it from the classical ED pathway. From the pyruvate major fermentation products acetate, formate, ethanol and hydrogen are formed. Similar pathways are also occurring in *Clostridium* species (Andreesen et al., 1969, Andreesen et al., 1970, Bender et al., 1971). However, strain GluBS11 differs from other strain that it produced no butyrate with glycerol as well as gluconate or glucose.

## **2. Energy metabolism in BoGlc83 and GluBS11**

The fermentation of glucose by *B. stamsii* was studied previously and found to occur via EMP (Embden-Meyerhof-Parnas) pathway (Müller et al., 2008). To avoid the overproduction of NADH, fermentative organisms usually do not have a complete citric acid cycle and have slightly different sets of enzyme systems. Ferredoxin and NADH reoxidizing enzymes and possible bifurcating systems were studied by enzymatic assays as well as confirmed by proteomic analysis in *A. acetethylicum*. The genome search was performed for the identification of respective genes and gene clusters to relate it to the activities found in respective enzymes in cell-free extract. The activity staining was also performed in native gels with respective cell free extracts in different trials and stained bands were analyzed by peptide-mass-fingerprinting analysis. The gene clusters are present in *A. acetethylicum* for NADP hydrogenase (HndD \_ 1001466, HndC\_1001467, HndB\_1001468, DNA gyrase\_1001469, HndA\_1001470), ferredoxin hydrogenase (Ga0116910-100545) and ferredoxin NADP reductase (Ga0116910-1001164) and iron containing hydrogenase (Ga0116910-100543) for the reoxidation of reduced equivalents and formate dehydrogenase for ferredoxin reoxidation to a lower extent.

In addition to this *A. acetethylicum* also produced ethanol via acetyl-CoA by acetaldehyde dehydrogenase and alcohol dehydrogenase enzymes which oxidizes NADH into NAD. As *A. acetethylicum* has alcohol dehydrogenase enzymes it is able to produce ethanol and NADH reoxidation occurs in more efficient ways than *B. stamsii*. This is the reason why it does not

---

need external syntrophic partner organism and grows in higher densities than *B. stamsii*. The presence of separate gene clusters contained the presence of gene encoding individual enzymes responsible for reoxidation and no bifurcating enzyme activities could be seen. The strain uses modified ED pathway which produces lower amounts of NADH makes strain energetically more efficient than EMP pathway. It has hydrogenases as main oxidizing enzymes and lacks formate dehydrogenase or bifurcating enzymes.

The fermentation of glucose by *B. stamsii* occurs with the syntrophic partner organism (methanogen) and acetate and methane was found to be major fermentation products but no ethanol was produced (Müller et al., 2015). The growth was possible in pure culture form only if pyruvate was added as a co-substrate by EMP pathway. When grown with glucose and pyruvate as a co-substrate in pure culture, strain BoGlc83 produced acetate, lactate and formate as major fermentation products. Since it is facultative anaerobic and also syntrophic bacterium the enzymes for reoxidation of reduced equivalents are different than the obligate anaerobic *A. acetethylicum*. The second reason is it lacks the enzyme alcohol dehydrogenase for ethanol production that makes strain difficult to oxidize NADH. Strain produced lactate that is also one way to get rid of excess NADH. Lactate was not produced (negligible) during syntrophic growth.

The redox enzymes in *B. stamsii* were studied by enzymatic assays with riboflavin and ferredoxin as an electron acceptors were proposed. The presence of riboflavin/FAD in cell free extracts was done by isolating riboflavin from the cells of *B. stamsii* shows that riboflavin is an important cofactor in *B. stamsii* and it is involved in enzyme activities for energy conservation. Flavins serve as an electron carrier in a wide range of electron transfer reactions (Edward, 2014), e.g., bifurcating reactions in which two high potential electrons from a single donor are bifurcated into two single electron acceptors (Hasse et al., 2014, Buckel and Thauer, 2018). It was shown that riboflavin biosynthesis increases the reduction of extracellular Fe<sup>3+</sup> (Crossley et al., 2007). Earlier studies have shown that ferredoxin ( $E_0' = -400$  mV) and flavodoxin ( $E_0' = -420$  mV) alternate to catalyze the dehydration reactions depending on the state of iron during the fermentation of glutamate in *Acidaminococcus fermentans* (Thamer et al., 2003).

Based on the genome analysis, proteome analysis and results of an enzyme activities, we proposed the NADH and ferredoxin reoxidizing enzymes. The strain found to contain

---

riboflavin reducing system involving PFL (pyruvate formate lyase) and ferredoxin reducing system. The comproportionating PFOR is used by the strain to oxidize the NADH by pyruvate oxidation. The comproportionating PFOR complex was proposed from the specific arrangements of the genes in the genome of *B. stamsii*. Such enzymes themselves are special in a way that it produced acetyl-CoA for generation of ATP and skips the step of NAD reduction used by normal pyruvate dehydrogenase complex. Further formate was found to be formed by formate dehydrogenase by reoxidation of reduced flavins and ferredoxin. The complete mechanism of both the enzyme complex had been discussed in details which differs it from *A. acetethylicum*.

Further separate NADH dehydrogenases are also studied by an enzyme activity measurement as a candidate for NADH oxidation in *B. stamsii*. It makes clear now why *B. stamsii* needs pyruvate as a cosubstrate in the absence of external partner for growth. Since it needs to reduce the flavins and ferredoxin for skipping the step of production of NADH to conserve energy through reduction of flavins and ferredoxin as it lacks alcohol dehydrogenase enzymes for NADH reoxidation and has formate dehydrogenase as a main reoxidizing enzyme. The glucose fermenting organism *B. stamsii* and gluconate fermenting organism *A. acetethylicum* have a different sets of enzymes involved in pyruvate oxidation as well as oxidation of reducing equivalents such as NADH and ferredoxin. Summarized redox enzymes system present in *A. acetethylicum* and *B. stamsii* are shown in figure 1 that describes the basic differences in energy metabolism in these two organisms.

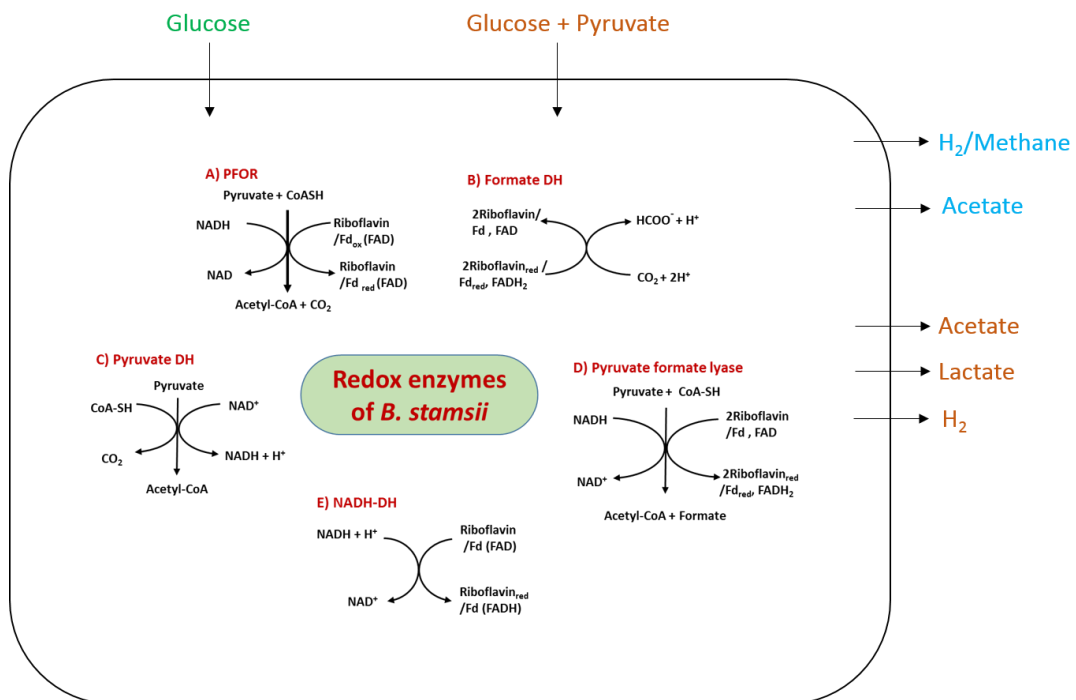
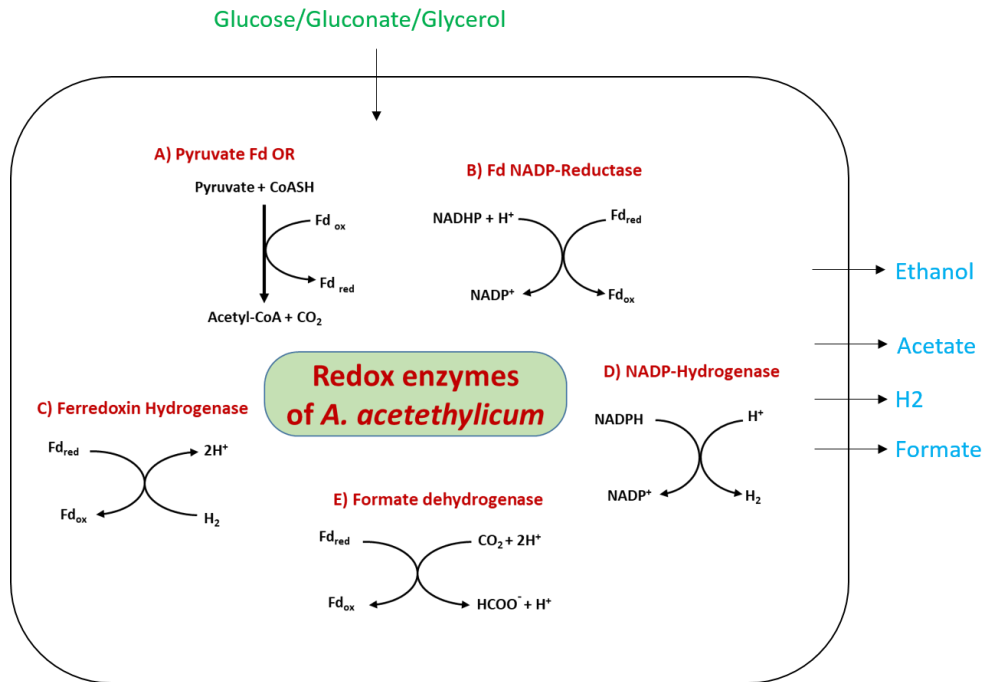


**Figure 1.** Summary of key redox enzymes of *A. acetethylicum* and *B. stamsii* involved in reoxidation of reducing equivalents (NAD(P)H and ferredoxin) and energy metabolisms.

---

## List of publications

### Published

1. **Patil, Y.**, Junghare, M. and Müller, N. (2017). Fermentation of glycerol by *Anaerobium acetethylicum* and its potential use in biofuel production. *Microbial Biotechnology*.10:203-17.
2. **Patil, Y.**, Müller N., Schink, B. et al., and Junghare, M. (2016). High-quality-draft genome sequence of the fermenting bacterium *Anaerobium acetethylicum* type strain GluBS11T (DSM 29698). *Standards in Genomic Sciences Stand Genomic Sci. doi:10. 1186/s40793-017-0236-4*.

### Under-review

3. **Patil Y**, Junghare M, Müller N. (2019). Gluconate-fermentation by *Anaerobium acetethylicum*: an evidence for the involvement of modified Entner-Doudoroff pathway (Under review, Microbial Cell Factories).

### Draft manuscript

4. **Patil Y**, Müller N. (2019). Enzymes involved in re-oxidation of reducing equivalents in glucose and gluconate fermentation (To be submitted).

### Research not included in the thesis

5. **Patil, Y.**, Junghare, M., Pester, M., Müller, N., and Schink, B. (2019). Genus *Anaerobium*. In: Bergey's Manual of Systematic Bacteriology. (Under review).
6. Junghare, M., **Patil, Y.**, and Schink, B. (2015). Draft genome sequence of a nitrate-reducing, *o*-phthalate degrading bacterium *Azoarcus sp.* PA01T. *Standards in Genomic Sciences*, 10; 90.
7. **Patil, Y.**, Junghare, M., Pester, M., Müller, N., and Schink, B. (2015). *Anaerobium acetethylicum* gen. nov., sp. a strictly anaerobic, gluconate-fermenting bacterium isolated from a methanogenic bioreactor. *International Journal of Systematics and Evolutionary Microbiology*, 65(10); 3289-3296.

---

## Achievements and individual contribution

Unless stated otherwise, all the wet-lab experiments were performed by me under the guidance of Dr. Nicolai Müller and Prof. Dr. Bernhard Schink. All the proteomic identification work was performed by Mr. Marquat at the Proteomics Facility, University of Konstanz. The draft manuscript mentioned in chapter 5 needs improvement with some additional results (awaiting proteomic results). The chapters 2 to 5 co-authors contributions are mentioned.

### Chapter 2

High-quality-Draft genome sequence of fermenting bacterium *Anaerobium acetethylicum* type strain GluBS11T (DSM99698).

**Yogita Patil**, Nicolai Müller<sup>1\*</sup>, Bernhard Schink<sup>1\*</sup>, William B. Whitman<sup>3</sup>, Marcel Huntemann<sup>4</sup>, Alicia Clum<sup>4</sup>, Manoj Pillay<sup>4</sup>, Krishnaveni Palaniappan<sup>4</sup>, Neha Varghese<sup>4</sup>, Natalia Mikhailova<sup>4</sup>, Dimitrios Stamatis<sup>4</sup>, T. B. K. Reddy<sup>4</sup>, Chris Daum<sup>4</sup>, Nicole Shapiro<sup>4</sup>, Natalia Ivanova<sup>4</sup>, Nikos Kyrpides<sup>4</sup>, Tanja Woyke<sup>4</sup> and Madan Junghare<sup>1,2\*</sup>

YP, MJ, NM and BS initiated the project and YP performed DNA preparation. MJ and YP performed the comparative genomics, investigated the genome for general metabolic features and fermentation pathways. MJ, YP and NM drafted the manuscript that was critically reviewed and corrected by BS, NM, WW, NS and NK, respectively. Marcel Huntemann, Alicia Clum, Manoj Pillay, Krishnaveni Palaniappan, Neha Varghese, Natalia Mikhailova, Dimitrios Stamatis, T.B.K. Reddy, Chris Daum, Natalia Ivanova, and Tanja Woyke performed the technical work for sequencing, assembly and annotation of the genome. All authors read and approved the final manuscript.

### Chapter 3

Fermentation of glycerol by *Anaerobium acetethylicum* and its potential use in biofuel production.

**Yogita Patil**, Madan Junghare, Nicolai Muller

YP and MJ contributed equally. Experiments were conducted by YP, MJ and NM. NM, YP and MJ designed experiments and wrote the manuscript.

---

## Chapter 4

Gluconate-fermentation by *Anaerobium acetethylicum*: an evidence for the involvement of modified Entner-Doudoroff pathway.

**Yogita Patil**, Madan Junghare, Nicolai Muller

YP, MJ, and NM designed experiments which were conducted by YP. YP, MJ, and NM analyzed the data and wrote the manuscript. All authors read and approved the final version of the manuscript.

## Chapter 5

Reoxidation systems for reduced equivalents involved in glucose and gluconate fermentation by *A. acetethylicum* and *B. stamsii*.

**Yogita Patil**, Nicolai Mueller

YP and NM designed the experiments and YP conducted the experiments. YP and NM analyzed the data and wrote the manuscript.

---

## References

- Abdel-Hamid, A. M. Attwood, Margaret, M., Guest, J. R. (2001). Pyruvate oxidase contributes to the aerobic growth efficiency of *Escherichia coli*. *Microbiology*, 147: 1483-98.
- Adams, MW. (1990). The structure and mechanism of iron hydrogenases. *Biochim Biophys Acta*, 1020: 115-145.
- Adnan, A.A.N., Suraini, S.S., Aziz-Abd, S., Hassan, M.A., Phang, L.Y. (2014). Optimization of bioethanol production from glycerol by *Escherichia coli* SS1. *Renew Energ*, 66: 625-633.
- Ahmed H, Ettema TJG, Tjaden B, Geerling ACM, Van der Oost J, Siebers B. (2005). The semi-phosphorylative Entner–Doudoroff pathway in hyperthermophilic archaea: a re-evaluation. *Biochem J*, 390: 529-540.
- Al-Awqati Q. (1986). Proton-translocating ATPases. *Annu Rev Cell Biol*, 2: 179-199.
- Altschul SF, Gish W, Miller W, Myers EW, Lipman DJ. (1990). Basic local alignment search tool. *J Mol Biol*, 215: 403-410.
- Andreesen JR, Gottschalk G, Schlegel HG. (1970). *Clostridium formicoaceticum* nov. spec. Isolation, description, and distinction from *C. aceticum* and *C. thermoaceticum*. *Arch Mikrobiol*, 72: 154-174.
- Andreesen JR, Gottschalk G. (1969). The occurrence of a modified Entner-Doudoroff pathway in *Clostridium aceticum*. *Arch Mikrobiol*, 1969; 69:160-170.
- Andreesen, A.A., Stier, T.J.B. (1954). Anaerobic nutrition of *Saccharomyces cerevisiae*. II. Unsaturated fatty acid requirement for growth in a defined medium. *J Cell Comp Physiol*, 43: 271-281.
- Ashburner M, Ball CA, Blake JA, Botstein D, Butler H, Cherry JM, Davis AP, Dolinski K, Dwight SS, Eppig JT, Harris MA, Hill DP, Issel-Tarver L, Kasarskis A, Lewis S, Matese JC, Richardson JE, Ringwald M, Rubin GM, Sherlock G. (2000). *Gene*

- 
- ontology: tool for the unification of biology. The gene ontology consortium. *Nat Gene*, 25: 25-29.
- Ashwell G, et al., (1960). Uronic acid metabolism in bacteria. I. Purification and properties of uronic acid isomerase in *Escherichia coli*. *J Biol Chem*, 235: 1559-1565.
- Bankevich A, et al., (2012). SPAdes: a new genome assembly algorithm and its applications to single-cell sequencing. *J Comput Biol*, 19: 455-477.
- Barbirato, F., Chedaille, D., Bories, A. (1997a). Propionic acid fermentation from glycerol: comparison with conventional substrates. *Appl Microbiol Biotechnol*, 47: 441-446.
- Barbirato, F., Himmi, E.H., Conte, T., Bories, A. (1998b). 1, 3-Propanediol production by fermentation: an interesting way to valorize glycerin from the ester and ethanol industries. *Ind Crops Prod*, 7: 281-289.
- Barcenilla A, Pryde SE, Martin JC, Duncan SH, Stewart CS, Henderson C, Flint HJ. (2000). Phylogenetic relationships of butyrate-producing bacteria from the human gut. *Appl Environ Microbiol*, 66: 1654-1661.
- Bar-Even A, Flamholz A, Noor E, Milo R. (2012). Rethinking glycolysis: On the biochemical logic of metabolic pathways. *Nat Chem Biol*, 8: 509-517.
- Batstone, J. Keller, I. Angelidaki, S.V. Kalyuzhnyi, S.G. Pavlostathis, A. Rozzi, W.T. Sanders, H. Siegrist, V.A. Vavilin. (2002). The IWA Anaerobic Digestion Model No 1 (ADM1). *Water Sci Technol.*, 45: 65-73.
- Bender R, Andreesen JR, Gottschalk G. (1971). 2-keto-3-deoxygluconate, an intermediate in the fermentation of gluconate by *Clostridia*. *J Bacteriol*, 107: 570-573.
- Bennett S. (2004). Solexa Ltd. *Pharmacogenomics*, 5: 433-438.
- Bergmeyer HU, Bernt E. (1974). Determination of D-glucose with glucose oxidase and peroxidase. In: Bergmeyer HU, editor. *Methods of Enzymatic Analysis*. 3rd ed., vol. 3. New York & London: Academic Press; p. 1205-1215.

- 
- Bianchi TS. (2011). The role of terrestrially derived organic carbon in the coastal ocean: a changing paradigm and the priming effect. *PNAS*, 108: 19473–81.
- Biddle A, Stewart L, Blanchard J, Leschine S. (2013). Untangling the genetic basis of fibrolytic specialization by *Lachnospiraceae* and *Ruminococcaceae* in diverse gut communities. *Diversity*, 5: 627-640.
- Biebl, H. (2001). Fermentation of glycerol by *Clostridium pasteurianum* - batch and continuous culture studies. *J Ind Microbiol Biotech*, 27: 18-26.
- Biebl, H., Pfennig, N. (1978). Growth yields of green sulfur bacteria in mixed cultures with sulfur and sulfate reducing bacteria. *Arch Microbiol*, 117: 9-16.
- Boll M, Fuchs G, Tilley G, Armstrong FA, Lowe DJ. (2000). Unusual spectroscopic and electrochemical properties of the 2[4Fe-4S] ferredoxin of *Thauera aromatica*. *Biochemistry* 39:4929–4938.
- Booth, I.R., Ferguson, G.P., Miller, S., Li, C., Gunasekera, B., Kinghorn, S. (2003). Bacterial production of methylglyoxal: a survival strategy or death by misadventure? *Biochem Soc Trans*, 31: 1406-1408.
- Bradford, M.M. (1976). A rapid and sensitive method for the quantification of microgram quantities of protein utilizing the principle of protein-dye binding. *Analytical Biochemistry*, 72: 248-254.
- Braune A, Bendrat K, Rospert S, Buckel W: (1999). The sodium ion translocating glutaconyl-CoA decarboxylase from *Acidaminococcus fermentans*: cloning and function of the genes forming a second operon. *Mol Microbiol*, 31: 473–487.
- Bryan R. et al., (2011). "Formate Formation and Formate Conversion in Biological Fuels Production," *Enzyme Research*, 532536. Bryant, M.P., Wolin, E.A., Wolin, M.J., Wolfe, R.S. (1967). *Methanobacillus omelianskii*, a symbiotic association of two species of bacteria. *Arch Microbiol*, 59: 20-31

- 
- Buckel W, Thauer RK. (2018). Flavin-based electron bifurcation, ferredoxin, flavodoxin, and anaerobic respiration with protons (Ech) or NAD<sup>+</sup> (Rnf) as electron acceptors: a historical review. *Front Microbiol*, 9: 401.
- Buckel, W., Thauer, R. K. (2013). Energy conservation via electron bifurcating ferredoxin reduction and proton/Na<sup>+</sup> translocating ferredoxin oxidation. *Biochim Biophys Acta*, 1827: 94–113.
- Buckel, W., Thauer, R. K. (2018). Flavin-based electron bifurcation. A new mechanism of biological energy coupling. *Chem Rev* 118: 3862–3886.
- Bushnell B. BB Tools software package, URL <http://sourceforge.net/projects/bbmap/>
- Campbell, C.J., Laherrere, J.H. (1998). The end of cheap oil. *Sci Am*, 3: 78-83.
- Canfield DE, Rosing MT, Bjerrum C. (2006). Early anaerobic metabolisms. *Phil Trans Roy Soc B Biol Sci*, 361: 1819–1834.
- Capone D.G. Kiene R.P. (1988) Comparison of micro-bial dynamics in marine and freshwater sediments: Contrasts in anaerobic carbon catabolism. *Limnology and Oceanography*, 33: 725-749.
- Casalot L, De Luca G, Dermoun Z, Rousset M, de Philip P. (2002). Evidence for a fourth hydrogenase in *Desulfovibrio fructosovorans*. *J Bacteriol*, 184; 853-6.
- Ceremuga, T. E., et al., (2014). Effects of L-theanine on posttraumatic stress disorder induced changes in rat brain gene expression. *The Scientific World Journal*, 419032.
- Chen, P.Y., Aman, H., Can, M., Ragsdale, S.W., Drennan, C.L. (2018). Binding site for coenzyme A revealed in the structure of pyruvate: ferredoxin oxidoreductase from *Moorella thermoacetica*. *Proc Natl Acad Sci*, 115: 3846-3851.
- Choi, W.J. (2008). Glycerol-based biorefinery for fuels and chemicals. *Recent Pat Biotechnol*, 2: 173-180.
- Clomburg, J.M., Gonzalez, R. (2011). Metabolic engineering of *Escherichia coli* for the production of 1, 2-propanediol from glycerol. *Biotechnol Bioeng*, 108: 867-879.

- 
- Clomburg, J.M., Gonzalez, R. (2013). Anaerobic fermentation of glycerol: a platform for renewable fuels and chemicals. *Trends Biotechnol*, 31: 20-28.
- Colin, T., Bories, A., Lavigne, C., Moulin, G. (2001). Effects of acetate and butyrate during glycerol fermentation by *Clostridium butyricum*. *Curr Microbiol*, 43: 238-243.
- Collins MD, et al., (1994). The phylogeny of the genus *Clostridium*: proposal of five new genera and eleven new species combinations. *Int J Syst Bacteriol*. 1994; 44:812–26.
- Conway T. (1992). The Entner-Doudoroff pathway: History, physiology and molecular biology. *FEMS Microbiol Rev*, 9: 1–27.
- Cole JJ, Prairie YT, Caraco NF, McDowell WH, Tranvik, LJ, Striegl RG, Duarte, CM, Kortelainen P, Downing JA, Middelburg JJ, and Melack. (2007). Plumbing the global carbon cycle: Integrating inland waters into the terrestrial carbon budget. *Ecosystems*, 10: 172–185.
- Cotta M, Forster R. (2006). The Family *Lachnospiraceae*, Including the Genera *Butyrivibrio*, *Lachnospira* and *Roseburia*. In: Dworkin M, Falkow S, Rosenberg E, Schleifer, KH, Stackebrandt, E, editors. *The prokaryotes. Bacteria: firmicutes, cyanobacteria a handbook on the biology of bacteria*. Springer-Verlag, New York; p. 1002-1021.
- Cray, J.A., Stevenson, A., Ball, P., Bankar, S.B., Eleutherio, E.C., Ezeji, T.C., Singhal, R.S., Thevelein, J.M., Timson, D.J., Hallsworth, J.E. (2015). Chaotropicity: a key factor in product tolerance of biofuel-producing microorganisms. *Curr Opin in Biotech*, 33: 228-259.
- Crossley, R. A., Gaskin, D. J. H., Holmes, K., Mulholland, F., Wells, J. M., Kelly, D. J., et al. (2007). Riboflavin biosynthesis is associated with assimilatory ferric reduction and iron acquisition by *Campylobacter jejuni*. *Appl Environ Microbiol*, 73: 7819–7825.
- Crueger A, Crueger W. (1990). Glucose transforming enzymes. In: Fogarty WM, Kelly CT, editors. *Microbial Enzyme and Biotechnology*, 2nd edn. London, New York: Elsevier Applied Science, p. 177–226.

- 
- Da Silva, G.P., Mack, M., Contiero, J. (2009). Glycerol: a promising and abundant carbon source for industrial microbiology. *Biotechnol Adv*, 27: 30-39.
- Dabrock, B., Bahl, H., Gottschalk, G. (1992). Parameters affecting solvent production by *Clostridium pasteurianum*. *Appl Microbiol and Biotechnol*, 58: 1233-1239.
- Das A, Kundu PN. (1987). Microbial production of gluconic acid. *J Sci Ind Res*, 46: 307-331.
- De Ley, J., Doudoroff, M. (1957). The metabolism of D-galactose in *Pseudomonas saccharophila*. *J Biol Chem* 227, 745–757
- De Rosa M, Gambacorta A, Nicolaus B, Giardina P, Poerio E, Buonocore V. (1984). Glucose metabolism in the extreme thermoacidophilic archaeobacterium *Sulfolobus solfataricus*. *Biochem J*, 224: 407-414.
- Deka RK, Brautigam CA, Bidy BA, Liu WZ, Norgard MV. (2013). Evidence for an ABC-type riboflavin transporter system in pathogenic spirochetes. *mBio*. 4: e00615–00612.
- Demirbas, M.F., Balat, M. (2006). Recent advances on the production and utilization trends of biofuels: a global perspective. *Energy Convers Mgmt*, 47: 2371-2381.
- Demmer JK, Huang H, Wang S, Demmer U, Thauer RK, Ermler U. (2015). Insights into Flavin-based Electron Bifurcation via the NADH-dependent Reduced Ferredoxin: NADP Oxidoreductase Structure. *J Biol Chem*, 290: 21985-21995.
- Dermoun, Z., G. De Luca, M. Asso, P. Bertrand, F. Guerlesquin., B. Guigliarelli. (2002). The NADP-reducing hydrogenase from *Desulfovibrio fructosovorans*: functional interaction between the C-terminal region of HndA and the N-terminal region of HndD subunits. *Biochim Biophys Acta*, 1556: 217-225.
- Deutscher J., Francke C., Postma P.W. (2006). How phosphotransferase system-related protein phosphorylation regulates carbohydrate metabolism in bacteria [published correction appears in *Microbiol Mol Biol Rev*. 2008 Sep; 72(3):555]. *Microbiol Mol Biol Rev*, 70: 939–1031.

- 
- Dharmadi, Y., Gonzalez, R. (2005). A better global resolution function and a novel iterative stochastic search method for optimization of high-performance liquid chromatographic separation. *J Chromatogr A*, 1070: 89-101.
- Dharmadi, Y., Murarka, A., Gonzalez, R. (2006). Anaerobic fermentation of glycerol by *Escherichia coli*: a new platform for metabolic engineering. *Biotechnol Bioeng*, 94: 821-829.
- Diekert, Thauer. (1978). Carbon monoxide oxidation by *Clostridium thermoaceticum* and *Clostridium formicoaceticum*. *J Bacteriol*, 136: 597-606
- Dong, X., Stams, A.J.M. (1995). Evidence for H<sub>2</sub> and formate formation during syntrophic butyrate and propionate degradation. *Anaerobe*, 1:35-39.
- Duan J, Senger M, Esselborn J, Engelbrecht V, Wittkamp F, Apfel UP, Hofmann E, Stripp ST, Happe T, Winkler M. (2018). Crystallographic and spectroscopic assignment of the proton transfer pathway in [FeFe]-hydrogenases, 9:4726.
- Duncan SH, Barcenilla A, Stewart CS, Pryde SE, Flint HJ. (2002). Acetate utilization and butyryl coenzyme A (CoA): acetate-CoA transferase in butyrate-producing bacteria from the human large intestine. *Appl Environ Microbiol*, 68: 5186-5190.
- Eagon R.G., Wang C.H. (1962). Dissimilation of glucose and gluconic acid by *Pseudomonas natriegens*. *J Bacteriol*, 83:879-886.
- EBB - European Biodiesel Board. (2006). EU biodiesel production growth hits record high in 2005. EBB publishes annual biodiesel production statistics. Press release. Available in [http://www.ebbeu.org/EBBpressreleases/EBB%20press%20release%202005%20statistics%20\(final\).pdf](http://www.ebbeu.org/EBBpressreleases/EBB%20press%20release%202005%20statistics%20(final).pdf).
- Edwards AM. (2014). Structure and general properties of flavins. *Methods Mol Biol Clifton NJ*, 1146: 3–13.
- Eisenberg, R. C., Dobrogosz, W. J. (1967). Gluconate metabolism in *Escherichia coli*. *J Bacteriol*, 93, 941–949.

- 
- Elmekawy, A., Diels, L., De Wever, H., Pant, D. (2013). Valorization of cereal based biorefinery byproducts: Reality and expectations. *Environ Sci Technol*, 47: 9014-9027.
- Entner N, Doudoroff M. (1952). Glucose and gluconic acid oxidation of *Pseudomonas saccharophila*. *J Biol Chem*, 196: 853-862.
- Euzéby J. (2010). List of new names and new combinations previously effectively, but not validly, published. List no. 132. *Int J Syst Evol Microbiol*, 60: 469-472.
- Felsenstein J. (1985). Confidence limits on phylogenies: an approach using the bootstrap. *Evol*, 39: 783-791.
- Ferry, J.G., Smith, P.H., Wolfe, R.S. (1974). *Methanospirillum*, a new genus of methanogenic bacteria, and characterization of *Methanospirillum hungatii* sp. nov., *Int J Syst Evol Microbiol*, 24: 465-469.
- Field D, Garrity GM, Gray T, Morrison N, Selengut J, Sterk P, et al. (2008). The minimum information about a genome sequence (MIGS) specification. *Nat Biotechnol*, 26: 541-557.
- Figueredo Juan Emilio Lago, Anny Armas Cayarga<sup>1</sup>, Yaimé Josefina González González, Teresa Collazo Mesa. (2017). A simple, fast and inexpensive method for mutation scanning of CFTR gene. *BMC Medical Genetics*, 18:58.
- Flamholz A, Noor E, Bar-Even A, Liebermeister W, Milo R. (2013). Glycolytic strategy as a tradeoff between energy yield and protein cost. *Proc Natl Acad Sci*, 110: 10039-10044.
- Forsberg CW, Donaldson L, Gibbins LN. (1987). Metabolism of rhamnose and other sugars by strains of *Clostridium acetobutylicum* and other *Clostridium* species. *Can J Microbiol*, 33:21-26.
- Fraenkel D. *Escherichia coli* and *Salmonella*. In: Neidhardt FC, editor. *Cellular and Molecular Biology*, Vol. 1. Washington, DC: American Society for Microbiology; 1996. p. 189-199.

- 
- Fraenkel DG, Horecker BL. (1964). Pathways of D-glucose metabolism in *Salmonella typhimurium*. A study of a mutant lacking phosphoglucose isomerase. *J Biol Chem*, 239: 2765-2771.
- Fuchs, G. (2011). Alternative Pathways of Carbon Dioxide Fixation: Insights into the Early Evolution of Life? *Annu Rev Microbiol*, 65: 631– 658.
- Fuchs, G. H.G. Schlegel. (2014). *Allgemeine Mikrobiologie*. Georg Thieme Verlag, Stuttgart, ed. 9:411-413
- Fuhrer T, Fischer E, Sauer U. (2005). Experimental identification and quantification of glucose metabolism in seven bacterial species. *J Bacteriol*, 187: 1581-1590.
- Furdui, C., Ragsdale, S. W. (2000). The Role of Pyruvate Ferredoxin Oxidoreductase in Pyruvate Synthesis during Autotrophic Growth by the Wood-Ljungdahl Pathway *J Biol Chem*, 275: 28494–28499.
- Garsin DA. (2010). Ethanolamine utilization in bacterial pathogens: roles and regulation: *Nature Reviews Microbiology*, 8: 290-295.
- Gersonde K, Trittelvitz E, Schlaak H-E, Stahel H-H. (1971).The influence of the dimeriation on the stoichiometry of the active center in ferredoxin from *Clostridium pasteurianum*. *Eur J Biochem*, 22:57–65.
- Gibbons NE, Murray RGE. (1978). Proposals concerning the higher taxa of bacteria. *Int J Syst Bacteriol*, 28: 1-6.
- Gibson DT, Subramanian V. (1984). Microbial degradation of aromatic hydrocarbons. In: Gibson DT (ed) *Microbial degradation of organic compounds*. Dekker, New York, pp 181–252..
- Gibson, M.I., Brignole, E.J., Pierce, E., Can, M., Ragsdale, S.W., Drennan, C.L. (2015). The Structure of an Oxalate Oxidoreductase Provides Insight into Microbial 2-Oxoacid Metabolism. *Biochemistry*, 54: 4112-4120.

- 
- González JM, Fernández-Gómez B, Fernández-Guerra A, Gómez-Consarnau L, Sánchez O, Coll-Lladó M, Del Campo J, Escudero L, Rodríguez-Martínez R, Alonso-Sáez L, Latasa M, Paulsen I, Nedashkovskaya O, Lekunberri I, Pinhassi J, Pedrós-Alió C. (2008). Genome analysis of the proteorhodopsin-containing marine bacterium *Polaribacter* sp. MED152 (Flavobacteria). *Proc Natl Acad Sci*, 105: 8724-8729.
- Gosalbes MJ, et al. (2011). Metatranscriptomic approach to analyze the functional human gut microbiota. *PLoS One*, 6: 17447.
- Grissa, I., Vergnaud G., Pourcel C. (2007). The CRISPR db database and tools to display CRISPRs and to generate dictionaries of spacers and repeats. *BMC Bioinformatics*, 8: 172.
- Grupe H, Gottschalk G. (1992). Physiological events in *Clostridium acetobutylicum* during the shift from acidogenesis to solventogenesis in continuous culture and presentation of a model for shift induction. *Appl Environ Microbiol*, 58: 3896-3902.
- Gupta, A., Murarka, A., Campbell, P., Gonzalez, R. (2009). Anaerobic fermentation of glycerol in *Paenibacillus macerans*: metabolic pathways and environmental determinants. *Appl Environm Microbiol*. 75: 5871-5883.
- Gutiérrez-Preciado A, Torres AG, Merino E, Bonomi HR, Goldbaum FA, García-Angulo VA. (2015). Extensive Identification of Bacterial Riboflavin Transporters and Their Distribution across Bacterial Species. *PLoS ONE*, 10: e0126124.
- Haase, I., Gräwert, T., Illarionov, B., Bacher, A., Fischer, M. (2014). Recent advances in riboflavin biosynthesis. *Methods Mol Biol*. 1146: 15–40.
- Hall, R.H., Stern, E.S. (1950). Acid-catalysed hydration of acraldehyde. Kinetics of the reaction and isolation of p-hydroxypropaldehyde. *J Chem Soc*. 1950: 490-498.
- Hallsworth, J.E., Nomura, Y., Iwahara, M. (1998). Ethanol-Induced Water Stress and Fungal Growth. *J of ferment and bioeng*, 86: 451-456.
- Hansen, A.C., Zhang, Q., Lyne, P.W.L. (2005). Ethanol diesel fuel blends – a review. *Bioresour Technol*, 96: 277-285.

- 
- Henry J. Lamb, Christine C. Milburn, Garry L. Taylor, David W. Hough, Michael J. Danson. Gluconate dehydratase from the promiscuous Entner–Doudoroff pathway in *Sulfolobus solfataricus*. *FEBS Letters* 576 (2004) 133–136
- Herrmann, G., Jayamani, E., Mai, G., Buckel, W. (2008). Energy conservation via electron-transferring flavoprotein in anaerobic bacteria. *J Bacteriol*, 190: 784-791.
- Homann T, Tag C, Biebl H, Deckwer WD, Schink B. (1990). Fermentation of glycerol to 1,3-propanediol by *Klebsiella* and *Citrobacter* strains. *Appl Microbiol Biotechnol*, 33: 121-126.
- Huang, H., Wang, S., Moll, J., Thauer, R. K. (2012). Electron bifurcation involved in the energy metabolism of the acetogenic bacterium *Moorella thermoacetica* growing on glucose or H<sub>2</sub> plus CO<sub>2</sub>, *Journal of bacteriology*, 194: 3689-99.
- Huntemann M, Ivanova NN, Mavromatis K, Tripp HJ, Paez-Espino D, Palaniappan K, Szeto E, Pillay M, Chen IM, Pati A, et al. (2015). The standard operating procedure of the DOE-JGI Microbial Genome Annotation Pipeline (MGAP v.4). *Stand Genomic Sci*, 2015: 10: 86.
- Hyatt D, Chen GL, Locascio PF, Land ML, Larimer FW, Hauser LJ. (2010). Prodigal: prokaryotic gene recognition and translation initiation site identification. *BMC Bioinformatics*, 11: 119.
- Iannotti L, Iannotti, E., Kafkewitz, David., Wolin, Meyer., P Bryant, M. (1973). Glucose Fermentation Products of *Ruminococcus albus* Grown in Continuous Culture with *Vibrio succinogenes*: Changes Caused by Interspecies Transfer of H<sub>2</sub>. *Journal of bacteriology*, 114: 1231-40.
- Imkamp, F., Biegel, E., Jayamani, E., Buckel, W., Müller, V. (2007). Dissection of the caffeate respiratory chain in the acetogen *Acetobacterium woodii*: identification of an Rnf-type NADH dehydrogenase as a potential coupling site. *J Bacteriol*, 189: 8145-8153.
- Ingram, L. O. (1990). Ethanol tolerance in bacteria. *Crit Rev Biotechnol*, 9: 305-319.

- 
- Jennifer S. McDowall, Bonnie J. Murphy, Michael Haumann, Tracy Palmer, Fraser A. Armstrong, Frank Sargent. (2014). Bacterial formate hydrogen lyase complex. PNAS, 23: 111.
- Jiménez, A., Santos, M.A., Pompejus, M., Revuelta, J.L. (2005) Metabolic engineering of the purine pathway for riboflavin production in *Ashbya gossypii* Appl. Environ. Microbiol, 71, pp. 5743-575.
- Johnson MJ, Peterson WH, Fred EB. (1931). Oxidation and reduction relations between substrate and products in the acetone-butyl alcohol fermentation. J Biol Chem, 91: 569-591.
- Jukes TH, Cantor CR. (1969). Evolution of protein molecules. In: Munro HN, editor, Mammalian protein metabolism. Academic Press, New York;. p. 21-132.
- Jungerman, K., Thauer, R.F., Leimenstoll, G. and Decker, K. (1973). Function of reduced pyridine nucleotide-ferredoxin oxidoreductases in saccharolytic *Clostridia*. Biochim Biophys Acta, 305: 268-280.
- Junghare M, Patil Y, Schink B. (2015). Draft genome sequence of a nitrate-reducing, o-phthalate degrading bacterium, *Azoarcus* sp. strain PA01T. Stand Genomic Sci, 10: 90.
- Junghare, M., Spitteller, D., Schink, B. (2016). Enzymes involved in the anaerobic degradation of ortho-phthalate by the nitrate-reducing bacterium *Azoarcus* sp. strain PA01. Environ Microbiol, 2920.13447.
- Jurgens G., Glockner F. O., Amann R., Saano A., Montonen L., Likolammi M., Munster U. (2000). Identification of novel Archaea in bacterioplankton of a boreal forest lake by phylogenetic analysis and fluorescent in situ hybridization. FEMS Microbiology Ecology, 34: 45–56.
- Kallmeyer J., Pockalny R., Adhikari R. R., Smith D. C., D'Hondt S. (2012). Global distribution of microbial abundance and biomass in seafloor sediment. Proc Natl Acad Sci, 109: 16213–16216.

- 
- Kapatral V, Anderson I, Ivanova N, Reznik G, Los T, Lykidis A, Bhattacharyya A, Bartman A, Gardner W, Grechkin G, Zhu L, Vasieva O, Chu L, Kogan Y, Chaga O, Goltsman E, Bernal A, Larsen N, D'Souza M, Walunas T, Pusch G, Haselkorn R, Fonstein M, Kyrpides N, Overbeek R: (2002). Genome sequence and analysis of the oral bacterium *Fusobacterium nucleatum* strain ATCC 25586. *J Bacteriol*, 184: 2005–2018.
- Kaster, A. K., Moll, J., Parey, K., Thauer, R. K. (2011). Coupling of ferredoxin and heterodisulfide reduction via electron bifurcation in hydrogenotrophic methanogenic archaea, *Proc Natl Acad Sci*, 108: 2981-6.
- Kerstens, K., De Lay, J. (1968). The occurrence of the Entner-Doudoroff pathway in bacteria. *Antonie van Leeuwenhoek Journal of Microbiology and Serology*, 34:393–408.
- Kim BH, Gadd GM. (2008). *Bacterial Physiology and Metabolism*. Cambridge, UK: Cambridge Univ Press.
- Kim S, Lee SB. (2005). Identification and characterization of *Sulfolobus solfataricus* D-gluconate dehydratase: a key enzyme in the non-phosphorylated Entner–Doudoroff pathway. *Biochem J*, 387: 271-280.
- Kittelman S, Seedorf H, Walters WA, Clemente JC, Knight R, Gordon JI, Janssen PH. (2013). Simultaneous amplicon sequencing to explore co-occurrence patterns of bacterial, archaeal and eukaryotic microorganisms in rumen microbial communities. *PLoS One*, 8: 47879.
- Knauth, P., Sabbah, R. (1990). Energetics of inter- and intramolecular bonds in alkanediols. IV. The thermochemical study of 1, 2-alkanediols at 298.15 K. *Thermochim Acta*, 164: 145-152.
- Kortelainen P, Pajunen H, Rantakari M, Saarnisto M. (2004). A large carbon pool and small sink in boreal Holocene lake sediments. *Global Change Biol*, 10: 1648–53.
- Kruger, Nicholas J; von Schaewen, Antje. (2003). The oxidative pentose phosphate pathway: structure and organisation. *Current Opinion in Plant Biology*, 6: 236–246.

- 
- Krumholz, L.R., and Bryant, M.P. (1986). *Syntrophococcus sucromutans* sp. nov. gen. nov. uses carbohydrates as electron donors and formate, methoxy benzenoids or Methanobrevibacter as electron acceptor systems. Arch Microbiol, 143: 313–318.
- Kumar S, Stecher G, Tamura K. (2016). MEGA7: molecular evolutionary genetics analysis version 7.0 for bigger datasets Mol Biol Evol, 33: 1870-1874.
- Kyrpides NC, Hugenholtz P, Eisen JA, Woyke T, Göker M, Parker CT, et al. (2014). Genomic encyclopedia of bacteria and archaea: sequencing a myriad of type strains. PLoS Biol, 12: 1001920.
- Laemmli U. K. (1970). Cleavage of structural proteins during the assembly of the head of bacteriophage T4. In: Nature. Bd. 227, S. 680–685.
- Lam, F.H., Ghaderi, A., Fink, G.R., Stephanopoulos, G. (2014). Engineering alcohol tolerance in yeast. Science. 346: 71-75.
- Lamble, H. J., Milburn, C. C., Taylor, G. L., Hough, D. W. & Danson, M. J. (2004). Gluconate dehydratase from the promiscuous Entner–Doudoroff pathway in *Sulfolobus solfataricus*. FEBS Letters, 133–136.
- Lee, K. H., Humbarger, S., Bahnvadia, R., Sazinsky, M.H., Crane EJ. (2014). Characterization of the mechanism of the NADH-dependent polysulfide reductase (Npsr) from *Shewanella loihica* PV-4: formation of a productive NADH-enzyme complex and its role in the general mechanism of NADH and FAD-dependent enzymes. Biochim Biophys Acta, 1844: 1708-1717.
- Li, F., Hindenberger, J., Seedorf, H., Zhang, J., Buckel, W., Thauer, R.K. (2008). Coupled ferredoxin and crotonyl coenzyme A (CoA) reduction with NADH catalyzed by the butyryl-CoA dehydrogenase/Etf-complex from *Clostridium kluyveri*. J Bacteriol, 190: 843-850.
- Liolios, K., Mavromatis, K., Tavernarakis, N., Kyrpides, N.C. (2008). The Genomes On Line Database (GOLD) in 2007: status of genomic and metagenomic projects and their associated metadata. Nucleic Acids Res, 36: D475-D479.

- 
- Losey NA, Mus F, Peters JW, Le HM, McInerney MJ. (2017). *Syntrophomonas wolfei* uses an NADH-dependent, ferredoxin independent [FeFe]-hydrogenase to reoxidized NADH. *Appl Environ Microbiol*, 83: e01335-17.
- Lowe TM, Eddy SR. tRNA scan-SE: (1997). A program for improved detection of transfer RNA genes in genomic sequence. *Nucleic Acids Res*, 25: 955-964.
- Lubner Carolyn E, David P Jennings, David W Mulder, Gerrit J Schut, Oleg A Zadvornyy, John P Hoben, Monika Tokmina-Lukaszewska, Luke Berry, Diep M Nguyen, Gina L Lipscomb et al., (2017). Mechanistic insights into energy conservation by flavin-based electron bifurcation. *Nature Chemical Biology*, 13: 655–659.
- M.F. Temudo, R. Kleerebezem, M.V. (2007). Loosdrecht Influence of the pH on (open) mixed culture fermentation of glucose: a chemostat study. *Biotechnol Bioeng*, 98: 69-79.
- Malki S, Saimmaime I, De Luca G, Rousset M, Dermoun Z, Belaich JP. (1995). Characterization of an operon encoding an NADP-reducing hydrogenase in *Desulfovibrio fructosovorans*. *J Bacteriol*, 177: 2628-36.
- Manzoor, S., Bongcam-Rudloff, E., Schnurer, A., and Muller, B. (2016). Genome guided analysis and whole transcriptome profiling of the mesophilic syntrophic acetate oxidising bacterium *Syntrophaceticus schinkii*. *PLoS ONE*, 11:e0166520.
- Marcus I. Gibson, Edward J. Brignole, Elizabeth Pierce, Mehmet Can, Stephen W. Ragsdale, and Catherine L. Drennan. (2015).The Structure of an Oxalate Oxidoreductase Provides Insight into Microbial 2-Oxoacid Metabolism. *Biochemistry*, 54: 4112-4120.
- Markowitz VM, Chen IM, Palaniappan K, Chu K, Szeto E, Pillay M, Ratner A, Huang J, Woyke T, Huntemann M, et al. (2014). IMG 4 version of the integrated microbial genomes comparative analysis system. *Nucleic Acids Res*, 42: 560-567.
- Markowitz, V.M., Mavromatis, K., Ivanova, N.N., Chen, I.M.A., Chu, K., and Kyrpides, N.C. (2009). IMG ER: a system for microbial genome annotation expert review and curation. *Bioinformatics*, 25: 2271-2278.

- 
- Marone, A., Varrone, C., Fiocchetti, F., Giussani, B., Izzo, G., Mentuccia, L., Rosa, S., and Signorini, A. (2015). Optimization of substrate composition for biohydrogen production from buffalo slurry co-fermented with cheese whey and crude glycerol, using microbial mixed culture. *Int J Hydrogen Energy*, 40: 209-218.
- Mavromatis K, Land ML, Brettin TS, Quest DJ, Copeland A, Clum A, Goodwin L, Woyke T, Lapidus A, Klenk HP, et al. (2012). The fast changing landscape of sequencing technologies and their impact on microbial genome assemblies and annotation. *PLoS One*, 7: 48837.
- Mayhew, S. G., Tollin, G. (1992). General properties of flavodoxins. in *Chemistry and Biochemistry of Flavoenzymes* (Müller, F. ed.), CRC Press, Inc., Boca Raton. pp 389-426.
- McDowall J. S., Murphy B. J., Haumann M., Palmer T., Armstrong F. A., Sargent F. (2014). Bacterial formate hydrogenlyase complex. *Proc Natl Acad Sci*, 111: E3948–E3956.
- McInerney MJ, Rohlin L, Mouttaki H et al. (2007). The genome of *Syntrophus aciditrophicus*: life at the thermodynamic limit of microbial growth. *P Natl Acad Sci*, 104: 7600–7605.
- McInerney, M. J., M. P. Bryant, N. Pfennig. (1979). Anaerobic bacterium that degrades fatty acids in syntrophic association with methanogens. *Arch Microbiol*, 122: 129–135.
- McInerney, M.J. et al. (2008). Physiology, ecology, phylogeny, and genomics of microorganisms capable of syntrophic metabolism. *Ann. NY Acad Sci*, 1125: 58-72.
- Meléndez-Hevia E, Waddell TG, Heinrich R, Montero F. (1997). Theoretical approaches to the evolutionary optimization of glycolysis-chemical analysis. *Eur J Biochem*, 244: 527-543.
- Menon, N.K., Chatelus, C.Y., Dervartanian, M., Wendt, J.C., Shanmugam, K.T., Peck, H.D., Jr, Przybyla, A.E. (1994). Cloning, sequencing, and mutational analysis of the hybrid operon encoding *Escherichia coli* hydrogenase 2. *J Bacteriol*, 176: 4416–4423.

- 
- Mitchell, P. (1975). Proton motive redox mechanism of the cytochrome b-c1 complex in the respiratory chain: proton motive ubiquinone cycle. *FEBS Lett.* 56: 1–6.
- Monteverde, D. R., Gómez-Consarnau, L., Suffridge, C., Sañudo-Wilhelmy, S. A. (2017). Life's utilization of B vitamins on early Earth. *Geobiology*, 15: 3–18.
- Müller N., Griffin B.M., Stingl U. Schink B. (2008). Dominant sugar utilizers in sediment of Lake Constance depend on syntrophic cooperation with methanogenic partner organisms. *Environmental Microbiology*, 10: 1501-1511.
- Müller et al., (2010). Syntrophic butyrate and propionate oxidation processes: from genomes to reaction mechanisms. *Environmental Microbiology Reports*, 2: 489–499.
- Müller N, Frank D. Scherag, M, Schink B. (2015). *Bacillus stamsii* sp. nov, a facultatively anaerobic sugar degrader that is numerically dominant in freshwater lake sediment. *Systematic and Applied Microbiology*, 38: 379-389
- Müller V. (2001). Bacterial Fermentation. *ENCYCLOPEDIA OF LIFE SCIENCES*. Nature Publishing Group.
- Müller V., Chowdhury N. P., Basen M. (2018). Electron bifurcation: a long-hidden energy-coupling mechanism. *Annu Rev Microbiol*, 72: 331–353.
- Murarka, A., Clomburg, J.S., Sean, M., Jacqueline, V. S., Gonzalez, R. (2010). Metabolic Analysis of Wild-type *Escherichia coli* and a Pyruvate Dehydrogenase Complex (PDHC)-deficient Derivative Reveals the Role of PDHC in the Fermentative Metabolism of Glucose. *JBC*, 8:285: 31548-58.
- Murarka, A., Dharmadi, Y., Yazdani, S. S., Gonzalez, R. (2008). Fermentative utilization of glycerol by *Escherichia coli* and its implications for the production of fuels and chemicals. *Appl Environ Microbiol*, 74: 1124-1135.
- Murray RGE. (1984). The higher taxa, or, a place for everything...? In: Krieg NR, Hol JG, editors. *Bergey's Manual of Systematic Bacteriology*, vol. 1. Baltimore: Williams & Wilkins Co. pp. 31–34.

- 
- Nawrocki EP, Eddy SR. (2013). Infernal 1.1: 100-fold faster RNA homology searches. *Bioinformatics*. 29: 2933-2935.
- Nei M, Kumar S. (2000). *Molecular Evolution and Phylogenetics*. Oxford University Press, New York.
- Neuhoff V., Arnold N., Taube D., Ehrhardt W. (1988). Improved staining of proteins in polyacrylamide gels including isoelectric focusing gels with clear background at nanogram sensitivity using Coomassie Brilliant Blue G-250 and R-250. *Wiley Online Library*, 9: 255-262.
- Ng H, Vaughn RH. (1963). *Clostridium rubrum* sp. n. and other pectinolytic *Clostridia* from Soil. *J Bacteriol*, 85: 1104.
- Nicol, R.W., Marchand, K., Lubitz, W.D. (2012). Bioconversion of crude glycerol by fungi. *Appl Microbiol Biotechnol*, 93: 1865-1875.
- Nwachukwu, R.E.S, Shahbazi, A., Wang, L., Ibrahim, S., Worku, M., and Schimmel, K. (2012) Bioconversion of glycerol to ethanol by a mutant *Enterobacter aerogenes*. *AMB Express*, 2: 20.
- Nwachukwu, R.E.S., Shahbazi, A., Wang, L., Worku, M., Ibrahim, S., Schimmel, K. (2013). Optimization of cultural conditions for conversion of glycerol to ethanol by *Enterobacter aerogenes* S012. *AMB Express*, 3: 12.
- Otero, J.M., Panagiotou, G., and Olsson, L. (2007) Fueling industrial biotechnology growth with bioethanol. *Adv Biochem Eng Biotechnol* 108: 1-40.
- Patil Y, Junghare M, Müller N. (2017). Fermentation of glycerol by *Anaerobium acetethylicum* and its potential use in biofuel production. *Microbiol Biotechnol*, 10: 203-17.
- Patil Y, Junghare M, Müller N. (2019). Gluconate-fermentation by *Anaerobium acetethylicum*: an evidence for the involvement of modified Entner-Doudoroff pathway (submitted to microbial cell factories).

- 
- Patil Y, Junghare M, Pester M, Müller N, Schink B. (2015). Characterization and phylogeny of *Anaerobium acetethylicum* gen. nov., sp. nov., a strictly anaerobic gluconate-fermenting bacterium isolated from a methanogenic bioreactor. *Int J Syst Evol Microbiol*, 65: 3289-3296.
- Patil Y, Müller N, Schink B, Whitman WB, Huntemann M, Clum A, Pillay M, Palaniappan K, Varghese N, Mikhailova N, Stamatis D, Reddy TBK, Daum C, Shapiro N, Ivanova N, Kyrpides N, Woyke T, Junghare M. (2016). High-quality-draft genome sequence of the fermenting bacterium *Anaerobium acetethylicum* type strain GluBS11T (DSM 29698). *Stand Genomic Sci.* doi: 10. 1186/s40793-017-0236-4.
- Patil Y, Müller N. (2019). Enzymes involved in reoxidation of reduced equivalents in glucose and gluconate fermentation (manuscript to be submitted).
- Peekhaus N, Conway T. (1988). What's for dinner? Entner-Doudoroff metabolism in *Escherichia coli*. *J Bacteriol*, 180: 3495-3502.
- Peters, J. W., Miller, A. F., Jones, A. K., King, P. W., Adams, M. W. (2016). Electron bifurcation. *Current opinion in chemical biology* 31, 146-152.
- Peters, J. W., Schut, G. J., Boyd, E. S., Mulder, D. W., Shepard, E. M., Broderick, J. B., et al. (2015). [FeFe]- and [NiFe]-hydrogenase diversity, mechanism, and maturation. *Biochim Biophys Acta*, 1853: 1350-1369.
- Petit E, LaTouf WG, Coppi MV, Warnick TA, Currie D, Romashko I, Deshpande S, Haas K, Alvelo-Maurosa JG, Wardman C, Schnell DJ, Leschine SB, Blanchard JL. Involvement of a bacterial microcompartment in the metabolism of fucose and rhamnose by *Clostridium phytofermentans*. *PLoS ONE*, 8: 54337.
- Pfennig, N. (1978). *Rhodocyclus purpureus* gen. nov. sp. nov., a ring-shaped, vitamin B12-requiring member of the family *Rhodospirillaceae*. *Int J Syst Bacteriol*, 28: 283-288.
- Porebski S, Bailey L, Baum B. (1997). Modification of a CTAB DNA extraction protocol for plants containing high polysaccharide and polyphenol components. *Plant Mol Biol Rep*, 15: 8-15.

- 
- Prévot AR. In: Hauderoy P, Ehringer G, Guillot G, Magrou J, Prévot AR, Rosset D, Urbain A, editors. *Dictionnaire des Bactéries Pathogènes*, second 2nd ed. Masson et Cie, Paris, Paris; 1953. p. 1-692.
- Pruesse, E., Quast, C., Knittel, K., Fuchs, B. M., Ludwig, W., Peplies, J., Glöckner, F. O. (2007). SILVA: a comprehensive online resource for quality checked and aligned ribosomal RNA sequence data compatible with ARB. *Nucleic Acids Res*, 35: 7188-7196.
- Przybyla AE, Robbins J, Menon N, Peck HD Jr: (1992). Structure-function relationships among the nickel-containing hydrogenases. *FEMS Microbiol Rev*, 88: 109-136.
- Rae BD, Long BM, Whitehead LF, Förster B, Badger MR, Price GD. (2013). Cyanobacterial carboxysomes: microcompartments that facilitate CO<sub>2</sub> fixation. *J Mol Microbiol Biotechnol*, 23: 300-307.
- Rainey FA. Class II Clostridia class., nov. In: De Vos P, Garrity GM, Jones D, Krieg NR, Ludwig W, Rainey FA, Schleifer KH, Whitman WB, editors. *Bergey's Manual of Systematic Bacteriology*, second edition, volume 3, Springer-Verlag, New York; 2009. p. 736-1297.
- Rainey FA. Family V. Lachnospiraceae fam., Nov. In: De Vos P, Garrity GM, Jones D, Krieg NR, Ludwig W, Rainey FA, Schleifer KH, Whitman WB, editors. *Bergey's Manual of Systematic Bacteriology*, second edition, volume 3, Springer-Verlag, New York; 2009. p. 921.
- Ramachandran S, Fontanille P, Pandey A, Larroche C. (2006). Gluconic acid: properties, applications and microbial production. *Food Technol Biotechnol*, 44: 185-195.
- Reddy TBK, Thomas AD, Stamatis D, Bertsch J, Isbandi M, Jansson J, Mallajosyula J, Pagani I, Lobos EA, Kyrpides NC. (2015). The Genomes OnLine Database (GOLD) v.5: a metadata management system based on a four level (meta) genome project classification. *Nucleic Acids Res*, 43: 1099-1106.

- 
- Richard P, Hilditch S. (2009). D-galacturonic acid catabolism in microorganisms and its biotechnological relevance. *Appl Microbiol Biotechnol*, 82: 597-604.
- Roger, V., Fonty, G., Andre, C., Gouet, P. (1992) Effects of glycerol on the growth, adhesion, and cellulolytic activity of rumen cellulolytic bacteria and anaerobic fungi. *Curr Microbiol*, 25: 197-201.
- Röhr M, Kubicek CP, Komínek J. Gluconic Acid. In: Rehm HJ, Reed G, editors. *Biotechnology*, Vol. 3. Weinheim: Verlag Chemie; 1983. p. 455-465.
- Rossi, D.M., Da Costa, J.B., De Souza, E.A., Peralba, M.C.R., and Ayub, M.A.Z. (2012) Bioconversion of residual glycerol from biodiesel synthesis into 1,3-propanediol and ethanol by isolated bacteria from the environmental consortia. *Renew Energy*, 39: 223-227.
- Rzhetsky A, Nei M. (1992). A simple method for estimating and testing minimum-evolution trees. *Mol Biol Evol*, 9: 945-967.
- Saitou N, Nei M. (1987). The neighbor-joining method: a new method for reconstructing phylogenetic trees. *Mol Biol Evol*, 4: 406-425.
- Sarma, S.J., Brar, S.K., Sydney, E.B., Bihan, Y.L., Buelna, G., and Soccol, C.R. (2012) Microbial hydrogen production by bioconversion of crude glycerol: a review. *Int J Hydrog Energy*, 37: 6473-6490.
- Sawers, R. G., Clark, D. P. (2004). Fermentative pyruvate and acetyl-coenzymeA metabolism. In *EcoSal—Escherichia coli and Salmonella: Cellular and Molecular Biology*. Edited by R. Curtis III. Washington, DC: American Society for Microbiology.
- Sawyer DT. (1964). Metal-gluconate complexes. *Chem Rev*, 64: 633-644.
- Schink B, Zeikus JG. (1983). Characterization of pectinolytic enzymes of *Clostridium thermosulfurogenes*. *FEMS Microbiol Lett*, 17:295-298.

- 
- Schink, B. (1997). Energetics of syntrophic cooperation in methanogenic cooperation. *Microbiol Mol Biol Rev*, 61: 262-280.
- Schink, B., Alfons J., Stams, M., 2006. Syntrophism among Prokaryotes. In: DWORKIN, Martin, ed. *The Prokaryotes / Vol. 2*. New York: Springer, pp. 309-335
- Schönheit P, Wäscher C, Thauer RK. A rapid procedure for the purification of ferredoxin from *Clostridia* using polyethyleneimine. *FEBS Lett*, 1987; 89: 219-222.
- Schuchmann, K. and Müller, V. (2012). A Bacterial Electron-bifurcating Hydrogenase. *J Biol Chem*, 287: 31165-31171.
- Schut, G.J., Adams, W.W. (2009). The iron-hydrogenase of *Thermotoga maritima* utilizes ferredoxin and NADH synergistically: a new perspective on anaerobic hydrogen production. *J. Bacteriol*, 191: 4451-4457.
- Servinsky MD, Liu S, Gerlach ES, Germane KL, Sund CJ. (2014). Fermentation of oxidized hexose derivatives by *Clostridium acetobutylicum*. *Microb Cell Fact*, 13: 139.
- Skerman VBD, McGowan V, Sneath PHA. (1980). Approved Lists of Bacterial Names. *Int J Syst Bacteriol*, 30: 225-420.
- Sleat R, Mah RA. (1985). *Clostridium populeti* sp. nov., a cellulolytic species from a woody-biomass digester. *Int J Syst Bacteriol*, 35: 160-163.
- Sokatch JT, Gunsalus IC. Aldonic acid metabolism. I. (1975). Pathway of carbon in an inducible gluconate fermentation by *Streptococcus faecalis*. *J Bacteriol*, 73: 452-460.
- Solomon, B.O., Zeng, A.P., Biebl, H., Schlieker, H., Posten, C., Deckwer, W.D. (1995). Comparison of the energetic efficiencies of hydrogen and oxychemicals formation in *Klebsiella pneumoniae* and *Clostridium butyricum* during anaerobic growth on glycerol. *J Biotechnol*, 39: 107-17.
- Speers, A.M., Young, J.M., and Reguera, G. (2014) Fermentation of glycerol into ethanol in a microbial electrolysis cell driven by a customized consortium. *Environ Sci Technol*, 48: 6350-6358.

- 
- Stackebrandt E, Kramer I, Swiderski J, Hippe H. (1999). Phylogenetic basis for a taxonomic dissection of the genus *Clostridium*. FEMS Immunol Med Microbiol, 24: 253-258.
- Stadtman, E. R. (1966). Some considerations of the energy metabolism of anaerobic bacteria, p. 39–62. *In* N. O. Kaplan and E. P. Kennedy (ed.), Current aspects of biochemical energetics. Academic Press, New York, NY.
- Stams A. J., Plugge C. M. (2009). Electron transfer in syntrophic communities of anaerobic bacteria and archaea. Nat Rev Microbiol, 7:568–577.
- Sung JS, Xu DP, Galloway CM, Black CC. (1988). A reassessment of glycolysis and gluconeogenesis in higher plants. Physiol Plant, 72: 650-654.
- Suresh K, Prakash D, Rastogi N, Jain RK. (2007). *Clostridium nitrophenolicum* sp. nov., a novel anaerobic p-nitrophenol-degrading bacterium, isolated from a subsurface soil sample Int J Syst Evol Microbiol, 57: 1886-1890.
- Sweet, G., Gandor, C., Voegelé, R., Wittekindt, N., Beuerle, J., Truniger, V., Lin, E.C., Boos, W. (1990). Glycerol facilitator of *Escherichia coli*: cloning of *glpF* and identification of the *glpF* product. J Bacteriol, 172: 424-430.
- Swings, J., and De Ley, J. (1977). The biology of *Zymomonas*. Bacteriol Rev 41: 1-46.
- Swings, J., and De Ley, J. (1977). The biology of *Zymomonas*. Bacteriol Rev, 41: 1-46.
- Szymona M, Doudoroff, M. (1960). Carbohydrate metabolism in *Rhodospseudomonas sphaeroides*. Microbiology, 22: 167-183.
- Tewes FJ, Thauer RK. (1980). Regulation of ATP-synthesis in glucose fermenting bacteria involved in interspecies hydrogen transfer. In: Gottschalk G, Pfennig N, Werner H (eds), Anaerobes and anaerobic infections. Gustav Fischer, Stuttgart New York, pp. 97–104
- Thamer, W., Cirpus, I., Hans, M., Pierik, A. J., Selmer, T., Bill, E., et al. (2003). A two [4Fe-4S]-cluster-containing ferredoxin as an alternative electron donor for 2-hydroxyglutaryl-CoA dehydratase from *Acidaminococcus fermentans*. Arch. Microbiol, 179: 197–204.

- 
- Thauer, R. K., Kaster, A.K., Seedorf, H., Buckel, W., and Hedderich, R. (2008) Methanogenic archaea: ecologically relevant differences in energy conservation. *Nature Reviews Microbiology* 6, 579-591.
- Thauer, R.K. Rupprecht, E. (1972). C1-Einheiten-Synthese aus CO<sub>2</sub> in *Clostridien*: Der reduktive Monocarbonsäurezyklus. *Zbl. Bakt. Hyg. I. Abt Orig A*, 220, 420-423.
- Thauer, R.K. (2008) Biologische Methanbildung: Eine erneuerbare Energiequelle von Bedeutung? In *Die Zukunft der Energie* (Gruss P. und Schüth, F. Herausgeber) Verlag C. H. Beck, pp. 119-137
- Thauer, R.K., Jungermann, K., Decker, K. (1977). Energy conservation in chemotrophic anaerobic bacteria. *Bacteriol Rev*, 41: 100–180.
- Thauer, R.K., Shima, S. (2008) Methane as fuel for anaerobic micro-organisms. *Annals of the New York Academy of Sciences*. 1125, 158-170.
- Trchounian, K., and Trchounian, A. (2015). Hydrogen production from glycerol by *Escherichia coli* and other bacteria: An overview and perspectives. *Appl Energy*, 156: 174–184.
- Truninger, V., and Boos, W. (1993). Glycerol uptake in *Escherichia coli* is sensitive to membrane lipid-composition. *Res Microbiol*, 144: 565-574.
- Tsukahara T, Koyama H, Okada M, Ushida K. (2002). Stimulation of butyrate production by gluconic acid in batch culture of pig fecal digesta and identification of butyrate-producing bacteria. *J Nutr*, 132: 2229-2234.
- Uyeda, K., and Rabinowitz, J.C. (1971). Pyruvate-ferredoxin oxidoreductase III. Purification and properties of the enzyme. *J Biol Chem*, 246: 3111–3119.
- Uyeda, K., Rabinowitz, J.C. (1971). Pyruvate-ferredoxin oxidoreductase III. Purification and properties of the enzyme. *J Biol Chem* 246: 3111–3119.
- Van Gylswyk NO, Morris EJ, Els HJ. (1980). Sporulation and cell wall structure of *Clostridium polysaccharolyticum* comb. nov. (Formerly *Fusobacterium polysaccharolyticum*). *J Gen Microbiol*, 121: 491-493.

- 
- Van Rijssel M, Smidt MP, Van Kouwen G, Hansen TA. (1993). Involvement of an intracellular oligogalacturonate hydrolase in the metabolism of pectin by *Clostridium thermosaccharolyticum*. *Appl Environ Microbiol*, 59: 837-842.
- Varel VH, Tanner RS, Woese CR. (1995). *Clostridium herbivorans* sp. nov., a cellulolytic anaerobe from the pig intestine. *Int J Syst Bacteriol*, 45: 490-494.
- Vignais, P.M., Billoud, B. (2007). Occurrence, classification, and biological function of hydrogenases: an overview. *Chem Rev*, 107: 4206–4272.
- Vitreschak AG, Rodionov DA, Mironov AA, Gelfand MS. Regulation of riboflavin biosynthesis and transport genes in bacteria by transcriptional and translational attenuation. *Nucleic Acids Res*, 2002; 30: 3141–3151. PMID: 12136096
- Wahl RC, Orme-Johnson WH (1987) Clostridial pyruvate oxidoreductase and the pyruvate-oxidizing enzyme specific to nitrogen fixation in *Klebsiella pneumoniae* are similar enzymes. *J Biol Chem*, 262: 10489–10496.
- Wallrabenstein C., Schink B. (1994). Evidence of reversed electron transport in syntrophic butyrate or benzoate oxidation by *Syntrophomonas wolfei* and *Syntrophus buswellii*. *Arch Microbiol*, 162: 136-142.
- Wang S, Huang H, Moll J, Thauer RK. (2010). NADP-reduction with reduced ferredoxin and NADP reduction with NADH are coupled via an electron-bifurcating enzyme complex in *Clostridium kluyveri*. *J Bacteriol*, 192: 5115–5123.
- Wang S, Huang H, Moll J, Thauer RK. 2010. NADP reduction with reduced ferredoxin and NADP reduction with NADH are coupled via an electron-bifurcating enzyme complex in *Clostridium kluyveri*. *J. Bacteriol.* 192:5115–5123.
- Wang, S., Huang, H., Kahnt, J., Müller, A.P., Köpke, M., R.K. Thauer (2013). NADP specific electron-bifurcating [FeFe]-hydrogenase in a functional complex with formate dehydrogenase in *Clostridium autoethanogenum* grown on CO. *J Bacteriol*, 195: 4373-4386.

- 
- Wang, S., Huang, H., Kahnt, J., Thauer, R. K. (2013). *Clostridium acidurici* electron-bifurcating formate dehydrogenase, Applied and environmental microbiology, 79: 6176-9.
- Weghoff M. C., Bertsch J., Müller V. (2015). A novel mode of lactate metabolism in strictly anaerobic bacteria. Environ Microbiol, 17: 670–677.
- Weissbach A., Hurwitz J. (1959). The Formation of 2-Keto-3-deoxyheptonic Acid in Extracts of *Escherichia coli* B : I. IDENTIFICATION J Biol Chem, 234: 705-9.
- Wendt A, Birnir B, Buschard K, Gromada J, Salehi A, Sewing S, Rorsman P, Braun M.(2004) Glucose inhibition of glucagon secretion from rat  $\alpha$ -cells is mediated by GABA released from neighboring  $\beta$ -cells. Diabetes.53: 1038–1045.
- Westermann P. (1993). Wetland and swamp microbiology. In: Ford TE (ed) Aquatic microbiology—an ecological approach. Blackwell, Boston, pp. 215–238
- Whitman W. B., Coleman D. C., Wiebe W. J. (1998). Prokaryotes: the unseen majority. Proc. Natl. Acad. Sci. U.S.A. 95, 6578–6583.
- Whitman, W.B., Woyke, T., Klenk, H.-P., Zhou, Y., Lilburn, T.G., Beck, B.J., De Vos, P., Vandamme, P., Eisen, J.A., Garrity, G., Hugenholtz, P., and Kyrpides, N.C. (2015) Genomic encyclopedia of bacterial and archaeal type strains, phase III: the genomes of soil and plant-associated and newly described type strains. Stand Genomic Sci 10: 26.
- Williams, K., Lowett, P.N., and Leadlay, P.F. (1987) Purification and characterization of pyruvate: ferredoxin oxidoreductase from the anaerobic protozoon *Trichomonas vaginalis*. Biochem J 246: 529–536.
- Woese CR, Kandler O, Wheelis ML. (1990). Towards a natural system of organisms: proposal for the domains Archaea, Bacteria, and Eucarya. Proc Natl Acad Sci, 87: 4576-4579.
- Yazdani, S.S., Gonzalez, R. (2007). Anaerobic fermentation of glycerol: a path to economic viability for the biofuels industry. Curr Opin Biotechnol, 18: 213-219.

- 
- You, K.M., Rosenfield, C.L., Knipple, D.C. (2003) Ethanol tolerance in the yeast *Saccharomyces cerevisiae* is dependent on cellular oleic acid content. *Appl Environ Microbiol*, 69: 1499-1503.
- Zelkus, J.G., G. Fuchs, W. Kenealy, R.K.Thauer. (1977). Oxidoreductases involved in cell carbon synthesis of *Methanobacterium thermoautotrophicum*. *J Bacteriol*, 132: 604-6
- Ziegenhom J., Senn M., Bucher T. (1976). Molar absorptivities of beta NADH and beta NADPH. *Clin Chem*, 22: 151-160.
- Znad H, Marcos J, and Bales V. Production of gluconic acid from glucose by *Aspergillus niger*: growth and non-growth conditions. *Process Biochemistry*. 2004; 39: 1341-1345.

---

## Abbreviations

IMG	Integrated Microbial Genomes
CoA	Coenzyme A
Da	Dalton
K	Kilo
DNA	Deoxyribonucleic acid
EDTA	Ethylene diamine tetraacetic acid
FAD	Flavin adenine dinucleotide
FMN	Flavin mononucleotide
L	Litre
µl	micro liter
M	Molar
mM	Milli molar
µM	Micro molar
Min	Minute
s/sec	Seconds
OD <sub>600</sub>	Optical density at 600nm
rpm	Revolutions per minute
SDS-PAGE	Sodium dodecyl sulphate polyacrylamide gel electrophoresis
HPLC	Ultra high performance liquid chromatography
UV	Ultra violet
MS	Mass spectrometry
GC	Gas chromatography
HPLC	High pressure liquid chromatography
HGAP3	Hierarchical Genome Assembly Process
CTAB	Cetyl Trimethyl Ammonium Bromide
NCBI	National Center for Biotechnology Information
IMG-ER	Integrated Microbial Genomes-Expert Review
CDSs	Codind DNA sequences
GOLD	Genomes Online Database
COG	Clusters of Orthologous Groups
ORF	Open reading frame
CFA	Cellular fatty acid
DTT	Dithiotritol

---

## **Acknowledgements**

I would like to acknowledge the people who supported me during the challenging journey of my life. My first words are of course for Prof. Schink who specially kept his trust on me from beginning. I would like to thank to him for giving me a chance to work in his lab and support, his helping nature and amazing ways to come out from the hard situations. I highly appreciate his guidance and scientific ideas and knowledge during my research project. I would like to thank him for his full support by all ways during the project.

Secondly I would like to thank my second guide Dr. Nicolai Müller for accepting the request to guide me during this project. Thanks for his guidance in lab work and sharing his ideas and scientific knowledge. I appreciate his efforts in this project from the beginning and helping me to correct the thesis and to reach final findings and the conclusions.

I would like to thanks to Prof. Peter Kroth for being my second supervisor during this project. I would like to thanks to Prof. Dieter Spiteller for being the chairman of my thesis committee. I like to acknowledge and thank Prof. Dr. David Schleheck for allowing me to work in his lab and his kind support. I would like to thanks Dr. Jasmin Frey for the discussions and sharing her knowledge. I would like to thanks to Sarah Sagin for her initial work on the topic before me. I also thanks to Julia Schmidt and Antje Weise for their technical support and help. Further I like to thanks to all the people from Prof. Schink lab for giving the company and nice environment. I like to acknowledge LGFG (Landesgraduiertenförderung), University of Konstanz for providing me a scholarship for doing my doctoral research.

I would like to thanks to my husband Dr. Madan Junghare for his support during this time and his efforts and help to complete this journey. I highly appreciate his efforts for correcting my thesis and papers during this study. I would like to thank him for his ideas and finding the starting ways to begin from. I like to thank my both families and my parents especially for their unconditional support who always have faith on me and my amazing lovely daughter Grishma for giving me motivation for everything from her presence in my life and her endless love.